Natural Resources Canada
Ressources naturelles Canada

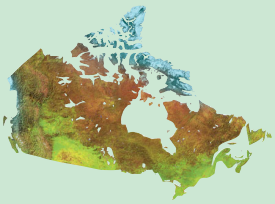

Geological Survey of Canada
Bulletin 596

Quaternary geology of Fort Liard map area, Northwest Territories

J.M. Bednarski

2008

Canada

The CD-ROM accompanying this publication contains the full report, including any oversized figures and/or A-series maps, in Portable Document Format (PDF). Oversized items may be purchased separately as paper plots from any Geological Survey of Canada Bookstore location:

Geological Survey of Canada Bookstore (Ottawa)
601 Booth Street
Ottawa, Ontario
K1A 0E8
Tel.: (613) 995-4342
Tel.: (888) 252-4301 (toll-free)
Fax: (613) 943-0646
E-mail: gscbookstore@nrcan.gc.ca
Web: http://gsc.nrcan.gc.ca/bookstore/index_e.php

Geological Survey of Canada Bookstore (Vancouver)
101-605 Robson Street
Vancouver, B.C.
V6B 5J3
Tel.: (604) 666-0271
Fax: (604) 666-1337
E-mail: gscvan@gsc.nrcan.gc.ca
Web: http://gsc.nrcan.gc.ca/org/vancouver/bookstore/index_e.php

Geological Survey of Canada Bookstore (Atlantic)
1 Challenger Drive
P.O. Box 1006
Dartmouth, Nova Scotia
B2Y 4A2
Tel.: (902) 426-4386
Fax: (902) 426-4848
E-mail: Jennifer.Bates@nrcan-rncan.gc.ca
Web: http://gsca.nrcan.gc.ca/pubprod/pubprod_e.php

Geological Survey of Canada Bookstore (Québec)
490, rue de la Couronne
Québec, Quebec
G1K 9A9
Tel.: (418) 654-2677
Fax: (418) 654-2660
E-mail: cgcq_librairie@rncan.gc.ca
Web: http://www.gscq.nrcan.gc.ca/bibliotheque/

Le CD-ROM qui accompagne cette publication renferme le rapport au complet, y compris les figures surdimensionnées ou les cartes de série A, en format PDF. Pour acheter des copies papier des éléments surdimensionnés, adressez-vous à la Librairie de la Commission géologique du Canada :

Librairie de la Commission géologique du Canada (Ottawa)
601, rue Booth
Ottawa (Ontario)
K1A 0E8
Tél. : (613) 995-4342
Tél. : (888) 252-4301 (sans frais)
Télécopieur : (613) 943-0646
Courriel : librairiecgc@nrcan.gc.ca
Web : http://cgc.rncan.gc.ca/librairie/index_f.php

Librairie de la Commission géologique du Canada (Vancouver)
101-605 Robson Street
Vancouver (C.-B.)
V6B 5J3
Tél. : (604) 666-0271
Télécopieur : (604) 666-1337
Courriel : gscvan@gsc.nrcan.gc.ca
Web : http://cgc.rncan.gc.ca/org/vancouver/bookstore/index_f.php

Librairie de la Commission géologique du Canada (Atlantique)
1 Challenger Drive
P.O. Box 1006
Dartmouth (Nouvelle-Écosse)
B2Y 4A2
Tél. : (902) 426-4386
Télécopieur : (902) 426-4848
Courriel : Jennifer.Bates@nrcan-rncan.gc.ca
Web : http://gsca.nrcan.gc.ca/pubprod/pubprod_f.php

Librairie de la Commission géologique du Canada (Québec)
490, rue de la Couronne
Québec (Québec) G1K 9A9
Tél. : (418) 654-2677
Télécopieur : (418) 654-2660
Courriel : cgcq_librairie@rncan.gc.ca
Web : http://www.cgcq.rncan.gc.ca/bibliotheque/

Geological Survey of Canada
Bulletin 596

Quaternary geology of Fort Liard map area, Northwest Territories

J.M. Bednarski

2008

ISSN 0068-7626
Catalogue No. M42-596E
ISBN 978-0-660-19841-5

Available in Canada from the Geological Survey of Canada Bookstore
(see inside front cover for details)

A copy of this publication is also available for reference in depository libraries across Canada through access to the Depository Services Program's Web site at http://dsp-psd.pwgsc.gc.ca

A free digital download of this publication is available from GeoPub: http://geopub.nrcan.gc.ca/index_e.php

Recommended citation

Bednarski, J.M., 2008. Quaternary geology of Fort Liard map area, Northwest Territories; Geological Survey of Canada, Bulletin 596, 59 p.

Cover illustration
The photograph was taken from the crest of the Liard Range, looking due north at Mount Flett, the highest distinct point on the horizon. Glacial erratics transported from the Canadian Shield are found all along the crest of the range. The broad valley in the foreground is a former meltwater channel that drained northward when the Laurentide Ice Sheet occupied the plains to the east (right) and abutted the outlying ridges. An old, partially forested landslide can be seen on the base of the cliff, centre left of the photograph. GSC 2008-124

Critical reviewers
A. Dyke
R. Smith

Author
J.M. Bednarski (jbednars@nrcan.gc.ca)
Geological Survey of Canada
9860 West Saanich Road, P.O. Box 6000
Sidney, British Columbia V8L 4B2

CONTENTS

Appendices

Figures

Tables

Quaternary geology of Fort Liard map area, Northwest Territories

Abstract

Detailed mapping of the surficial geology of the Fort Liard area (NTS 95 B) provides insight into the dynamics of the Laurentide Ice Sheet as it impinged against the Cordilleran Ice Sheet during the last glacial maximum. Overall, ice advance over the plains was from the northeast, but as the ice sheet approached the mountain front, the flow was deflected southward, up the lower Liard River valley. In the southern part of the map area, curving flowlines record the collision and northward deflection of the Laurentide Ice Sheet when it impinged on the Cordilleran Ice Sheet in the mountains west of the map area. High-elevation striations and Canadian Shield erratics show that the entire region was glaciated during this time. Once deglaciation began, an expanding corridor between the two ice sheets was instrumental in channelling meltwater from at least 500 km of the Laurentide ice margin, northward, into the Mackenzie Basin. During early deglaciation, drainage divides connecting northward-trending mountain valleys controlled proglacial lakes levels (>600 m a.s.l.). With eastward retreat of the Laurentide ice margin, glacial lake levels continued to fall as lower outlets became ice-free. About 11.5 ka BP, a large glacial lake formed in Liard River valley when the Laurentide ice margin disengaged from the mountain front. The entire map area was deglaciated shortly after 11 ka BP. Glacial Lake Liard finally drained into Mackenzie River valley when the ice margin retreated east of the confluence of the Liard and Mackenzie rivers.

Résumé

La cartographie détaillée de la géologie de surface de la région de Fort Liard (SNRC 95 B) fournit un aperçu de la dynamique de l'Inlandsis laurentidien pendant qu'il entrait en collision avec l'Inlandsis de la Cordillère lors du dernier pléniglaciaire. Dans l'ensemble, la glace s'est avancée dans les plaines depuis le nord-est, mais alors que l'inlandsis s'approchait du front montagneux, l'écoulement a été dévié vers le sud pour remonter la basse vallée de la rivière Liard. Dans la partie méridionale de la région cartographique, des lignes de flux incurvées témoignent de la collision et de la déviation vers le nord de l'Inlandsis laurentidien lorsqu'il s'est buté à l'Inlandsis de la Cordillère dans les montagnes à l'ouest de la région cartographique. Des stries glaciaires et des blocs erratiques du Bouclier canadien observés à haute altitude révèlent que toute la région était englacée à cette époque. Une fois la déglaciation commencée, un corridor en expansion entre les deux inlandsis a contribué à canaliser vers le nord dans le bassin du Mackenzie l'eau de fonte provenant d'un segment de la marge de l'Inlandsis laurentidien d'au moins 500 km. Lors du début de la déglaciation, les lignes de partage des eaux reliant les vallées de montagne orientées vers le nord ont contrôlé les niveaux des lacs proglaciaires (> 600 m a.n.m.). Pendant le retrait vers l'est de la marge de l'Inlandsis laurentidien, les niveaux des lacs glaciaires ont continué à baisser à mesure que sont devenu libres de glace des exutoires à moindre altitude. Il y a environ 11,5 ka, un grand lac glaciaire s'est formé dans la vallée de la Liard lorsque la marge de l'Inlandsis laurentidien s'est dégagée du front montagneux. Toute la région cartographique était libre de glace peu après 11 ka avant le présent. Le Lac glaciaire Liard s'est finalement vidé dans la vallée du fleuve Mackenzie lorsque la marge glaciaire s'est retirée à l'est de la confluence de la rivière Liard et du fleuve Mackenzie.

SUMMARY

This report on the Quaternary geology of the Fort Liard map area (NTS 95 B) is the result of detailed (1:50 000 scale) surficial geology mapping. The map area encompasses an abrupt boundary between the western edge of the Interior Plains and the Cordillera. During the last glaciation (Late Wisconsinan (McConnell) time), Liard Range, southern Franklin Mountains, in the western part of the map area may have been first glaciated by limited montane ice, but the continental Laurentide Ice Sheet dominated the ice cover in this region during the last glacial maximum. The continental Laurentide Ice Sheet advanced from the northeast, based on the provenance of Canadian Shield erratics and extensive glacial flutings. This flow was diverted southward within Liard River valley where the Laurentide Ice Sheet encountered the abrupt mountain front of Liard Range. Flutings in the southwest part of the map area that line up to form a curved path show that when the Laurentide Ice Sheet encountered Cordilleran ice west of the map area, it was forced to flow northward, against the regional topography into the southern end of Liard Range. Laurentide incursion into Liard Range extended beyond the western limit of the map area, overtopping a ridge 1200 m a.s.l. On the plains, extensive glacial flutings, drumlinoid ridges, and subglacial furrows show the gradual northward deflection in ice-flow direction caused by the contact of the two ice sheets.

Deglaciation was marked by the downvalley retreat of the Laurentide (continental) ice out of mountain valleys, which became flooded because of ice-dammed drainage. An ice-free corridor along Kotaneelee River valley, west of Liard Range, routed meltwater northward along a 500 km sector of the Laurentide Ice Sheet. With farther northeastward retreat of the ice front, meltwater was channelled through various valleys of Liard Range. When the Laurentide Ice Sheet disengaged from the southern Liard Range, smaller proglacial lakes combined outside the mountain front to form glacial Lake Liard. At about 11.5 ka BP, glacial Lake Liard joined glacial Lake Tetcela and glacial Lake Nahanni. Northward drainage continued west of Nahanni Range until the ice front receded northeastward and exposed lower outlets east of Nahanni Range. Lake levels were maintained because as the ice margin retreated down the lower Liard River it continued to occupy the upper Mackenzie River valley. The final stages of glacial Lake Liard are marked by a prominent delta near Fort Liard townsite at about 254 m a.s.l. and extensive sand deposited within Liard River valley in the northern part of the map area. Meltwater issuing from retreating ice and glacial-lake drainage cut several large meltwater channels across the region, although some channels may have

SOMMAIRE

Ce rapport sur la géologie du Quaternaire de la région cartographique de Fort Liard (SNRC 95 B) découle de la cartographie détaillée (à l'échelle de 1/50 000) de la géologie de surface. La région cartographique englobe une limite bien définie entre la bordure occidentale des Plaines intérieures et la Cordillère. Pendant la dernière glaciation (glaciation de McConnell au Wisconsinien supérieur), le chaînon Liard des monts Franklin méridionaux, dans la partie ouest de la région cartographique, peut avoir été d'abord englacé par une quantité limitée de glace de montagne, mais c'est l'Inlandsis laurentidien continental qui a dominé la couverture de glace de cette région pendant le dernier pléniglaciaire. L'Inlandsis laurentidien s'est avancé depuis le nord-est, comme en témoignent des blocs erratiques provenant du Bouclier canadien et d'abondantes rainures glaciaires. Cet écoulement a été dévié vers le sud dans la vallée de la Liard où l'Inlandsis laurentidien a rencontré l'abrupt front montagneux du chaînon Liard. Des rainures glaciaires dans la partie sud-ouest de la région cartographique, qui s'alignent en une trajectoire incurvée, révèlent que lorsque l'Inlandsis laurentidien a rencontré l'Inlandsis de la Cordillère à l'ouest de la région cartographique, son écoulement a été dévié vers le nord à l'encontre de la topographie régionale et dans l'extrémité sud du chaînon Liard. La glace laurentidienne dans le chaînon Liard s'est avancée au-delà de la limite ouest de la région cartographique, débordant une crête de 1200 m au-dessus du niveau de la mer. Dans les plaines, d'abondantes rainures glaciaires, des drumlinoïdes et des sillons sous-glaciaires révèlent la progressive déviation vers le nord de la direction d'écoulement glaciaire engendrée par le contact des deux inlandsis.

La déglaciation a été marquée par le retrait de la glace laurentidienne (continentale) vers l'aval des vallées de montagne qui ont alors été noyées parce que le drainage y a été bloqué par la glace. Un corridor libre de glace le long de la vallée de la rivière Kotaneelee, à l'ouest du chaînon Liard, acheminait l'eau de fonte vers le nord le long d'un secteur de l'Inlandsis laurentidien de 500 km. À mesure que le front glaciaire reculait davantage vers le nord-est, l'eau de fonte devenait canalisée par les diverses vallées du chaînon Liard. Lorsque l'Inlandsis laurentidien s'est dégagé du chaînon Liard méridional, de plus petits lacs proglaciaires se sont combinés hors du front montagneux pour former le Lac glaciaire Liard. Il y a environ 11,5 ka, le Lac glaciaire Liard a rejoint le Lac glaciaire Tetcela et le Lac glaciaire Nahanni. Le drainage vers le nord s'est poursuivi à l'est du chaînon Nahanni jusqu'à ce que le front glaciaire se soit retiré vers le nord-est pour laisser libre les émissaires plus bas à l'est du chaînon Nahanni. Les niveaux des lacs se sont maintenus parce que pendant que la marge glaciaire se retirait vers l'aval dans la basse vallée de la rivière Liard, la glace continuait à occuper la haute vallée du fleuve Mackenzie. Les stades ultimes du Lac glaciaire Liard sont marqués par un important delta près du site de l'agglomération de Fort Liard à environ 254 m au-dessus du niveau de la mer, et par de vastes dépôts de sable dans la vallée de la Liard dans la partie nord de la région cartographique. L'eau de fonte issue de la glace en retrait et l'eau de drainage du lac glaciaire ont entaillé plusieurs grand chenaux à travers la région, bien que certains d'entre eux aient emprunté

reoccupied segments of preglacial valleys. In particular, some channels were probably occupied by a proto–Petitot River, whereas others are partially filled with till and may have been tunnel valleys within or below the glacier.

A detailed record of the eastward-retreating Laurentide ice margin is provided by small end moraines and crevasse fillings that are found overlying glacial flutings at sharp angles. As opposed to the flutings, these features are only about 100–200 m wide and made up of short segments that can be traced for tens of kilometres. In some places, these moraines form sets of closely spaced, parallel ridges that may mark seasonal pulses of ice retreat.

Landslides are common along steep slopes in the area. Interbedded recessive shale and thick sandstone exposed along cliffs in Liard Range are prone to failures causing landslides ranging in size from a few tens of square metres to several square kilometres. Active and relic landslides suggest that mass wasting has been occurring throughout the postglacial time.

de nouveau des segments de vallées préglaciaires. Certains de ces chenaux avaient en particulier probablement été occupés par une proto-rivière Petitot, alors que d'autres sont en partie comblés de till et peuvent avoir été des vallées-tunnels dans le glacier ou sous celui-ci.

Les petites moraines frontales et les remplissages de crevasses qui recouvrent à angle aigu les rainures glaciaires, fournissent une histoire détaillée du retrait vers l'est de la marge de l'Inlandsis laurentidien. Par opposition aux rainures glaciaires, ces entités n'ont qu'environ 100 à 200 m de largeur et se composent de courts segments pouvant être suivis sur des dizaines de kilomètres. En certains endroits, ces moraines forment des ensembles de crêtes parallèles rapprochées qui peuvent marquer des périodes de recul saisonnier de la glace.

Les glissements de terrain sont communs le long des talus abrupts dans la région. Les épaisses couches de grès interstratifiées de shale récessif exposées le long des falaises dans le chaînon Liard sont sujettes aux effondrements causant des glissements de terrain dont l'ordre de grandeur varie de quelques dizaines de mètres carrés à plusieurs kilomètres carrés. Les glissements de terrain actifs et reliques font penser que les mouvements de masse se sont produits tout au long de l'époque postglaciaire.

INTRODUCTION

This paper describes the Quaternary geology of the Fort Liard map area (NTS 95 B), situated in the southwest corner of Northwest Territories (Fig. 1). The area continues to be the focus of intensive hydrocarbon exploration and development. Evidence of human occupation dates back several thousand years (Millar, 1968), and during deglaciation, it would have been part of the doorway to an ice-free corridor to the south.

Fieldwork was conducted during 2000, 2001, and 2002, as part of the Central Foreland Project, a multidisciplinary study of surficial, bedrock, and subsurface geology that covered parts of northeastern British Columbia and the southern Northwest Territories (NATMAP; Lane et al. (1999)). The surficial geology component resulted in 16 detailed 1: 50 000 scale GSC Open File maps of surficial materials and landforms of the Fort Liard map area (Bednarski, 2002, 2003a, b, c, d, e, f, g, h, i, j, k, l, m, n, o) and physical and geochemical data on 64 samples of glacial drift (Appendix A). The Central Foreland Project also included detailed surficial mapping of the adjacent La Biche River map area reported elsewhere (Smith, 2000, 2000a, b, 2003a, b, c, d, 2004a, b).

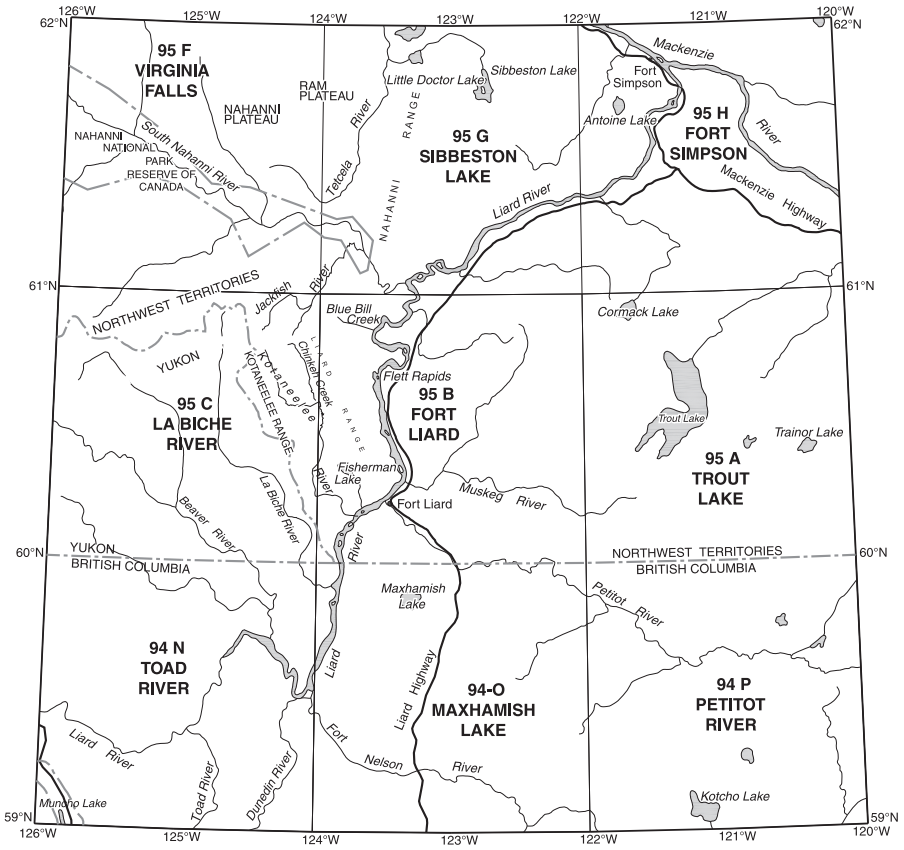

Figure 1. Location of the study area and surrounding NTS map areas. Geological Survey of Canada Open Files on the surficial geology of Fort Liard area (95 B) are shown on the index map.

Sawmill Mountain 95 B/13 GSC OF 4476	Netla River 95 B/14 GSC OF 4478	Emile Lake 95 B/15 GSC OF 4477	Arrowhead Lake 95 B/16 GSC OF 1775
Mount Flett 95 B/12 GSC OF 4481	Denedothada Creek 95 B/11 GSC OF 4480	Arrowhead River 95 B/10 GSC OF 4483	Pointe-de-flèche River 95 B/9 GSC OF 1773
Fisherman Lake 95 B/5 GSC OF 4360	Rabbit Creek 95 B/6 GSC OF 4486	Tourbière River 95 B/7 GSC OF 4487	Muskeg River 95 B/8 GSC OF 1753
Betalamea Lake 95 B/4 GSC OF 4502	Fort Liard 95 B/3 GSC OF 1760	Lake Bovie 95 B/2 GSC OF 1761	Celibeta Lake 95 B/1 GSC OF 1754

PHYSIOGRAPHY

The Fort Liard map area is dominated by the 600 m wide Liard River that separates the western mountains from the plains. The study area straddles several physiographic regions described by Bostock ((1970); Fig. 2). The Liard Range, a part of the southern Franklin Mountains, dominates the west side of the map area. It forms a nearly continuous, sharp-crested ridge, running north to south to about the middle of the map area, where it bifurcates into separate ridges running southwest and southeast that finally terminate just north of Liard River. Elevations range from a little more than 1550 m a.s.l. in the north, to about 840 m a.s.l. near the end of the southern ridges. Although the mountains are currently ice-free, a few small cirques below some ridges indicate minor local glaciation in the past. Most signs of glacial erosion in the mountains relate to the incursion of glaciers from beyond the mountains themselves.

The southwest map area also includes part of Liard Plateau, which is expressed as a distinct break in slope on the mountain flanks, forming a smooth, concordant surface incised by crosscutting streams that exit the mountains. The plateau includes the broad Kotaneelee River valley, west of Liard Range, and the broad area around Fisherman Lake, south of the bifurcation in the mountains. Elevations range from about 600 m in the north, to 300 m on the southern boundary along Liard River. The plateau is probably a Tertiary erosional surface, one of several ancient erosional surfaces that have been reported throughout the Cordillera (e.g. Tempelman-Kluit, 1980; Dyke, 1990; Duk-Rodkin et al., 1996). Glacial erosion does not seem to have affected the plateau much and till cover is usually thin.

The Fort Nelson Lowland covers most of the southern part of the map area where Liard River and a major tributary, Petitot River, are situated. The lowland extends northward along Liard River valley and eventually joins Great Slave Plain where Liard River valley widens in the northernmost part of the map area. In the central and eastern parts of the map area, smooth uplands rise gradually eastward to 700 m a.s.l., over 300 m above Liard River valley. These uplands are part of the Alberta Plateau, a collective term describing a ring of plateaus mainly composed of Cretaceous sediments on the Interior Plains, which are separated by wide valleys. Given the patterns of glacial flow in the Fort Liard area, the regional drainage patterns present today were probably not much different during preglacial times. Hage (1945)

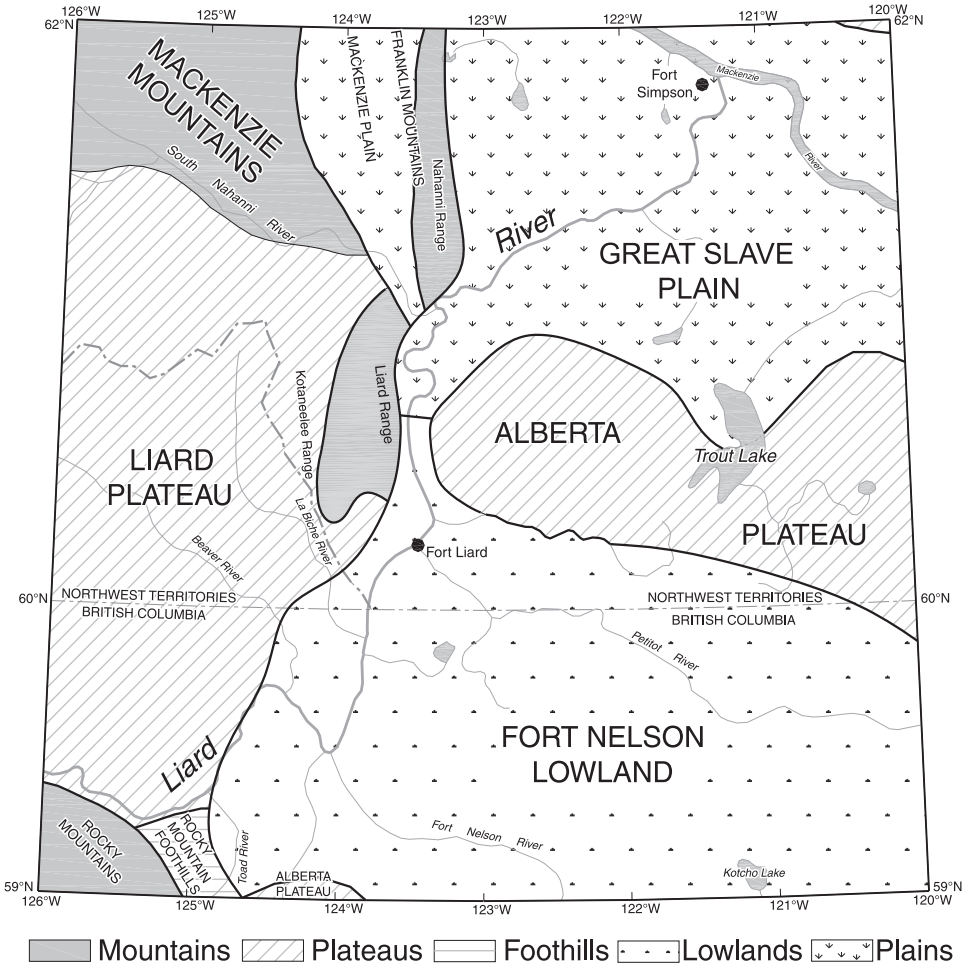

Figure 2. Physiographic regions surrounding the study area (*after* Bostock, 1970).

suggested that in the northern part of the study area, Liard River valley was preglacial in origin because he observed till on the valley floor, near the level of the river.

BEDROCK GEOLOGY

Most of the bedrock geology discussed here is based on Douglas and Norris (1959, 1976). Some detailed bedrock geology from the Central Foreland Project is found in Fallas and Lane (2001), Lane (2001, 2006), Hynes et al. (2002), and Lane and Hynes (2005). Figure 3 shows the regional bedrock distributions (Wheeler et al., 1997; Gordey and Makepeace, 1999; Massey et al., 2003)

The geological structure of the Fort Liard area includes the Mackenzie fold belt of the eastern Cordillera and the Interior Platform, the western part of the Interior Plains. In places, the structural elements of the mountains are not coincident with the physiographic boundary of the plains. Synclines, faulted anticlines, and west-dipping thrusts expressed in the mountains continue beneath the plains (Douglas and Norris, 1959). The strike is oriented along north-south axes, with folded and faulted Devonian to Mesozoic sedimentary rocks

Figure 3. Regional bedrock geology (*modified from* Wheeler et al., 1997; Gordey and Makepeace, 1999; Massey et al., 2003).

comprising the mountains in the western part of the map area, and gently folded to flat-lying Cretaceous sediments (Fort St. John Group) underlying the plains to the east. Although covered with thick glacial deposits, the northeastern part of the map area appears to be the western flank of a broad basin. In the southeast, a small area of flat-lying limestone (Mississippian Flett Formation) is exposed along Petitot River, likely an anticline underlying the area (Douglas and Norris, 1976).

The gentle topography of the plains is broken by a prominent ridge that runs from the confluence of the Arrowhead and Muskeg rivers, near the centre of the map area, for 50 km straight southward into British Columbia. The ridge is the result of the Bovie Lake thrust fault that brings gently west-dipping beds of upper Paleozoic Flett, Mattson, and Fantasque formations to the surface (Douglas and Norris, 1976). The ridge rises above the surrounding terrain by over 100 m and it formed a barrier to glacial flow from the east, as well as to meltwater and subsequent drainage. Hage (1945) reported on a restricted exposure of possible Tertiary strata along Petitot River near the border with British Columbia. Of interest was a 2 m layer of rusty gravel about 23 m above Petitot River that he believed to be at least preglacial in age. Unfortunately, this deposit could not be found during the present study. All the high-level gravel units located within the valley were found to contain granite clasts (continental glacial erratics) and are thus Quaternary.

REGIONAL QUATERNARY HISTORY

McConnell (1891) was the first to report on the glacial and postglacial features of the upper Mackenzie River basin, and was followed by others from the Geological Survey of Canada (e.g. Bell, 1900; Cameron, 1922). Craig (1965; Fig. 1, Douglas (1959)) was the first to compile a regional map of glacial features that included the present study area. Surficial materials of the region were mapped by various workers in the early 1970s as part of intensive research centred on developing the Mackenzie River valley transportation corridor. The culmination of this work was a 1:500 000 scale compilation by Rutter et al. (1980, 1993) showing the general surficial geology of the entire Mackenzie River region (including the Fort Liard map area), from the British Columbia border to 64°N latitude. The surficial geology of adjacent Yukon is less well known and is being addressed as a component of the Central Foreland NATMAP Project. General information can be obtained from the Surficial Materials Map of Canada (compiled by Fulton (1995)) and maps of continental deglaciation by Dyke and Prest (1987) and Dyke et al. (2003). To the south in British Columbia, Mathews (1980) compiled a 1:1 000 000 scale map of glacial features, essentially flutings, eskers, and meltwater channels.

Figure 4 shows the generalized ice-flow directions over the region compiled from the aforementioned sources. The ice-flow directions shown are thought to date from the last glaciation and are Late Wisconsinan. Drumlins, flutings, and striations show that the general flow over the plains was to the southwest, but near the mountain front, ice flow was to the west and northwestward in the southern Northwest Territories and southwestward in northeastern British Columbia. The source of the continental ice is from an ice divide of the Laurentide Ice Sheet situated over Great Slave Lake, the plains ice divide of Dyke and Prest (1987) and Dyke et al. (2003). At its maximum ca. 18 ka BP (last glacial maximum, the interval encompassing the last eustatic sea-level minimum centred on 18 ka BP; ca. 21.4 ka BP (calibrated); Mix et al. (2001)) the Laurentide Ice Sheet extended beyond the western border of Fort Liard map area, well into La Biche Range in the Yukon. At this time, the Laurentide ice probably abutted the Cordilleran Ice Sheet flowing northeastward from the Yukon Ice Divide and the central ice divide of the Cordilleran Ice Sheet over northern British Columbia (Dyke and Prest, 1987; Dyke, 1990; Dyke et al., 2003). To the south there is evidence that during the last glaciation the Cordilleran ice advanced prior the continental maximum, which occurred after a limited retreat of the Cordilleran ice (Mathews, 1978, 1980; Bednarski, 1996, 2001). In the north, the history is more complicated. Dud-Rodkin and Hughes (1991, 1992) recognized two montane glaciations in northeastern Mackenzie Mountains, tentatively correlated with the Reid (penultimate) and McConnell (last) glaciations. The last montane glaciation was the least extensive. Subsequently, Duk-Rodkin et al. (1996) used paleomagnetism and soil development to determine that the youngest montane glaciation was pre-Wisconsinan (Reid Glaciation) and that the only continental glaciation to reach Mackenzie Mountains was the Late Wisconsinan Laurentide Ice Sheet. This would imply that the two ice sheets did not impinge upon each other, which is in contrast to areas farther south. In Yukon, four major Cordilleran glaciations have long been recognized with the least extensive being Late Wisconsinan (McConnell Glaciation; Klassen (1987); Jackson et al. (1991)), but it appears the greatest variability between successive glaciations was experienced in central Yukon, with the least amount of variability in the southeast (Jackson et al., 1991).

Previous models of the last glacial maximum in this area suggested that the last glaciation was less extensive than suggested here. Work in the early 1970s reported evidence of two advances of continental ice (Rutter and Minning, 1972; Rutter and Boydell, 1973; Rutter, 1974). The first, and most extensive continental glacier advance left granite and gneiss erratics on summits of the southern Mackenzie Mountains at elevations of about 1555 m a.s.l. and a grey-black, stony till exposed as a basal unit in tributaries of Mackenzie River. Evidently, the ice was thick enough to flow across Mackenzie Mountains. The second Laurentide advance was evidenced by a light grey-brown, stony till that is separated from the lower till in stratigraphic sections by stratified sand

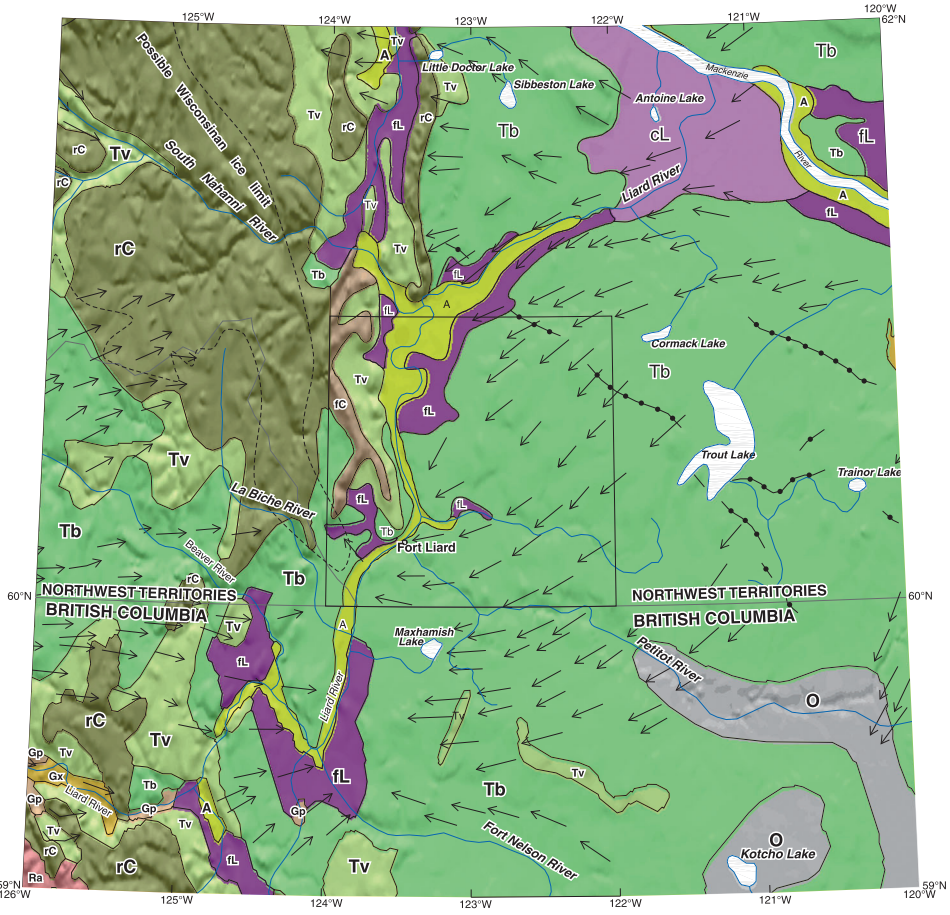

A — ***Alluvial deposits:*** *stratified silt, sand, clay, and gravel; floodplain, delta, and fan deposits; in places overlies and includes glaciofluvial deposits*

O — ***Organic deposits:*** *peat, muck, and minor inorganic sediments; large bog, fen, and swamp areas whereorganic fill masks underlying surficial materials; geneally >2 m thick*

Colluvial deposits: *colluvial and residual materials deposited as veneers and blankets of debris through downslope movement and in place disintigration of bedrock; includes areas of rock outcrop*

rC — ***Colluvial rubble:*** *rubble and silt; derived from carbonate and consolidated fine clastic sedimentary rock substrate*

fC — ***Colluvial fines:*** *silt, clay, and fine sand; derived from substrate weakly consolidated shale and siltstone substrate*

Glaciolacustrine and lacustrine deposits: *sediments deposited in a glacial lake during deglaciation and subsequent lake drainage*

fL — ***Fine grained:*** *silt and clay, locally containing stones; deposited as quiet-water sediments*

cL — ***Coarse grained:*** *sand, silt, and gravel; deposited as deltas, sheet sands, and lag deposits*

Glaciofluvial deposits: *gravel and sand deposited by meltwater streams*

Gp — ***Plain:*** *sand and gravel; deposited as outwash sheets, valley trains, and terrace deposits*

Gx — ***Complex:*** *sand and gravel and locally diamicton; undifferentiated ice-contact stratified drift, and outwash; locally includes till and rock*

Glacial deposits: *silty, sandy, and clayey diamicton; formed by the direct action of glacier ice*

Tb — ***Till blanket:*** *thick and continuous till*

Tv — ***Till veneer:*** *thin and discontinuous till; may include extensive areas of rock outcrop*

Rock: *areas of abundant (>75%) rock outcrop*

Ra — ***Alpine complexes:*** *rock, colluvium, and till; rock and Quaternary deposits complex in an area, characterized by alpine and glacial landforms*

Figure 4. Regional surficial geology with general ice-flow directions based on drumlins and flutings (arrows), the possible Wisconsinan ice limit (dashed line; from Fulton (1995)). Moraines near Trout Lake were added by the author (ball lines; some based on Rutter et al. (1993)). The Fort Liard study area is outlined by the box.

and gravel. This second advance was thought to have been relatively thin and was deflected northwest and south as the continental ice approached the mountains. The centre of deflection was just north of the Fort Liard map area at the south end of Nahanni Range (Fig. 4). Glacial deposits from the second advance were not found above about 670 m a.s.l., but tongues of ice penetrated through gaps in the mountain ranges. Day (1966) postulated that when the continental ice retreated eastward, the eastern mountain slopes below 480 m a.s.l. were inundated by a proglacial lake, glacial Lake Liard, between Fort Liard and Nahanni Butte.

Similarly, Ford (1976) described three continental ice advances into the South Nahanni River area. The most extensive advance overtopped Nahanni Range, which deposited glacial erratics up to 1400 m a.s.l. on Nahanni Plateau and 1500 m a.s.l. on Ram Plateau, and was thought to be pre-Illinoisan. This most extensive glaciation was followed by two younger, successively lesser advances that took place within the confines of South Nahanni River valley. Related to these continental advances were glacial lakes Nahanni (580–650 m a.s.l.) and Tetcela (400 m a.s.l.) that formed when eastward drainage was dammed during the last two glaciations. Only the least extensive of the continental advances was thought to have been Late Wisconsinan. For mountain glaciers, Ford (1976) proposed that Cordilleran glaciation during the Late Wisconsinan was restricted to minor advances of local cirque glaciers, but a more extensive eastward advance occurred during the previous Illinoisan glaciation. Ford's (1976) Cordilleran glacial zone extended as far east as Funeral Range, about 100 km west of the confluence of the South Nahanni and Liard rivers.

Notwithstanding, Dyke (1990), working east of the continental divide, found no earlier ice limits and argued that the extensive Cordilleran advance was Late Wisconsinan (McConnell Glaciation). Moreover, the all-time limit of continental glaciation in western Canada is now thought to have been reached during the last glaciation (Mathews, 1980; Lemmen et al., 1994; Duk-Rodkin et al., 1996). Recent advances in cosmogenic dating show that the Laurentide and Cordilleran ice sheets contacted each other during the last glacial maximum from northern British Columbia to southern Alberta (cf. Jackson et al., 1997; Bednarski, 2001). In La Biche Range, west of the study area, Smith (2003a) found that the Laurentide ice advanced into the area first, followed by a northeastward advance of the Cordilleran Ice Sheet, based on crosscutting ice-flow features. Sandstone erratics of unknown provenance were found up to 1820 m a.s.l. on the Kotaneelee Range (Smith, 2003c). The largest of these provided a ^{10}Be cosmogenic exposure date of 25.6 ± 3.2 ka BP (Smith, 2004a). There is stratigraphic evidence along the mountain front to the south, however, that Cordilleran ice advanced first, and retreated some distance before the continental ice reached its maximum western extent (Mathews, 1980; Bednarski, 2001; Bednarski and Smith, 2007). Moreover, there is also stratigraphic evidence that there were probably several readvances of continental ice (this study). Mathews (1963) identified two continental tills in section in the Fort St. John area and Hage (1944) identified several continental tills in wells drilled near Fort Nelson. Two distinct Laurentide tills separated by a boulder pavement were identified in section by the present author in NTS map area 94 P, northeast of Fort Nelson.

North of the study area, in Mackenzie Mountains the glacial record shows several early to late Pleistocene Cordilleran advances, but the all-time limit of the continental ice is thought to have occurred only during the last glaciation ca. 30 ka BP (Hughes, 1987; Duk-Rodkin and Hughes, 1995; Duk-Rodkin et al., 1996). In this area, the all-time Laurentide Ice Sheet limit, marked by the uppermost Canadian Shield erratics in the Mackenzie Mountains, is separated from a less extensive Laurentide margin by a system of meltwater channels and moraines. The less extensive margin is thought to be the result of a major readvance that came within 200 m in elevation of the earlier all-time Laurentide maximum at ca. 22 ka BP (Katherine Creek Phase, Duk-Rodkin and Hughes (1995)). The timing of the all-time maximum of the Laurentide Ice Sheet is contrary to the ca. 18 ka BP last glacial maximum reached by the Laurentide ice in most other areas (Dyke and Prest, 1987; Dyke et al., 2003).

According to Hughes (1987), build-up of continental ice in the region occurred prior to ca. 30 ka BP in the north, but on the Liard plain, east of the study area, the last glacial buildup of mountain glaciers occurred after a nonglacial interval that ended about 24 ka BP (Klassen, 1987). In the Fort Liard area, wood fragments between reworked till and glaciolacustrine sediment near Fisherman Lake radiocarbon dated 32.7 ka BP (I-3187, Millar (1968)), providing a maximum age for the last glaciation for the southern Liard Range. In British Columbia, about 45 km southwest of Fort Nelson, a fragment of wood recovered from gravel stratigraphically underlying till dated at 24.4 ka BP (Levson et al., 2004). In the Peace River area of northeast British Columbia, the Laurentide ice arrived sometime after 22 ka BP (Catto et al., 1996). In the Fort St. John area, a radiocarbon date on wood near the base of glacial Lake Peace sediments suggests that the Laurentide Ice Sheet retreated from the area by at least ca. 14 ka BP (TO-2742; Catto et al. (1996)). Deglaciation farther north is not well dated, but probably occurred as early as 12 ka BP in southeastern Yukon (Dyke, 1990, 2004; Lemmen et al., 1994; Dyke et al., 2003), whereas the northwesternmost part of the Laurentide Ice Sheet was undergoing retreat prior to 13 ka BP (Hughes, 1987). Dyke et al. (2003) showed that the Fort Liard area became deglaciated between 12 ka BP and 11 ka BP, but no dates on early deglaciation are available in the area. Pond sediments a few kilometres east of Fisherman Lake record continuous sedimentation since at least 9590 BP, with permafrost invading the site during the last 300–500 years (GSC-1890 and other dates, Matthews (1980)).

GLACIAL GEOMORPHOLOGY AND SURFICIAL LANDFORMS

The surficial material and landforms of the Fort Liard map area were mapped at 1:50 000 scale and presented on 16 Geological Survey of Canada Open File maps (Fig. 1). The mapping procedure consisted of airphoto interpretation followed by field checking by helicopter, truck, boat, and foot traverses during the 2000 to 2003 field seasons. Observations were recorded at 340 sites, and 64 samples of till and other surficial materials were obtained from shallow pits, natural exposures, and roadcuts throughout the study area (Fig. 5).

Sample collection and analyses

The surficial materials sampling program employed as part of this study was initially designed to characterize the regional till cover and to identify possible anomalies related to mineralization and glacial transport of heavy-mineral indicators; however, because of the scarcity of points in the some parts of the map area, statistical spatial analysis did not provide significant results. Consequently, only the general characteristics will be discussed below. The 63 bulk samples were analyzed for grain size, Atterberg limits, carbon and carbonate content, a suite of trace elements, and heavy-mineral concentrations (*see* Appendix A).

Geological Survey of Canada Sedimentology Laboratory, Ottawa measured the particle-size distributions, carbon contents, and carbonate analyses (Appendix A1). Grain size was measured by sieving and sedimentation into: more than 2 mm, sand (2 mm to 63 µm), and silt+clay (<63 µm) fractions. The silt-clay boundary was placed at 2 µm. Silt and clay fractions were determined by laser particle size analyzer (PSA, Galia Instrument) to obtain volume percentage. The sieved and PSA results are combined and calculated for weight percentage. Calcite, dolomite, and total carbonate content were analyzed by Chittick method and carbon content by the Leco method.

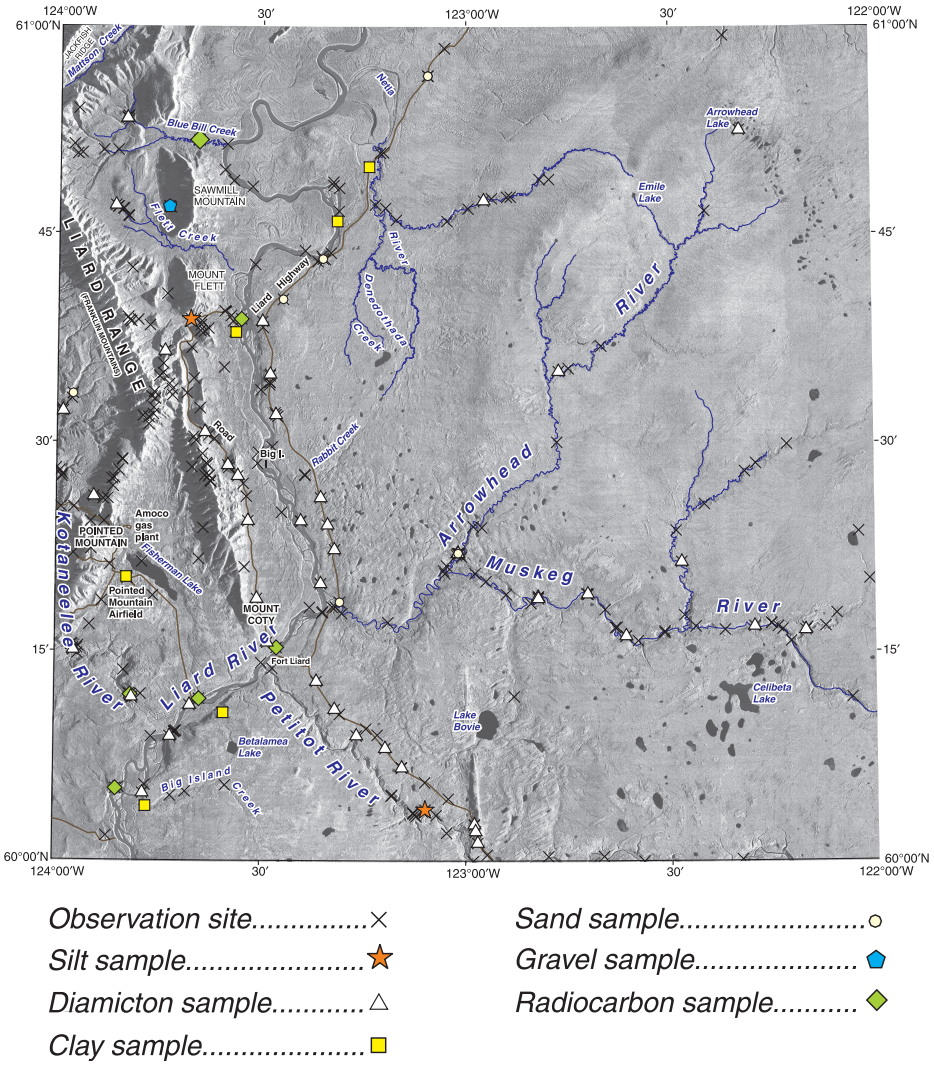

Figure 5. Locations of sample and observation sites in the study area (background map is synthetic aperture airborne radar image coloured by a Landsat overlay).

The trace elements were measured by Instrumental Neutron Activation Analysis (INAA) of the combined silt+clay fractions. The analytical precision of the INAA was assessed using laboratory duplicates. For the most part, the results are consistent, but occasional discrepancies arose when dealing with trace concentrations. Accuracy was determined by submitting a standard reference till with each batch. The INAA data are presented in Appendix A2 for all surficial materials sampled. Descriptive statistics for all the sample types combined are given in Appendix A3 and only for till samples in Appendix A4. Samples with anomalously high values are also identified in these appendices.

The 63 µm to 250 µm size fraction of 65 sediment samples were separated for ferromagnetic and heavy minerals (heavy-liquid separation, specific gravity 3.3 g/cm^3) by the GSC Sedimentology laboratory (Appendix A5). Consorminex Inc., Gatineau, Quebec analyzed the heavy-mineral fraction of the samples which were mounted in epoxy on 1 x 3 inch glass slides. A Zeiss, Stemi SR, stereoscopic microscope with polar and Nicol lenses, in conjunction with a petrographic microscope, were used to count the heavy minerals. The ribbon method was used to count 300 grains. A computer program was used to enter the data by keyboard in the same manner as a Swift blood-cell counter. Heavy-mineral counts are presented in Appendix A6.

Surficial materials mapping

The surficial geology was compiled onto 1:50 000 National Topographic Database (NTDB) digital base maps. The use of these base maps presented a problem because it was found that the positional accuracy of the maps was poor. Positional discrepancies of more than 100 m with repeated GPS (global positioning system) fixes were common. In particular, features and contours in map area 95 B/4 were more than 400 m off in several areas. Secondly, it was found that the course of Liard River has changed significantly since the NTDB maps were compiled. In contrast to the inaccuracies of the digital base maps, it was found that Landsat 7 GeoCover (orthorectified) images taken in 1991 agreed better with the GPS positions and also provided a more up-to-date position of Liard River. For these reasons, it was decided to correct the digital bases by using the GeoCover images as a datum. The GeoCover and NTDB maps were digitally overlaid and the updated course of Liard River was redigitized. Since most of the 1: 50 000 bases seemed to have a systematic error in position, it was possible to simply shift the entire digital map so that it would agree with the GeoCover image. Map area 95 B/4, however, also required extensive correction to the course of Kotaneelee River and adjacent contours. Consequently, the site locations reported here should be regarded as accurate, whereas some of the surficial geology polygon boundaries are only approximate in absolute location.

Fort Liard map area lies within the southern fringe of the discontinuous permafrost zone (Brown, 1967), where the dominant peatland landforms are peat plateaus, palsas, bogs, fens, and thermokarst features (collapse scars) (Tarnocai, 1973; Zoltai and Tarnocai, 1975). Although these features are common in the poorly drained glaciolacustrine deposits and till in the eastern part of the map area, no exposed ground ice was encountered during the course of summer fieldwork; however, Matthews (1980) reported segregated ice lenses at 150 cm depth in a bog near Fisherman Lake, and a single log from a seismic survey auger hole reported ice in gravel down to 14 m in depth, east of Arrowhead River in the east-central part of the study area. Common surface vegetation on peat plateaus includes *Sphagnum* mosses, abundant ericaceous plants, scrub birches, and open depauperate stands of black spruce (*Picea mariana*), whereas surrounding well drained sites are dominated by stands of quaking aspen (*Populus tremuloides*) (Matthews, 1980). Scattered stands of impoverished black spruce in these boggy areas are usually indicative of localized permafrost (Fig. 6).

Table 1. Areal extent of various surficial materials for the study area.

UNIT	Area (km^2)
Bedrock	620
Till and colluvial veneer	246
Till	4912
Glaciolacustrine deposit	2431
Glaciofluvial deposit	744
Colluvium	217
Lacustrine deposit	140
Alluvium	1111
Alluvial veneer	36
Alluvial terrace	203
Organic deposit	1293
Eolian deposit	<1

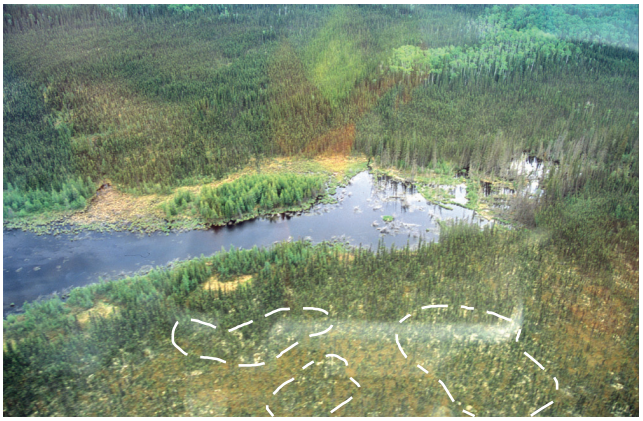

Figure 6. Bog area near Fisherman Lake. Note slumping peat along the far left of the pond and peat palsas (dashed lines; underlain by ground ice, forming islands about 30 m across in the foreground). Photograph by J.M. Bednarski. GSC 2007-215

The surficial materials of the map area, except for bedrock, are classed according to age, type of depositional environment, and genesis. The ages are broadly divided into either post–last glacial (Holocene) or Late Wisconsinan, and the depositional environments are classed into either nonglacial, glacial, or proglacial. Eight main genetic types include till, and deposits of glaciofluvial, glaciolacustrine, lacustrine, alluvial, colluvial, eolian, and organic origin (Fig. 7). No surficial materials were considered to predate the last glaciation, except for some limited exposures in sections that may relate to the advance phase of the last glaciation. Consequently, nearly all of the sediments mapped here are thought to be Late Wisconsinan and Holocene. Table 1 shows the areal coverage the main surficial materials units have in the Fort Liard map area.

Drift thickness

An estimate of the minimum glacial drift thickness overlying the central part of the map area was determined from over 2500 auger holes drilled during seismic surveys in 1970 and 1971 (Appendix B on CD-ROM). Although most of the descriptions are very general, the overburden is thought to be mostly till, gravel, and glaciolacustrine sediments. A limitation of this data set is that many of the auger holes did not penetrate the overburden completely in areas where drift thickness is deepest. Figure 8 shows isopachs of total drift thickness estimated by a natural neighbour-gridding analysis. In general, the thickest drift (>20 m) is in the floodplain of Liard River, with a maximum reported depth of 37 m, which is mostly sand and gravel. The thickest drift coincides with an area where the river begins a series of large meanders below Flett Rapids and coincides with extensive glaciofluvial delta and glaciolacustrine deposits on the surface (Fig. 7). Uplands flanking the east side of this area are

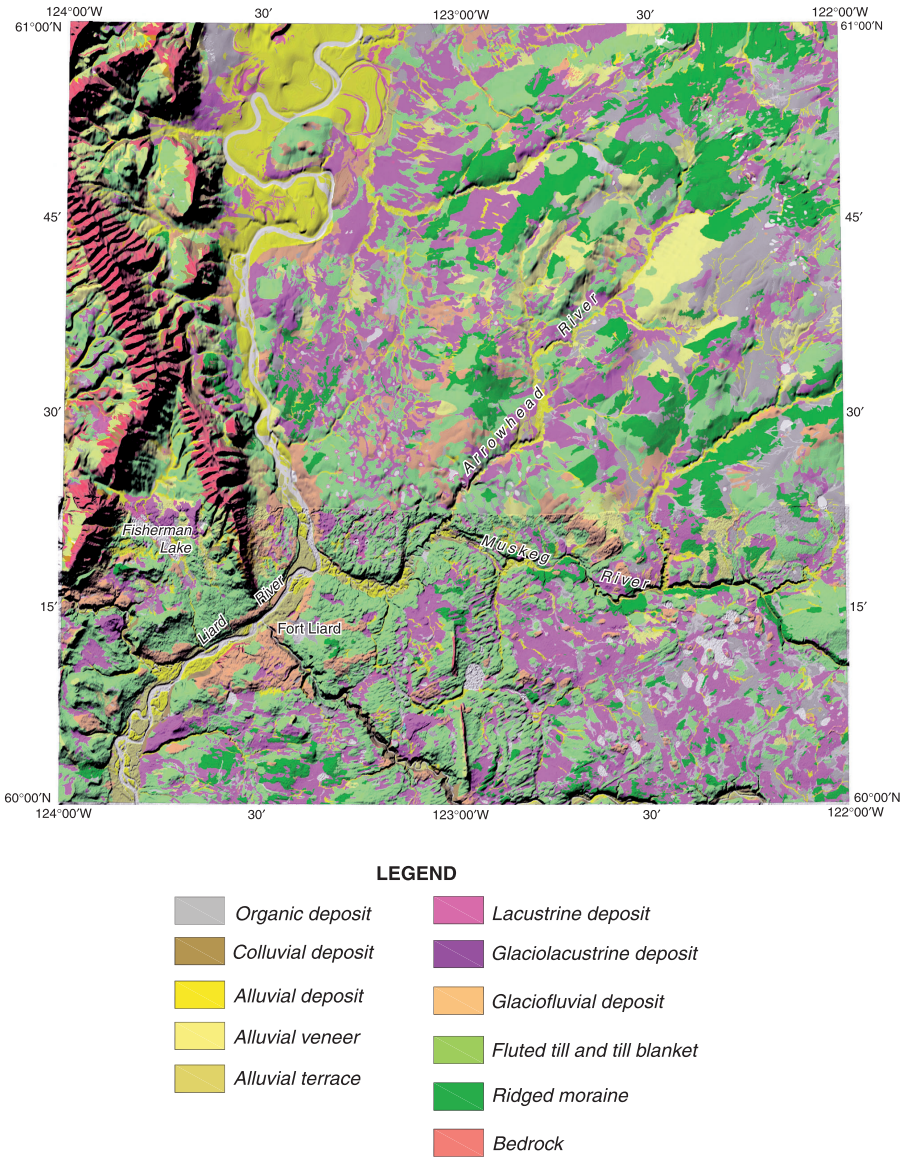

Figure 7. Surficial materials of the Fort Liard map area. Compiled from 1:50 000 scale GSC Open File maps (draped over USGS STRM30 DEM) .

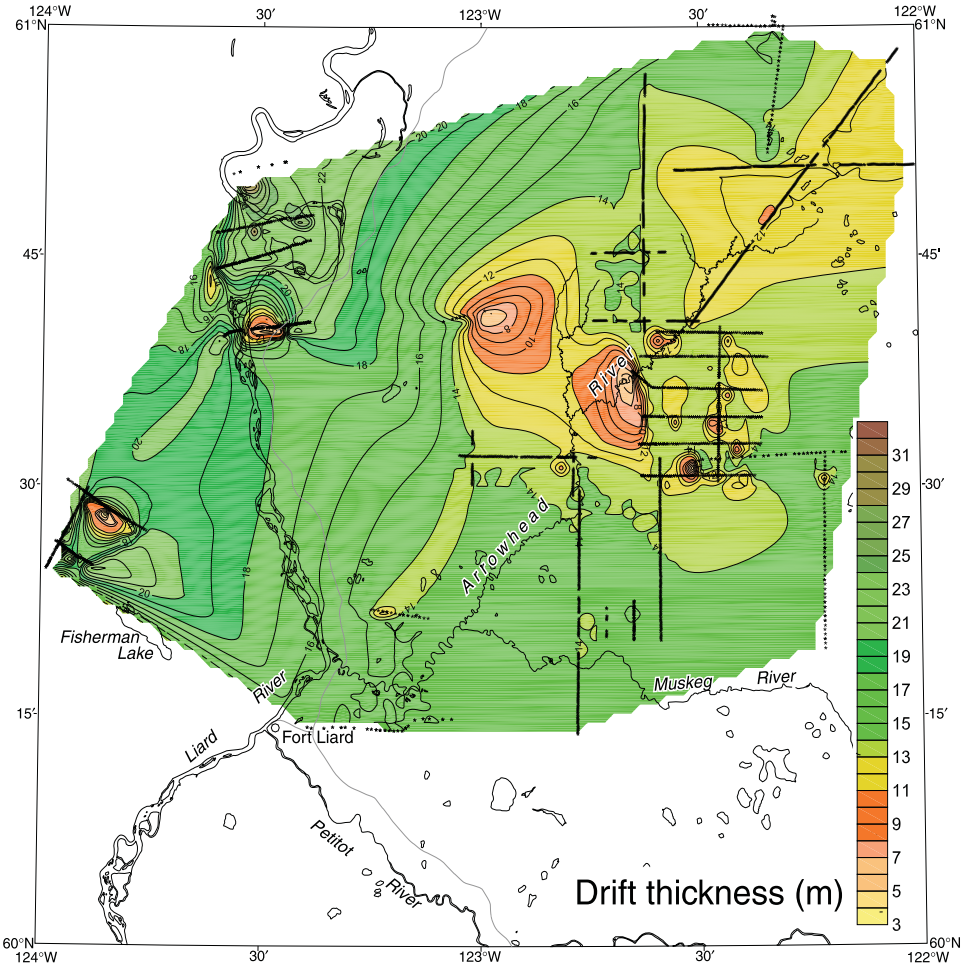

Figure 8. Approximate drift thickness (metres) over part of the study area derived from shotpoint auger holes (asterisks).

usually covered by at least 15 m of till, gravel, and lacustrine sediments. A second area of thick drift is north of Fisherman Lake. It is likely that drift thickness is much more variable than shown in the mountains west of Liard River. For example, stratigraphic sections show over 40 m of till and boulder gravel in the upper tributary valleys of Blue Bill Creek.

Drift is thinnest over the uplands between Liard and Arrowhead rivers, where it thins to less than 6 m. In the eastern parts, south of Arrowhead River, most of the auger holes in this area did not penetrate to bedrock, and therefore a minimum thickness of 15 m is indicated. Likewise, the area north of Muskeg River is mantled by at least 15 m of drift. The drift is composed of clay and rock underlain by up to 10 m of gravel and sand layers. Similar stratigraphy is exposed along 75 m high cliffs near the confluence of the Arrowhead and Muskeg rivers where gravel and sand underlies till.

Stratigraphy

Over ninety stratigraphic exposures were logged in the map area. The general Quaternary stratigraphy is depicted in Figures 9, 10, 11, and 12, with more detailed descriptions in Appendix C (on CD-ROM). Additional stratigraphic information is provided by the auger-hole data (Appendix B). The general stratigraphy of the study area can be divided into four general categories: stratified sediments found beneath glacial diamictons, glacial diamictons, glaciofluvial and glaciolacustrine deposits related to the retreat of the ice sheet, and Holocene sediments typically related to modern fluvial processes.

Stratified deposits that underlie till from the last glaciation were found in several exposures. The basal sediments range from very coarse gravel to fine silt and clay. Stratigraphically, these sediments are probably the oldest Quaternary deposits identified in the area, but they are not considered preglacial because they contain Canadian Shield clasts, implying distant transport from the east by glaciers. Based on the descriptions, several auger-hole logs also note gravel units interbedded with till-like sediments (Appendix B). For example, auger-hole data shows an area about 10 km north of Muskeg River that has at least 15 m of “clay and rock” diamicton underlain by up to 10 m of gravel and sand. Auger data also shows that the northern part of Liard River floodplain is typically underlain by 23 m of sand, gravel, and clay, and a line running east from the Mount Flett airfield reports 16 m of gravel overlying 7 m of clay. The auger data, however, do not record whether the lower units contain granite erratics.

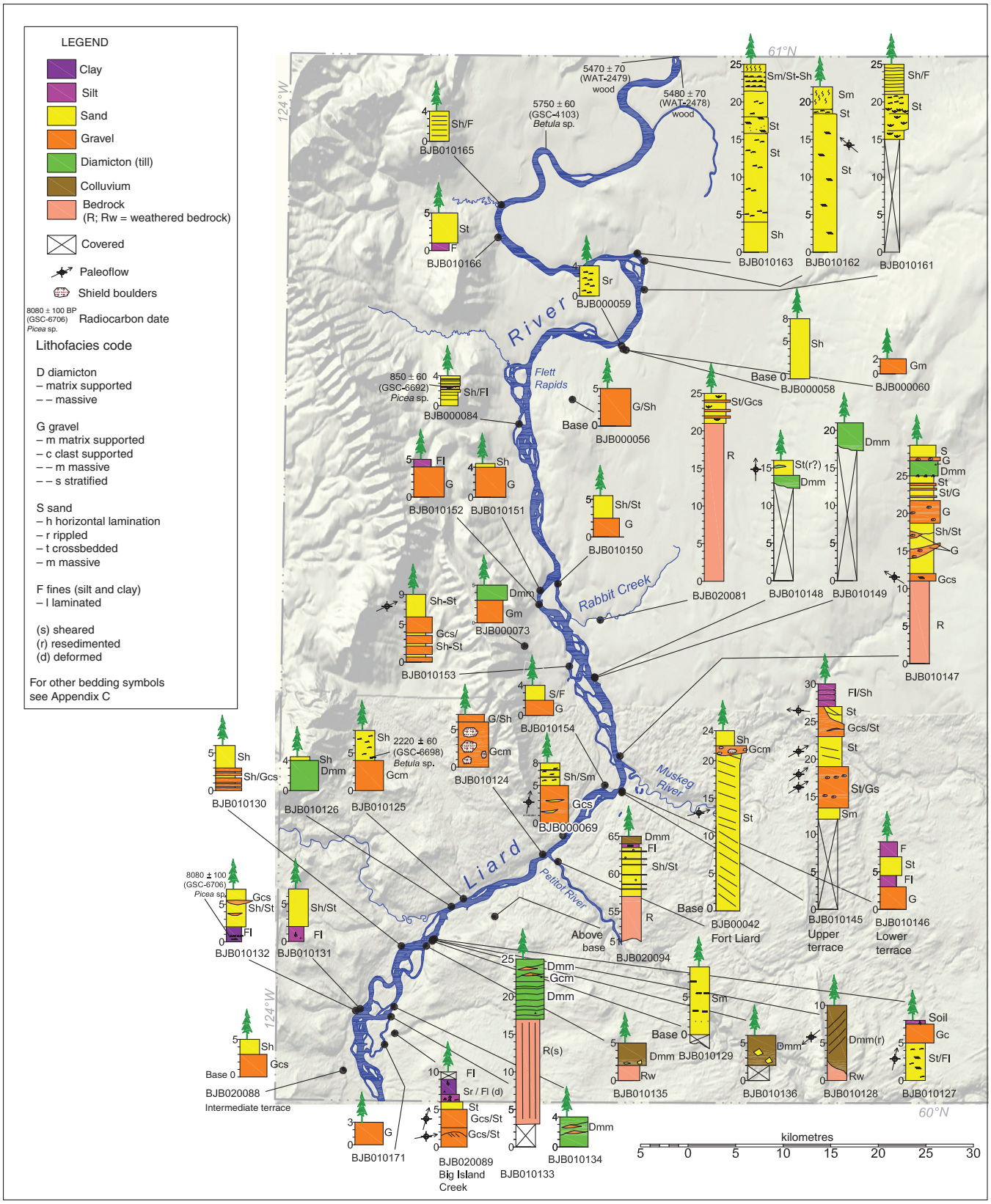

Figure 9. Major stratigraphic sections along Liard River. All elevations are in metres above the river level unless otherwise stated. More detailed descriptions of each section is found in Appendix C. Radiocarbon dates GSC-4103, WAT-2478, and WAT-2479 are from Piët (1992). / = interbedded units, - = mix of sediment types.

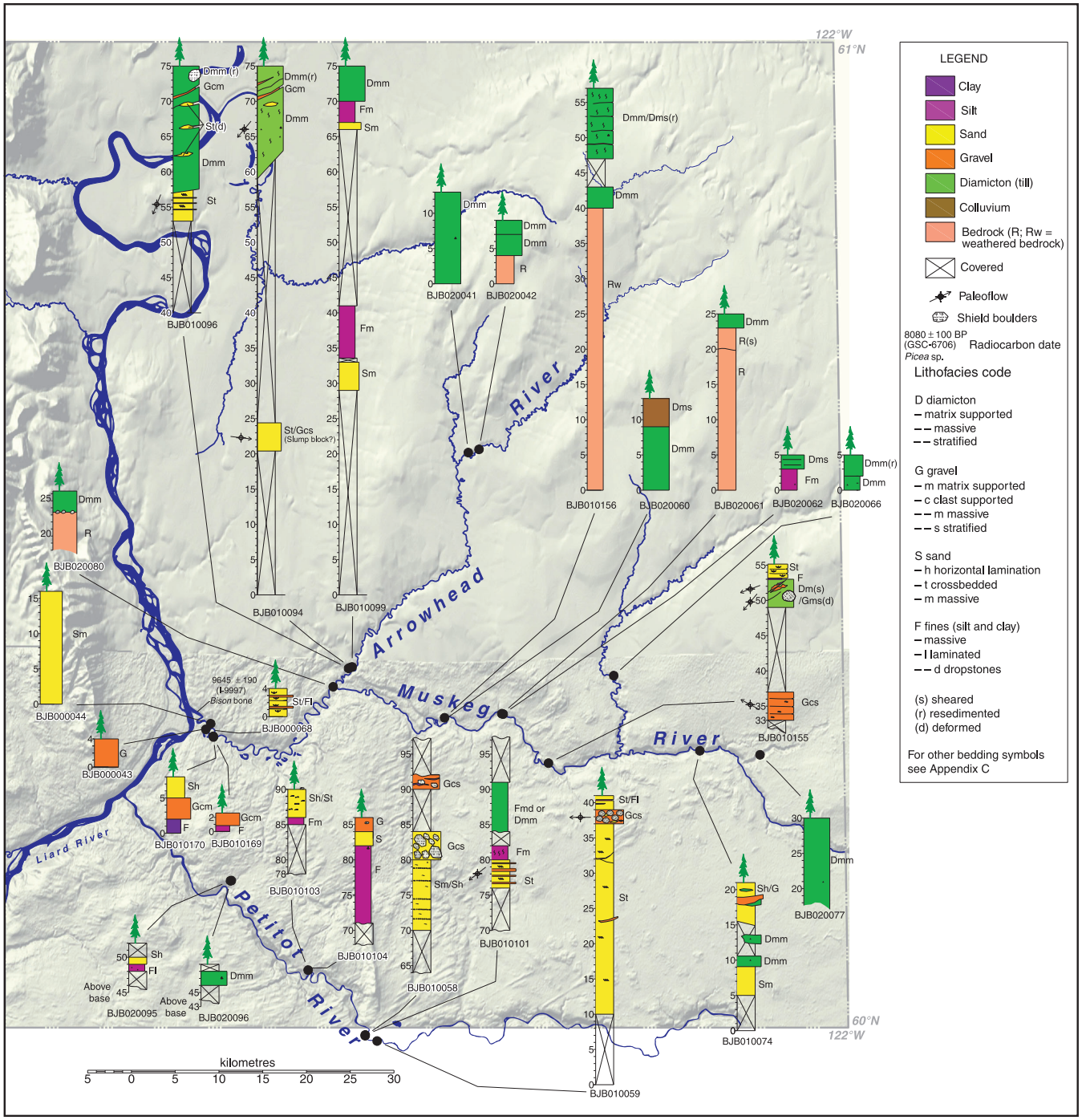

Figure 10. Major stratigraphic sections along the Petitot, Muskeg, and Arrowhead rivers. All elevations are in metres above the river level unless otherwise stated. More detailed descriptions of each section is in Appendix C. Radiocarbon date I-9997 is from Harington (2003). / = interbedded units

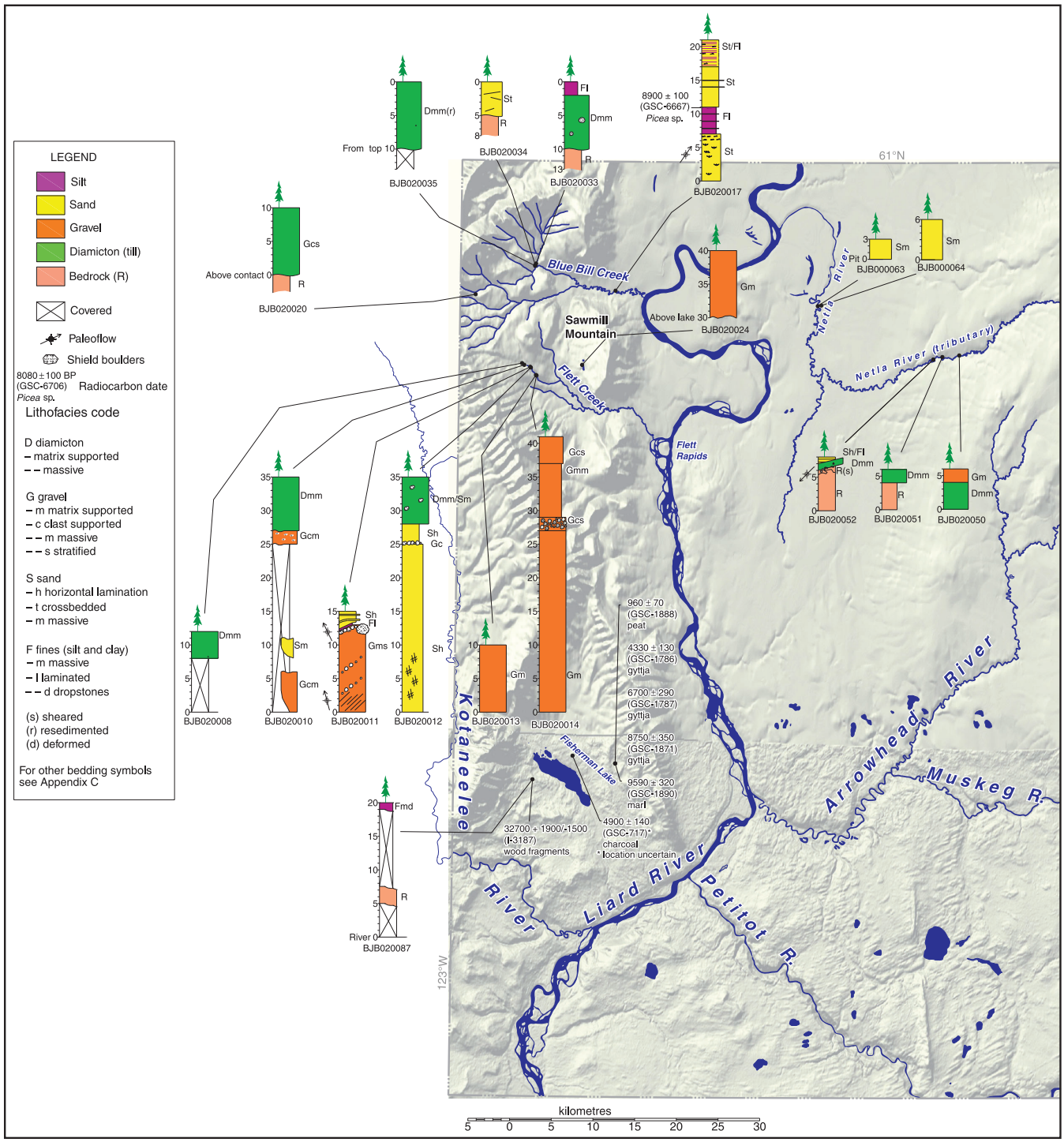

Figure 11. Major stratigraphic sections along various northern creeks and Fisherman Lake. All elevations are in metres above the river level unless otherwise stated. More detailed descriptions of each section are in Appendix C. Radiocarbon ages northeast of Fisherman Lake are from cores in 'John Klondike Bog' (informal name; Matthews (1980)). Date I-3187, near Fisherman Lake is from Millar (1968). There are numerous other radiocarbon dates on bone and charcoal from the Fisherman Lake area, related archeological investigations. These dates range from mid- to late Holocene. / = interbedded units

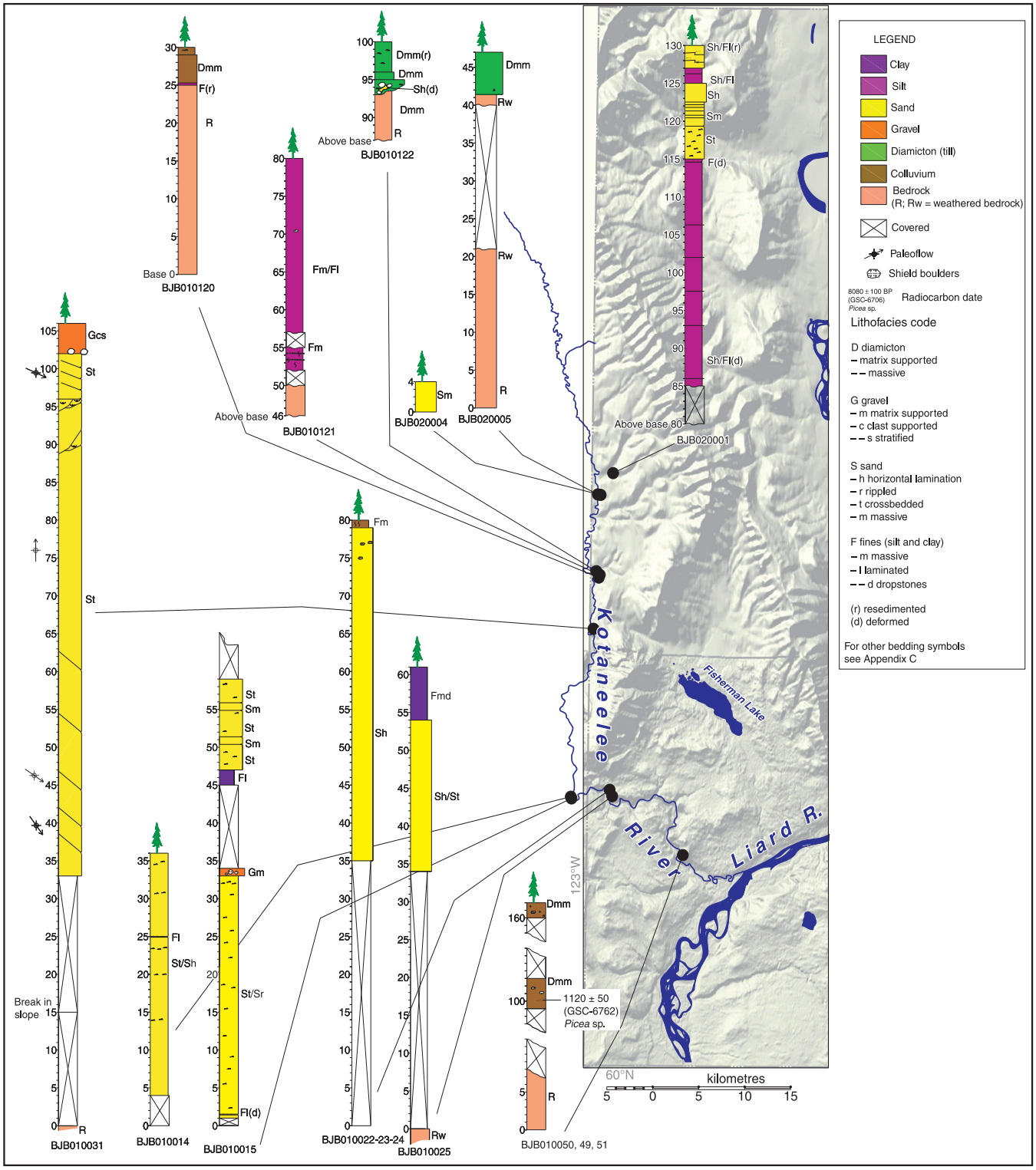

Figure 12. Major stratigraphic sections along Kotaneelee River. Elevations are in metres above the river level unless otherwise stated. More detailed descriptions of each section are in Appendix C. / = interbedded units

Stratified basal sediments that were examined in natural exposures were probably deposited in proglacial environments as the continental ice approached, either as outwash gravel or as silt and clay into ice-dammed lakes. Until contrary data is found, it is assumed that these sediments probably date from the last glaciation when the Laurentide Ice Sheet advanced from the northeast and blocked the regional drainage. With the exception of a lower sand and gravel layer in a section along Arrowhead River (Fig. 10), all the paleocurrent indicators in the gravel below till show a westward component to the flow, similar to the subsequent ice-flow direction. For example, basal gravel along the Petitot and Muskeg rivers, east of the mountains, show paleoflows to the southwest and northwest, respectively (Fig. 10). These flows are in the same direction as the modern drainage into Liard River, but basal gravel beds along a tributary to Flett Creek, within the mountain front, show paleoflows counter to the modern drainage (Fig. 11). In this case, very coarse gravel with northwest-dipping foreset beds dip upslope and could only have been deposited close to the glacial margin when the main valley to the east was occupied by ice. This marks a lobe of the Laurentide Ice Sheet that penetrated into the Liard Range, and implies that the slopes to the west were free of montane ice at this time. The incursion of Laurentide ice into the mountains is further documented by the regional flow pattern of the surface till and the mountain-ridge striations (discussed below). Thick glaciolacustrine sediments are found along upper Kotaneelee River, west of Liard Range, but it is not clear whether these sediments relate to the advance or retreat phase of glaciation (Fig. 12). Conversely, nearly all the exposures of glaciofluvial and glaciolacustrine deposits along Liard River appear to be either retreat phase or postglacial, and related to stages of glacial Lake Liard (Fig. 9). An exception is a site near the confluence of the Muskeg and Liard rivers (BJB010147; Fig. 9), where gravel occurs both under and above till.

Most of the glacial diamicton in the study area is regarded as till, the product of direct glacial deposition. Many of the tills found in stratigraphic sections in the study area comprise the uppermost unit and correspond to the surface till that was extensively moulded during the last glaciation (*see* 'Till and till landforms'). The till is typically an indurated diamicton with a calcareous, clayey, grey-brown matrix, but it tends to be stonier within the mountains east of Liard River than on the plains. In several places the till exposed in stratigraphic sections is not homogeneous, but comprises several distinct layers. This is especially evident along 75 m high cliffs near the confluence of the Arrowhead and Muskeg rivers and in exposures along Muskeg River farther upstream (Fig. 10; Appendix C) where distinct till sheets are separated by shear planes or intercalated with discontinuous layers of sand, gravel, and minor silt and clay. The sorted units are deformed in places, suggesting ice thrusting and dragging associated with the formation of shear planes (Fig. 13). This shearing and stacking of the till is likely to have occurred with compressive flow near the ice margin during minor readvances. Instability along the ice margin in this area may have been enhanced by the presence of glacial Lake Liard immediately to the west.

Several natural exposures in the study area contain diamictons that resemble till, but show signs of resedimentation in the form of interbeds of clay or thin gravel layers. For example, along Kotaneelee River (Fig. 12) the steep valley sides are underlain by shale and it is clear that recent slumping has occurred. At one site (BJB010050; Fig. 12) a radiocarbon date on enclosed wood confirms that the deposit is late Holocene colluvium. Other sites, however, show evidence that the till was resedimented during, or shortly after, deposition. For example, on the east side of Liard River (BJB010133; Fig. 9), recent fluvial erosion exposed a 15 m outcrop of Cretaceous sandstone (Dunvegan Formation) that was thrust by glacial ice so that its beds are nearly vertical. The sandstone is capped by 8 m of clayey grey diamicton. The upper 3 m of the diamicton appears to be in situ till, containing granite boulders, but the lower part contains pieces of lignite and is composed of layers, about 50 cm thick, interbedded by lenses of massive gravel. This stratigraphy is interpreted as subglacial slumping into a cavity beneath the advancing ice sheet. The fact that the former cavity coincides with the edge of the Cretaceous upland, which defines the Liard River valley, suggests that a valley with a similar orientation existed before the last glaciation. Adjacent sections along the east side of the river show 3–4 m of the upper till unit, but with many eroded sandstone blocks incorporated near the base.

A third type of glacial diamicton is represented in a section along Muskeg River (site BJB020062; Fig. 10), which is interpreted as glaciolacustrine in origin. Shale exposed just at the base of the section is conformably overlain by 3 m of massive indurated clay, silt, and fine sand. The lower unit is noncalcareous and contains a few weathered clasts near the base that may be dropstones. A planar erosional contact separates the lower unit with a calcareous upper unit composed of horizontally stratified clay, silt, and a few thin lenses of gravel. Although this 2 m thick unit is obviously stratified, a dispersal of clasts throughout it suggests that it may be glaciolacustrine in origin.

Sorted gravel, sand, and fines that are stratigraphically younger than till are found along most of the major rivers in the study area. These sediments were deposited as proglacial outwash, as deltas, or as glaciolacustrine fines into ice-dammed lakes. The depositional environment was similar to the advance-phase stratified sediments underlying the tills, but this time they relate to the retreat phase of the Laurentide Ice Sheet. During early retreat phase, the Laurentide Ice Sheet blocked the mouths of valleys exiting the mountains and produced high-level lakes above 400 m a.s.l. At this time tens of metres of stratified sand and fines were deposited within Kotaneelee River valley and its tributaries (Fig. 12), as well as the basin surrounding Fisherman Lake (Fig. 11). Early glacial lakes would have formed in Blue Bill and Flett creeks, which are also recorded in stratigraphic sections

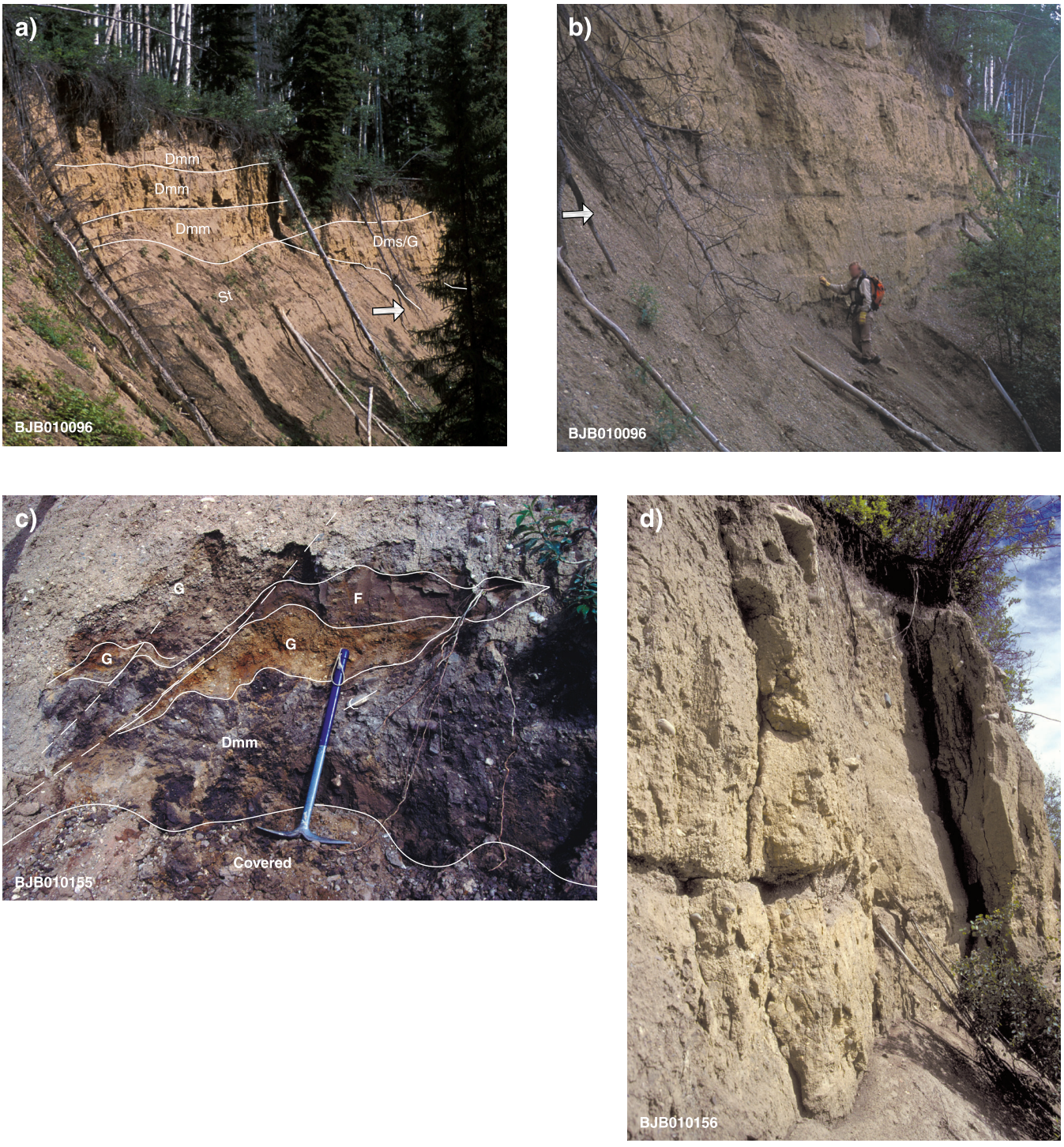

Figure 13. Examples of layered and sheared tills exposed along the Muskeg and Arrowhead rivers. **a)** Three distinct layers of till (Dmm) separated by thin bodies of sand. The till layers, which are each about 1–2 m thick, overlie 10 m of stratified sand and granular gravel (St). The far end of the exposure shows interbedded gravelly diamicton and gravel (Dms). The arrow provides a reference point for Figure 13b. Photograph by J.M. Bednarski. GSC 2007-216. **b)** A closer view of the gravelly diamicton and gravel. Person is approximately 177 cm. Photograph by J.M. Bednarski. GSC 2007-207. **c)** Shear planes (dashed lines) in till (Dmm) incorporating gravel (G) and clay (F). Note striated clasts that are embedded in the lower till. Direction of shear and striations is approximately orthogonal to a series of ridges in the area. Pick handle is 65 cm long. Photograph by J.M. Bednarski. GSC 2007-210. **d)** Indurated layers of till, 2 m thick, separated by a thin layer of pebbly gravel. Site locations are in Figure 10. The lower vertical layer of till is 2 m thick. Photograph by J.M. Bednarski. GSC 2007-212.

(Fig. 11). At a later stage of ice retreat when Liard River valley became ice-free, extensive gravel and sand were deposited into glacial Lake Liard, a lake that formed when the main northeastern drainage to the Mackenzie River was still blocked by the ice sheet. These sediments are now exposed along the banks of Liard River in terraces up to 30 m above the river (Fig. 9). Delta foreset beds near Fort Liard mark a prominent level of glacial Lake Liard at about 254 m a.s.l. (site BJB00042; Fig. 9). Progradation into the lake is also recorded farther downstream in sections near the confluence of Liard and Muskeg rivers, however, between the mouths of Muskeg River and Rabbit Creek, the stratigraphy also shows gravel deposition during advance of the ice margin (Fig. 9).

Extensive cliffs of well sorted, current-bedded sand, up to 25 m thick, are exposed along a large meander of Liard River in the northern part of the map area just downstream of Flett Rapids (Fig. 9). These sand units are thought to represent rapid sedimentation into glacial Lake Liard when the lake was at least 220 m a.s.l. The sand deposit probably extends over 10 km northward, underlying a shallow trough that joins two large bends in the river. The sand deposit was preserved when Liard River flowed westward around a prominent hill of more resistant material. The hill may be underlain by bedrock, but none is visible at the surface and auger data from the western edge of the hill record detrital shale from 11 m to 23 m below the surface (Appendix B). As noted previously, auger data from just northeast of here show that Liard River floodplain is typically underlain by 20 m of sand and gravel, with a maximum of at least 37 m; however, the stratigraphic age of this sediment cannot be determined from the auger data.

The age of glacial Lake Liard is not well constrained in the study area. As noted earlier, the study area was deglaciated between 12 ka BP and 11 ka BP, with continuous pond sedimentation near Fisherman Lake since at least 9590 BP (Table 2; Mathews (1980)). Two radiocarbon ages on detrital logs hint that remnants of former glacial Lake Liard persisted well into the Holocene. In the southern part of the study area, several sections show rhythmically bedded clay beds, which were likely deposited into glacial Lake Liard, at various elevations to at least 240 m a.s.l., about 9 m above the modern Liard River (e.g. site BJB020089; Fig. 9). On the west bank of the river, however, laminated clay layers are also exposed underlying gravel near the water. These clay beds may relate to a late phase of glacial Lake Liard, but a log extracted from the clay, exposed about 1 m above the river, radiocarbon dated 8080 ± 100 BP (GSC-6706), a time when the margin of the Laurentide Ice Sheet was hundreds of kilometres to the northeast (Dyke et al., 2003).

A second radiocarbon date that constrains that age of glacial Lake Liard in the study area comes from Blue Bill Creek in the northwest (site BJB020017; Fig. 11). Here, the creek exposed a 21 m section: almost 7 m of trough-crossbedded sand at the base, which is overlain by 4 m of laminated clayey silt, and then, another 10 m of stratified sand with pebbly layers. The uppermost stratified sand fines upward and interbeds with silt. The upper part of the middle clayey unit has a 40 cm thick layer of wood detritus from which a *Picea* sp. log radiocarbon dated 8900 ± 100 BP (GSC-6667). The basal sand exposed in this section is probably equivalent to the extensive deltaic sand exposed along Liard River, 20 km to the east (Fig. 9), and therefore should date from the time of glacial Lake Liard. The middle layer, however, was deposited some time after that because a planar contact separates the two units, implying a hiatus. Nonetheless, it is apparent that the clayey unit was deposited in a body of water and that the body of water existed prior to 8900 BP. Perhaps it was a remnant of glacial Lake Liard.

The last group of deposits shown in the stratigraphy of the study area relate to Holocene sedimentation during postglacial time. The watersheds became free of glaciers and fluvial processes began to dominate. It is likely that overall sedimentation was greatly reduced, but local accumulations of landslide debris and other colluvium remained significant. Fluvial sedimentation was especially prevalent along Liard River where pulses of terrace building followed initial valley incision. Alluvial terraces, usually about 3–4 m above the present river are common in the map area. Riverbank exposures typically show cobbly gravel overlain by rhythmically bedded silt and fine sand. Above Flett Rapids, reaches of Liard River are braided, but below the rapids Liard River is a meandering river dominated by sandy point-bar deposits (Piët, 1992).

Till and till landforms

Till (glacial diamicton) thick enough to completely mask underlying bedrock covers about 41% of the map area. Clayey till forms an almost continuous blanket on the plains east of Liard River, and probably underlies most of the other surficial materials where it is not continuously exposed. Till greater than 2 m thick covers most of the valley bottoms and some more gentle mountain flanks west of Liard River, but higher mountain slopes have only a discontinuous till veneer, typically less than 1 m thick. Small patches of till also occur in mountainous areas that were mapped as bedrock. The characteristics of till units in the map area ranges from bouldery, with very sandy textures, which is more common in the mountains, to a clay-rich matrix with few larger clasts, which is more prevalent on the plains (Fig. 14). All the till in the area contains distinctive erratics transported from the Canadian Shield.

In the map area, the till map unit was subdivided according to its surface expression and implied genesis. For example, ridges of till are found as morainal, crevasse-fill, and glacially moulded landforms. Glacially moulded and elongated landforms (flutings and drumlinoid ridges) are widespread on the plains east of Liard Range (unit Td on the Open File maps; Fig. 15, 16). Some of these ice-flow features are found in isolation, but more often they occur in swarms as parallel ridges and furrows extending for tens of

Table 2. Radiocarbon dates for the study area.

Lab. no.	Material	NTS	UTMX	UTMY	Latitude	Longitude	Elevation (m)	Uncorrected age	del ^{13}C	Normalized Age (a)	Comments	References
I-3187	Wood fragments	95 B/5	454378	6689414	60.3387°	123.8264°	400	32 700	—	32 700	Maximum date on last glaciation	Millar, 1968
GSC-1890	Marl, basal	95 B/5	464224	6691304	60.3567°	123.6467°	460	9590 ± 320	-0.06	9990 ± 320	John Klondike bog, basal date	Matthews, 1980
I-9997	*Bison* (sp.) cranial frag.	95 B/6	481504	6687279	60.3216°	123.3349°	~230	9565 ± 190	-20	9645 ± 190	Minimum date of deglaciation	Harington, 2003
GSC-6667	*Picea* (sp.)	95 B/13	464276	6747602	60.8621°	123.6577°	198	8880 ±100	-23.57	8900 ± 100	Minimum date of treeline advance	This publication
Gak-1275	Charcoal	95 B/5	453939	6692533	60.37°	123.83°	?	8720 ± 190	-25	8720 ± 190	From archeological site	Kigoshi et al., 1969
GSC-1871	Gyttja	95 B/5	464224	6691304	60.3567°	123.6467°	460	8750 ± 350	-28.3	8700 ± 350	John Klondike bog	Matthews, 1980
GSC-6706	*Picea* (sp.)	95 B/4	452771	6661261	60.0857°	123.8489°	220	8080 ± 100	-24.93	8080 ± 100	Date on glaciolacustrine deposits	This publication
GSC-1787	Gyttja	95 B/5	464224	6691304	60.3567°	123.6467°	460	6700 ± 290	-27.8	6660 ± 290	John Klondike bog	Matthews, 1980
GSC-4103	*Betula* (sp.)	95 C/15	472726	6753101	60.91°	123.5°	190	5810 ± 60	-28.5	5750 ± 60	Sandy point-bar deposit	McNeely and McCuaig, 1991; Piët, 1992
WAT-2478	Wood	95 B/14	486881	6762447	60.9967°	123.2425°	~175	—	—	5480 ± 70	Laminated silt	Piët, 1992
WAT-2479	Wood	95 G/3	486762	6762816	61°	123.2447°	~175	—	—	5470 ± 70	Sandy point-bar deposit	Piët, 1992
GSC- 717	Wood, charcoal	95 B/5	458493	6688765	60.333°	123.75°	~365	4900 ± 140	—	—	Overlying glaciolacustrine clay*	McNeely, 1989
GSC-1786	Gyttja	95 B/5	464224	6691304	60.3567°	123.6467°	460	4330 ± 130	-25.5	4320 ± 130	John Klondike bog	Matthews, 1980
GSC- 844	Charcoal	95 B/5	453939	6692533	60.37°°	123.83°	?	2460 ± 160	—	—	Archeological site, hearth*	Lowdon et al., 1970
GSC-1033	Charcoal	95 B/5	453939	6692533	60.3667°	123.8333°	?	2390 ± 130	-23.1	2420 ± 130	Archeological site, hearth*	Lowdon et al., 1970
GSC-6698	*Betula* (sp.)	95 B/4	464058	6673135	60.1935°	123.8489°	210	2220 ± 60	-25.41	2220 ± .60	Liard River aggradation, flood event	This publication
GSC-6762	*Picea* (sp.)	95 B/4	454797	6673740	60.0857°	123.8489°	350	1140 ± 50	-26.35	1120 ± 50	Age of landslide	This publication
GSC-1888	Peat (*Carex*)	95 B/5	464224	6691304	60.3567°	123.6467°	460	960 ± 70	-26.5	930 ± 70	John Klondike bog	Matthews, 1980
GSC-6692	*Picea* (sp.)	95 B/12	469887	6723704	60.648°	123.5507°	190	850 ± 60	-25.16	850 ± 60	Liard River aggradation, flood event	This publication
GSC-846	*Picea* (sp.)	95 B/5	453939	6692533	60.37°	123.83°	?	420 ± 140	—	—	From archeological site*	Lowdon et al., 1970

I = Teledyne Isotopes, Brown Engineering, U.S.A.
GSC= Geological Survey of Canada
GaK = Gakushuin University, Japan
WAT = Waterloo University, Canada
*Location approximate
? unknown
— no data

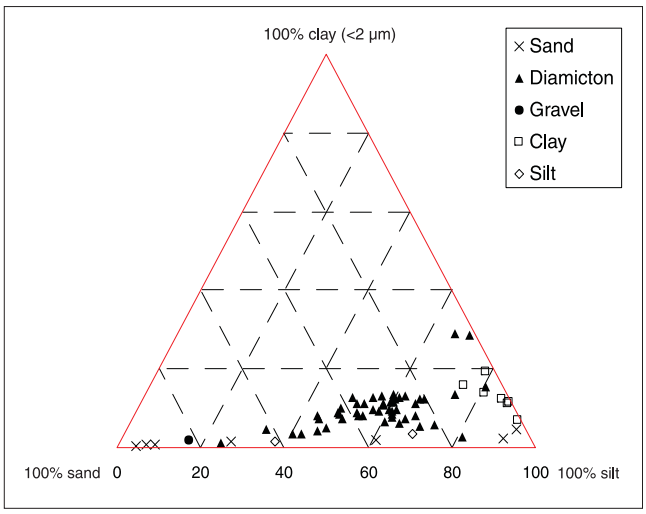

Figure 14. Measured ratios of sand, silt, and clay for various surficial materials in the Fort Liard area.

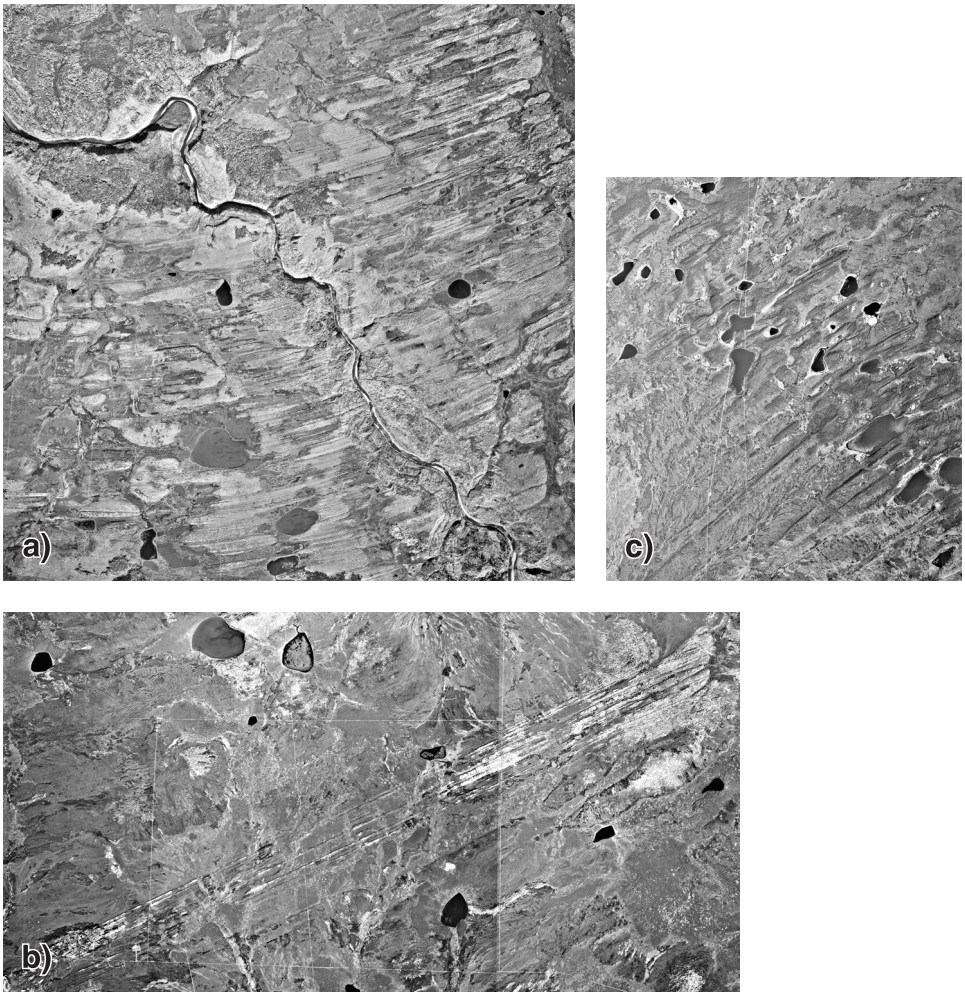

Figure 15. a) Finely spaced drumlins, flutings, and grooves following a curving path on either side of Petitot River. The flow was from the right to the left (NAPL A17442-109). **b)** Accumulations of till at the edge of an upland, probably an end moraine that has been streamlined to the southwest by overriding ice (NAPL A17439-57). **c)** Remarkably straight flutings stretching for 15 km downstream from a low hill east of Celibeta Lake (NAPL A17442-48, 49). Locations of airphotos and scale are shown in Figure 16.

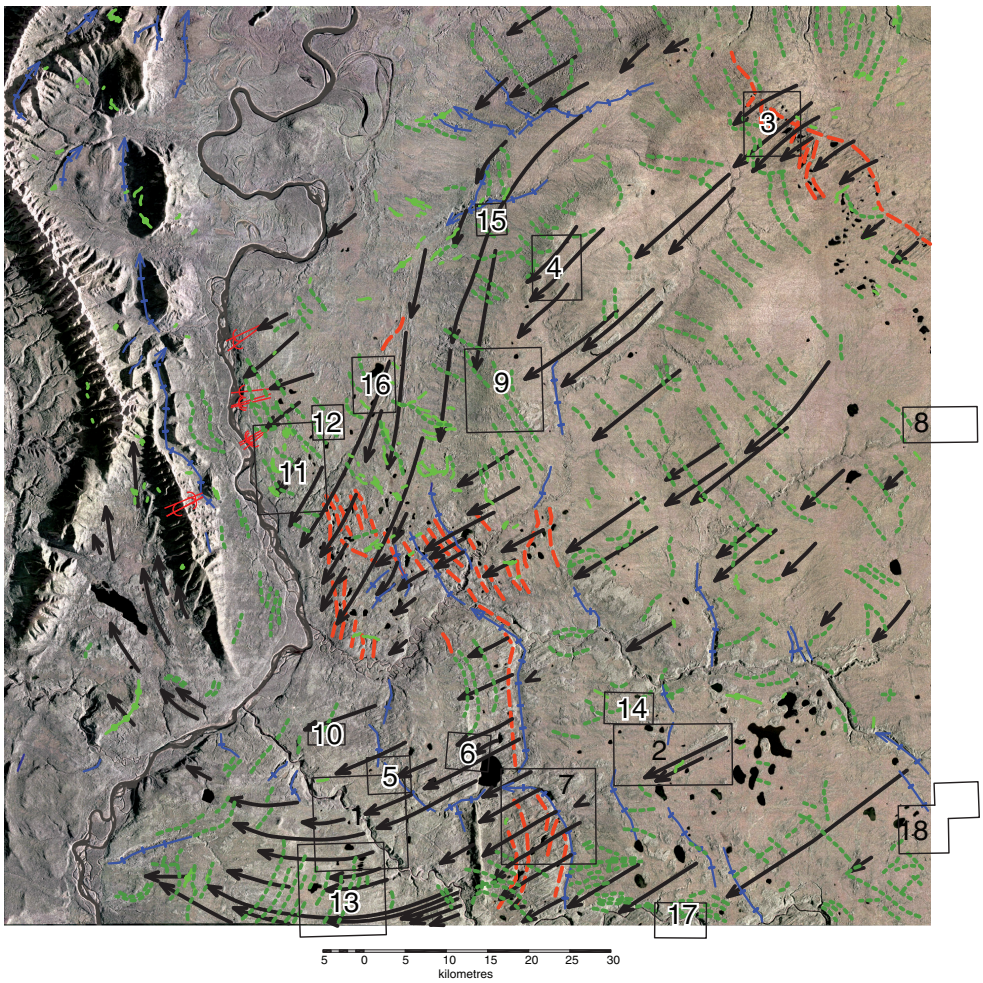

Figure 16. Patterns of former ice flow (arrows), striations on bedrock (symbol), and ice-marginal retreat (dashed green lines) in the study area. Some larger moraines (green), meltwater channels (blue), and overridden moraines (red) are also indicated.

1 = Figure 15a,
2 = Figure 15b,
3 = Figure 15c,
4 = Figure 17a,
5 = Figure 17b,
6 = Figure 17c,
7 = Figure 17d,
8 = Figure 18a,
9 = Figure 18b,
10 = Figure 18c,
11 = Figure 18d,
12 = Figure 18e,
13 = Figure 18f,
14 = Figure 18g,
15 = Figure 20a,
16 = Figure 20b,
17 = Figure 20c,
18 = Figure 20d.

kilometres. Individual features are commonly a few tens of metres wide and can extend unbroken for over 10 km. Some ridges or furrows are remarkably straight over distances of 15 km. Other flutings follow smooth curves with a radius of about 25 km. Collectively, these features formed parallel to glacial flow and hence record distinct flow events that took place during continental glaciation. It is assumed that ice-moulded features that form a single coherent pattern are likely to be contemporaneous, and hence mark a discrete interval of glacial flow during glaciation.

The provenance of Canadian Shield erratics and regional patterns of flutings show that the Laurentide Ice Sheet flowed into the area from the northeast. Nevertheless, major shifts occurred as the continental ice approached the Liard Range (Fig. 16) and ice was channelled southward down Liard River valley, which is expressed by extensive glacial flutings along the eastern side of the valley. This zone of southward flow extends for about 75 km and appears to be contained within a lowland that lies about 200 m below the uplands to the east where the northeast flow is preserved. Just north of Muskeg River, these south-trending flutings converge with the regional southwest flow pattern. The zone of convergence is marked by stubbier streamlined or complex landforms. In places, overlapping relationships suggest that the southern flow within Liard River valley is younger, but in most areas the converging flows appear to have an interference pattern, suggesting that they were contemporaneous. Farther north, on the east side of the Liard River, there is a secondary southwest flow recorded by flutings and striations on outcrops of limestone (Lower Carboniferous, Flett Formation) along road cuts. This flow is thought to date from local deglaciation when the eastern flank of Liard Range was becoming ice-free (Fig. 16).

A second major shift from the regional southwest ice flow occurs on the south side of Petitot River where the flow features curve gradually from southwest to west, and then sharply to the northwest over the Fisherman Lake area. The ice flowed up the mountain slopes across the Liard Range and northward into the Kotaneelee River valley. Well preserved glacial striae on a ridge crest at 1200 m a.s.l., show that this ice flow extended northward between Kotaneelee and Liard ranges (Fig. 16). This diversion was caused by the Laurentide Ice Sheet colliding with eastward-flowing Cordilleran ice farther west. The ice sheets accumulated along the contact zone until they were sufficiently thick to flow northward.

Glacial striae also occur on sandstone outcrops along the crest of the southeastern arm of Liard Range at about 1120 m a.s.l. (Fig. 16). Generally, the outcrops along the crest are very weathered and only a general east-northeast trend to the striae could be determined, without any sense of ice-flow direction. This general trend is similar to the trends found on the plains to the east. Consequently, a logical interpretation would be that the ridge crests were eroded by thick Laurentide ice as it flowed up and over Liard Range. Nonetheless, this simple model is probably wrong because one site shows that the striae were eroded by ice flowing toward the east-northeast. Consequently, two possibilities exist. Either the striae were produced by the same tongue of Laurentide ice that flowed northward over Fisherman Lake (described in the previous paragraph), or the striae record an older Cordilleran ice advance emanating from the west.

Fluting fields usually start along the stoss edge of uplands or topographic protuberances and stream down-ice for kilometres. This is particularly clear where linear obstructions were oriented obliquely to ice flow — an orientation that would have enhanced stress at the glacier bed and led to accelerated bed erosion and till deformation. In several places where the ice flow crossed valleys, it is evident that the downglacier side of the valley was also an obstruction to flow because flutings stream from some valley edges. From this, it can be deduced that these valleys existed prior to being overridden by the ice. Large parts of Petitot River valley, for example, probably predate the last glaciation, because the southern edge of the valley is commonly fluted. The rims of some north-trending meltwater channels on Liard plain are fluted, which also suggests that the channels were extant prior to being overridden by ice (Fig. 17). This suggests that these channels may have been part of a preglacial drainage pattern that is now partially obscured. Alternatively, either they may be meltwater channels formed during deglaciation that were overridden by a minor glacial readvance, or they may have been subglacial conduits formed during the last glaciation. If subglacial, some parts of the channels could also have been used by subaerial meltwater during deglaciation. Currently, some segments of these channels are occupied by rivers, but many are discontinuous and in places completely infilled with glacial sediment.

In addition to till landforms elongated in the direction of glacial flow, Liard plain is also covered by numerous ridges of till oriented transversely to the former ice flow (unit Tr on the Open File maps). These narrow ridges are usually made up of short segments that can be traced for several kilometres (Fig. 16, 18). Their relief is usually less than 3 m, but in some boggy places they are only recognizable on airphotos by changes in patterns of vegetation that are probably caused by subtle differences in soil moisture regimes. Successive ridges are usually subparallel and closely spaced (~150 m), but some crosscut each other in a rhomboid pattern. Although all the features mapped as unit Tr are similar in form, it is unlikely that all of these transverse ridges have the same genesis. In some places where the ridges are repetitive, they have a similar appearance to areas of 'corrugated ground moraine' in the southern Prairies (cf. Prest, 1983). Corrugated ground moraine is though to delineate the former position of marginal lobes, but not necessarily the ice terminus itself. The subglacial shearing implied may have been caused by surges along some margins of the retreating ice sheet. In fact, several of the landform associations mapped in the Fort Liard area are similar to ones left by surges in Icelandic glaciers (Evans et al., 1999). The chance of glacial surging leads to a second ridge-forming mechanism, that of crevasse filling. After a glacier experiences rapid extensional flow during a surge it is usually left extensively faulted. On modern glaciers, the faulting commonly produces a criss-crossing network of crevasses, which can penetrate from the surface, or upwards from the base of the glacier. If the glacier is thin, crevasses can penetrate its entire thickness. These crevasses are subsequently filled with sediment, either by subglacial material being squeezed from beneath and/or supraglacial and englacial material falling into the crevasse from above. Once the ice melts, the former crevasses form prominent ridges. Consequently, some of the reticulate patterns of till ridges in the study area are probably crevasse fills.

A third possible origin for some of the transverse ridges in the study area is that they are end moraines. This is most likely for individual ridges that can be traced for several kilometres, implying a continuous glacier margin. Some of these ridges are so closely spaced that they may mark individual winter stillstands of the retreating ice margin (cf. Sharp, 1984). If these moraines formed annually, the Fort Liard map area was deglaciated in less than 1000 years, from the west to the east, as the Laurentide Ice Sheet retreated northeastward. The existence of ice-marginal lakes may also have enhanced formation of seasonal ridges if the water was deep enough to promote calving along the ice front.

Large lateral moraine segments related to recessional stages of Laurentide ice are found along a few mountain flanks in the Liard Range. Some are nearly horizontal benches of till, whereas others form gravelly kame terraces. A good example is a boulder gravel ridge about 2 km long, on the west side of Sawmill Mountain. The ridge rises about 40 m above two lakes it dams on the uphill side.

On the plains, a broad ridge of glacially moulded till runs across the northeast corner of the map area. This ridge appears to be part of an extensive northwest-trending moraine system mapped near Trout Lake (Craig (1965); Rutter et. al. (1993); Fig. 4). This moraine appears to have been overridden by a subsequent glacial advance northwest of Trout Lake. Segments of the overridden moraine can be traced to the northwest where it abuts Nahanni Range, north of the confluence of the South Nahanni and Liard rivers, and to the southeast into British Columbia, a total distance of more than 200 km. Apparently a significant stillstand occurred during recession of the Laurentide Ice Sheet, which was then followed by a major readvance of the ice margin. The overridden parts of the moraine have many kettle lakes

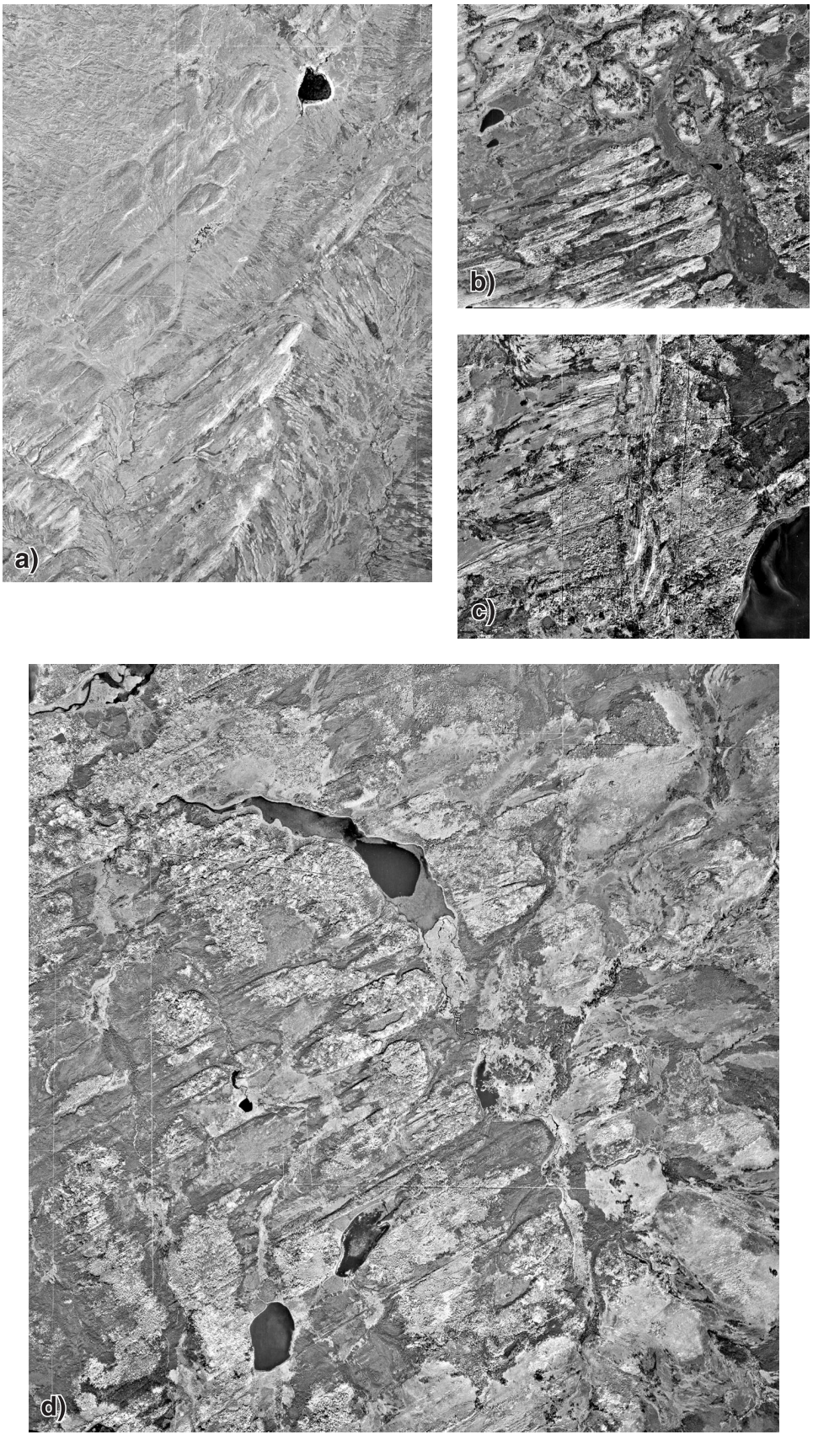

Figure 17. Drumlins and flutings which extend downflow from the rims of valleys and protuberances. **a)** Topographic knobs provided obstacles to glacial flow. Enhanced deformation of subglacial drift over and around these features resulted drumlin formation (NAPL A17434-63). **b)** Streamlined landforms on either side of an old channel. The southwest edge of the channel has been modified by the ice flow, indicating that the channel existed beneath the ice (NAPL A17442-57). **c)** Grooves and flutings on the lee side of the Bovie Lake Thrust, a prominent bedrock ridge (NAPL A17442-55). **d)** Drumlins formed on the downflow rim of a partially buried channel; probably an ancestral Petitot River (NAPL A17442-114). *See* Figure 16 for locations and scale.

elongated in the direction of flow. These kettle lakes suggest the meltout of buried ice. Subglacial stacking may have occurred as the overriding ice was decoupled along shear planes. It may also be argued that the overridden feature is not an end moraine, but an entirely subglacial form, such as a ribbed or Rogen moraine; however, the northwest trend of the overridden moraine is mimicked by at least two moraine systems 15–40 km east of Trout Lake (Rutter et al., 1993), which do not appear to be overridden. As noted above, stratigraphic evidence for glacial readvances in the form of till sheets separated by shear planes or deformed sediments is found in the cliffs near the confluence of the Arrowhead and Muskeg rivers, and farther upstream on Muskeg River (Fig. 10, Appendix C). See 'Patterns of glacial flow and ice retreat near Fort Liard' for further discussion about this moraine system.

Glaciofluvial deposits and landforms

For mapping purposes, glaciofluvial deposits are subdivided into proglacial outwash and ice-contact stratified drift. Proglacial outwash, the most extensive glaciofluvial deposit in the study area, was deposited by meltwater issuing from the ice margin, mainly in the form of braided channels. Outwash in the map area is generally composed of stratified gravel and sand, forming deposits 1–10 m thick. The gravel clasts are typically well rounded with maximum clast diameters of about 25 cm, but some outwash deposits may also contain diamictons. When first laid down, the proglacial outwash probably formed continuous sheets extending out from the ice margin. These deposits probably spanned entire valley floors or meltwater channels, but now only remnants are found on hill slopes and the flanks of valleys.

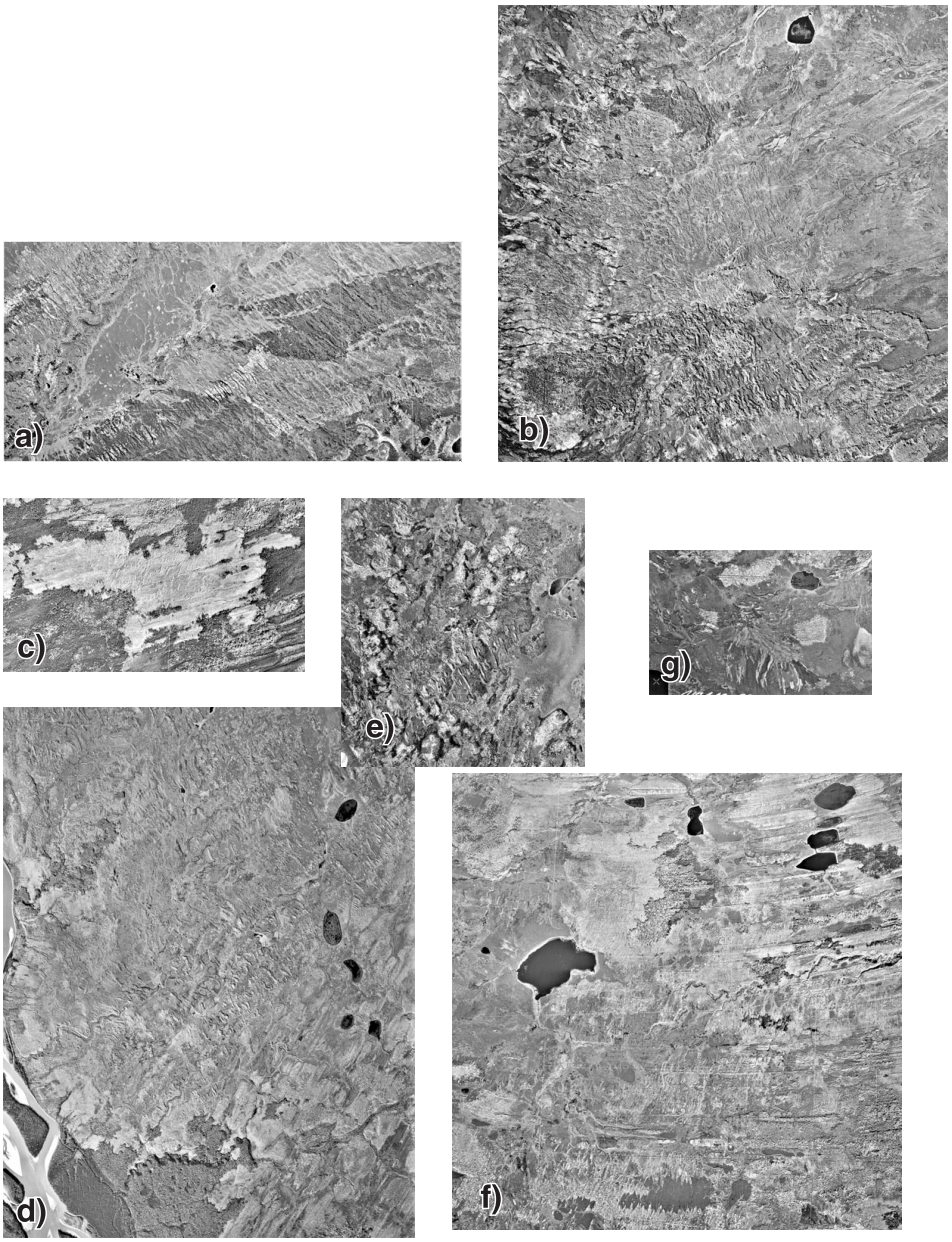

Figure 18. Transverse ridges. **a)**, **b)** Closely spaced end moraines and meltwater channels etched along the retreating ice margin (NAPL A17438-66 and A17438-77). **c)** Subtle end moraines lying obliquely across drumlinoid forms. The moraines are manifest as subtle changes in the vegetation (NAPL A17442-58). **d)**, **e)** End moraine segments oriented across the former glacial flow direction (NAPL A17438-81, A17438-45). **f)** Curvilinear flutings along the southwest side of Petitot River. The lower part of the figure shows numerous moraine segments lying obliquely to the former flow direction (NAPL A17442-43). **g)** Nested end moraines depicting an ice margin retreating to the northeast (NAPL A17442-32). *See* Figure 16 for locations and scale.

Most of the outwash deposits were removed by postglacial channel incision because modern drainage systems usually occupy the former meltwater drainage networks in this area. Consequently, glaciofluvial deposits are typically found as upper terraces along the major rivers of the study area (Fig. 7; unit Gt on the GSC Open File maps). The glaciofluvial deposits are commonly interrupted by fluvial sediments that form low terraces along the major rivers, about 5 m above modern floodplains. In places, the modern streams have reworked pre-existing glaciofluvial material and redeposited it in lower terraces. In the study area, more recent fluvial deposits are generally finer grained and usually have woody layers, compared to glaciofluvial sediments.

Glaciofluvial deltas were formed when proglacial meltwater streams entered glacial lakes. As noted previously, ice-dammed lakes flooded various parts of the map area, especially Liard River valley, during deglaciation when the Laurentide Ice Sheet retreated northeastward. Large foreset beds exposed along a prominent terrace at Fort Liard indicate that the feature is a delta that prograded into glacial Lake Liard (Fig. 19). The deposit is an erosional remnant, more than 20 m thick and more than 1 km² in area, but on airphotos the surface the delta is indistinguishable from adjacent glaciofluvial terraces and it is possible that larger remnants remain. Nearby Cretaceous outliers at the confluence of the Liard and Petitot rivers probably protected the deposit from erosion. More distal deltaic deposits in the form of thick, well sorted sand beds are preserved along the cut banks of Liard River and in the basal units of Blue Bill Creek (*see* stratigraphic section BJB020017; Fig. 11). These sand beds represent rapid sedimentation into glacial Lake Liard by currents, and mark a transition into eventual glaciolacustrine deposition by suspension. Terraces within the confines of Kotaneelee River valley, near the western edge of the map area (Fig. 12), show even thicker stratified sand units. These are also thought to record rapid aggradation into a glacial lake.

Ice-contact stratified drift, the second category of glaciofluvial deposit, is usually coarser than proglacial outwash and has chaotic bedding related to high-energy, highly variable conditions at the glacier margin. Grain size is extremely variable, with boulders greater than 1 m in diameter and interbedded diamictons common. Landforms produced by ice-contact stratified drift are usually related to some former configuration of the glacier at the time of deposition. The contact zone may be along the ice margin, or in some basal or englacial cavity. In places, the ice-contact sediments can be further modified as the ice subsequently melted out.

As noted, the map area has numerous small ridges that are oriented transversely to ice flow (*see* 'Till and till landforms' section). Some of these ridge patterns are very similar to crevasse networks seen on modern glaciers and likely formed by basal cavity infilling (Fig. 20). A few of these ice-contact ridges are composed of glaciofluvial material, implying that meltwater exploited the crevasses (unit Gr on the GSC Open File maps). Nevertheless, most of the crevasse ridges in the map area are composed of till and may have formed by some basal squeeze mechanism. It is difficult to distinguish the composition of particular ridges from airphotos; therefore, most of the ridges were collectively mapped as 'Tr'.

In contrast to the reticular crevasse-fill ridges, sinuous ridges several kilometres long were mapped in the study area as eskers. Eskers are former meltwater conduits in glaciers and thus composed of ice-contact stratified drift; however, many of these esker-like ridges, especially those with less

Figure 19. Foreset bedded gravel comprising a prominent delta near Fort Liard. The section is about 24 m thick. The paleocurrent was to the east-northeast, approximately the same direction as the modern Liard River. **a)** Photograph by J.M. Bednarski. GSC 2007-213; **b)** Photograph by J.M. Bednarski. GSC 2007-204

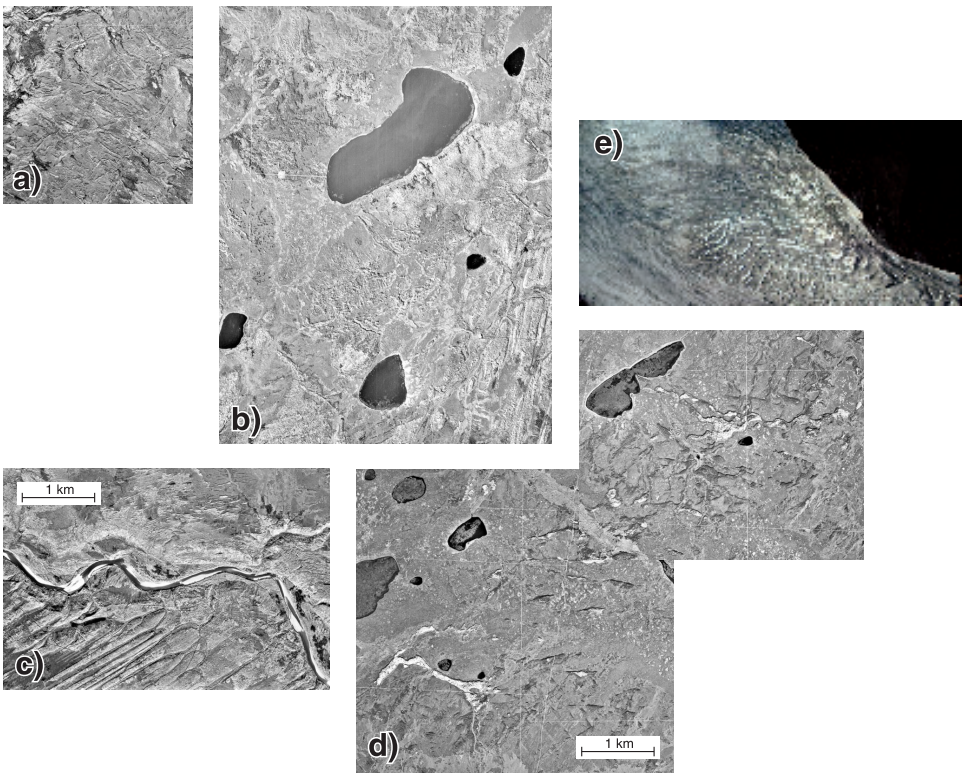

Figure 20. Basal crevasse patterns reflected by crosscutting ridges. **a)** Crosscutting crevasse fillings (NAPL A17434-88). **b)** Small moraines and crevasse fillings forming a crosscutting pattern in a low area. The high ground to the southeast is streamlined by glacial flow (NAPL A17438-81). **c)** Small till ridges along the north side of Petitot River, that are probably crevasse fills. En echelon drumlinoid forms south of the river have been enhanced by postglacial drainage (NAPL A17442-134). **d)** A complex pattern of moraines or crevasse fillings (NAPL A17442-124). **e)** The colour photograph shows crevasse patterns on a modern glacier in the high Arctic for comparison. Photograph by J.M. Bednarski. GSC 2007-205. *See* Figure 16 for locations and scale.

than 3 m in relief, were discovered to be composed of till rather than glaciofluvial material. This suggests that the eskers are nascent features where the flow of meltwater was very short-lived, and the aggregate quality of which is poor. Alternatively, the ridges may have formed when subglacial sediment was squeezed into cavities at the base of the ice sheet, much like crevasse-squeeze ridges.

Ice-contact stratified drift also underlies hummocky and kettled terrain produced by meltout of buried glacial ice. Kettled terraces are found at higher elevations along Liard River and in some mountain valleys. Some terraces also have distinct escarpments marking former ice margins. This is particularly evident in kame terraces on the flanks of valleys in Liard Range (e.g. on Sawmill Mountain, site BJB020024; Fig. 11).

Meltwater channels are glaciofluvial landforms that can be entirely erosional with no associated deposits. This is common in Liard Range where meltwater channels were cut into bedrock leaving only a clean floor or erosional notch. Evidently the material was transported downstream and deposited as outwash in the valleys or ultimately into glacial lakes. Meltwater channels cut into bedrock are also found on the plains east of Liard River, especially when the channels are incised into the deeper valleys. Nonetheless, there are also many broad, flat-floored channels that appear to be cut entirely into till. No glaciofluvial deposits were seen in these broad channels because the flat channel floors are usually poorly drained and covered by organic and lacustrine deposits. Individual channel systems can be traced along longitudinal profiles that go up and down. The channels appear to die out along their course as relief diminishes, only to reappear again farther downstream. It is possible that the depth of incision varied because of subsurface control, such as bedrock structure, but in many places the channel floors appear to rise because they become infilled with till. As noted earlier, numerous broad channels east of Liard River bear marks of being overridden by glacial ice, so till slumping from the sides is a possibility. Alternatively, if the channels were subglacial meltwater conduits (tunnel valleys) at some stage during deglaciation, the till may have been deposited from meltout as the tunnels collapsed during deglaciation. This interpretation is further supported by a series of subparallel moraines running on either side of some of the larger

meltwater channels, including parts of Petitot and Muskeg rivers in the eastern part of the map area. These moraines appear to confirm that the channel was walled by ice on both sides. This may have occurred when the subglacial tunnel channel became subaerial during deglaciation. As the position of the ice margin moved northeast of the map area, several other meltwater channels were cut as spillways when glacial lakes drained, especially a glacial lake that existed around present-day Trout Lake (Fig. 4).

The advance and retreat of the ice sheet was not only instrumental in cutting meltwater channels, but significant diversions of pre-existing drainage networks also took place. The best example is the shift in the course of Petitot River, which likely occurred during the initial advance and final retreat of the Laurentide Ice Sheet. It is hypothesized that prior to glaciation an ancestral Petitot River flowed northward along the east side of the Bovie structure, a prominent bedrock ridge west of Lake Bovie (Fig. 5), and entered the present-day Muskeg River valley, eventually flowing into Liard River. The former course of the river is marked by a series of northward-trending channels that extend as far north as Arrowhead and Muskeg river valleys. The westward edge of the larger channels are ice moulded, which undoubtedly shows that they existed prior to the last glacial advance. Northward drainage was obstructed when the ice margin advanced from the northeast and forced the ancestral Petitot River westward against the bedrock ridge. The ridge was breached twice by meltwater flowing westward, once near Lake Bovie and the second time where Petitot River flows today, near the border with British Columbia.

Glaciolacustrine deposits and landforms

Glaciolacustrine deposits are defined as fine sand, silt, and clay deposited in glacier-dammed lakes. Ephemeral glacial lakes covered much of the map area because the Laurentide Ice Sheet formed an extensive barrier to the northeast, the direction of regional drainage. As already mentioned, smaller lakes in the mountain valleys would have migrated and enlarged along the retreating ice margin, culminating into glacial Lake Liard when Liard River drainage into Mackenzie River was still blocked by the retreating ice sheet. During this time the lake levels fell from more than 400 m a.s.l. to about 254 m a.s.l., which is marked by a delta 60 m above the modern river at Fort Liard. Along Liard River, thick sequences of the sand and gravel were deposited into glacial Lake Liard when the lake level was at least 220 m a.s.l. These deposits were previously described in the section 'Glaciofluvial deposits and landforms'. Fluvial processes began to dominate Liard River valley during postglacial time when the watersheds became free of glaciers and ice-dammed lakes.

It is important to note that the glaciolacustrine deposits mapped (Fig. 7) are diachronous because of the transient nature of ice-dammed lakes. The configuration and extent of the lakes changed quickly as the ice front rapidly retreated northeastward and continually exposed new outlets. This also made lake shorelines notably absent in the map area. In the map area east of Liard River valley the local drainage is westward toward Liard River, meaning that the drainage would be away from the ice margin and large lakes along the ice margin would be inhibited. Consequently, glaciolacustrine sediments over 2 m thick are rare outside of the larger river valleys. Glaciolacustrine deposits are found in local depressions and are though to underlie large areas of flat organic deposits.

Alluvial deposits and landforms

Alluvium, defined as postglacial fluvial deposits, forms active floodplains with meander channels, oxbow lakes, and scroll marks. The most extensive alluvial deposits in the map area are in Liard River valley (Fig. 21). Over the 115 km length of this part of Liard River valley, the active floodplain ranges in width from about 3 km in the southwest to over 23 km in the north (Fig. 7). The southern reaches of Liard River are confined by Cretaceous outcrops that limit meandering and segments of the river are braided. North of Flett Rapids the river meanders through extensive glaciofluvial and glaciolacustrine deposits, and thick point-bar deposits dominate (Piët, 1992). Within the floodplain, Liard River is very dynamic, exhibiting rapid lateral erosion and frequent channel avulsion, especially during times of flood when large log jams form and divert flow (Fig. 22). Study of airphotos from 1961 and Landsat and radar images from the early 1990s show that parts of Liard River have shifted dramatically during this period, particularly where the river contacted sandy alluvial terraces (Fig. 23). Interestingly, comparison of GPS positions taken in 2001 with the 1991 imagery shown in Figure 22 shows that further erosion during the later interval was minimal.

Long, narrow, alluvial plains are also found along Arrowhead, Kotaneelee, Muskeg, and Petitot rivers. Many small deposits of alluvium are also found in pockets along smaller streams. Alluvial fans are numerous in the mountains where steep tributary streams flow onto valley floors. In the steepest areas, alluvial deposition is enhanced by seasonal torrents of avalanches and mudflows.

In general, postglacial alluvium deposited in the mountains is coarser than on the plains, owing to the steeper stream gradients. Nonetheless, when compared to glaciofluvial deposits in general, postglacial alluvium is finer grained, related to point-bar deposition and silty overbank deposits. In places, wood and other layers of organic detritus are common within the alluvium. In boggy areas in the eastern part of the map area, some gentle slopes are uniformly drained by small subparallel or anastomosing alluvial channels interspersed with fens (unit Ac on GSC Open File maps). The alluvium can be regarded as slope wash and is likely very thin.

Figure 21. Extensive meander plain on Liard River. Flett Rapids are located at the southern edge of the image. The main channel is about 600 m wide. (Airborne radar image colour enhanced with Landsat image.)

Alluvium is also found in low terraces along the larger rivers in the map area, usually 3–4 m above the active floodplain. The largest alluvial terraces lie along Liard River (Fig. 7). Riverbank exposures typically show cobbly gravel overlain by rhythmically bedded silt and fine sand. A distinct characteristic of Holocene alluvium exposed in terraces is the presence of interbedded organic debris, particularly in flood deposits when significant point-bar sedimentation took place. Piët (1992) described terraces of point-bar deposits on the lower Liard River containing wood that dated 5750 ± 60 (GSC-4103), 5480 ± 70 (WAT-2478), and 5470 ± 70 (WAT-2479)(Fig. 9). The dates suggest that at least 18 m of incision has taken place since the terraces were formed.

In many places organic material contained within terraces has been burnt, and charred logs commonly protrude from river cutbanks. Burnt-wood debris is exposed for tens of kilometres along cutbanks of Liard River. Radiocarbon dates indicate that the wood was deposited at various times, likely during flood events that postdated major forest fires. For example, downstream of the confluence of the Liard and Kotaneelee rivers, a charred log, which was exposed 4.3 m above the river in an 8 m high terrace, was radiocarbon dated at 2220 ± 60 BP (GSC-6698; Fig. 9). A second charred stump exposed in a low terrace near Mount Flett, was dated at 850 ± 60 BP (GSC-6692; Fig. 9). The ubiquity of charred wood in alluvium suggests that forest fires within a watershed may have contributed to periods of local fluvial aggradation. Two other radiocarbon dates suggest forest fires ca. 1120 ± 50 BP (GSC-6762; Fig. 12), near the confluence of the Kotaneelee and Liard rivers, and one ca. 4900 ± 140 BP (GSC-717, McNeely (1989); Fig. 11) in the Fisherman Lake area.

As noted earlier, alluvial terraces are lower in the valleys and have different sediment characteristics than glaciofluvial terraces; however, interpreting some terraces of intermediate elevation is less certain, particularly where glaciofluvial material might have been recycled. Older alluvial terraces with abandoned meander scrolls and oxbow lakes become infilled organic deposits where drainage is poor.

Lacustrine deposits

Deposits exposed by recent fluctuations in lake levels are limited in the study area (Table 1). Some of these recently exposed areas are probably due to recent climatic changes causing the lakes to dry up; however, along many of the smaller stream courses beaver dams seem to have a significant geomorphic impact, controlling lake levels and

Figure 22. Liard River above Flett Rapids is braided in places and channels often shift during times of flood when log-jams occur. **a)** Looking north. Photograph by J.M. Bednarski. GSC 2007-214. **b)** Distributary channels, looking south. Photograph by J.M. Bednarski. GSC 2007-200. **c)** Left side of photograph shows a log-jam across a side channel. Photograph by J.M. Bednarski. GSC 2007-203.

Figure 23. Lateral channel migration into a sandy alluvial terrace on Liard River eroded about 470 m in the period 1961 to 1991. The figure compares a 1961 black and white airphoto (NAPL A17442-23) with a Landsat 5 colour image taken in 1991. The 1991 cutbank is indicated by the arrows. The terrace is located just upstream of the confluence of the Liard and Muskeg rivers. The reddish plume is relatively clear tributary water that has not yet mixed with silt-laden Liard River water.

catastrophic drainage. Lacustrine deposits are usually more than 2 m thick and are generally overlain by organic deposits and, as such, were mapped as organic deposits.

Although fluvial processes dominate Liard River valley during postglacial time, there is stratigraphic evidence that a significant lake existed in the valley without the effects of glacial damming. A ^{14}C date of 8080 ± 100 BP (GSC-6706; Fig. 9) was obtained from a detrital log exposed in a low alluvial terrace, in the southwest part of the study area. The log was overlain by 2 m of dense, laminated clay, which was in turn overlain by 5 m of stratified sand with some gravel. The lake must have formed during a major flood event on Liard River.

Colluvial deposits and landforms

Most of the colluvium in the map area is associated with steep mountain slopes, whereas outside of the mountains, significant colluvium is usually confined to the riverbanks, especially along Petitot, Muskeg, and Liard rivers, where slumps are common. Colluvium in the mountains includes talus, landslide debris, and a few rock glaciers. The rock glaciers are confined to higher elevations at the base of steep northeast-facing cliffs.

The effects of weathering, particularly frost action, on steep mountain cliffs leads to the accumulation of rock-fall debris (talus) at the foot of slopes, forming cones or aprons. Talus is produced from most of the bedrock formations in the area, but the size of individual blocks is governed by rock type. Sandstone outcrops, such as in the Mattson Formation, produce talus with blocks up to several metres in diameter, but generally the material is smaller, although the total volume can still be large. In a few places rock debris at the foot of the slope has transverse and longitudinal furrows, suggesting past movement away from the cliff, likely as rock glaciers. Judging by their subdued, lichen-covered surfaces, these rock glaciers are considered inactive under current climatic conditions.

Catastrophic failures in the form of landslides and debris flows are common in the mountainous terrain, particularly where thick sequences of recessive shale are overlain by sandstone or limestone. In Liard Range, landslides range in size from a few tens of square kilometres to several square kilometres. Aggregate excavations into the toe of a large landslide near the Chevron Corporation K-29 gas plant shows that the colluvium can be well over 100 m thick near the base (Fig. 24). Large landslides tend to occur within bedrock, but the most common smaller landslides take place in till. A number of factors are necessary to initiate a landslide, but periods of intense rainfall or rapid snowmelt have been shown to trigger numerous landslides northwest of the

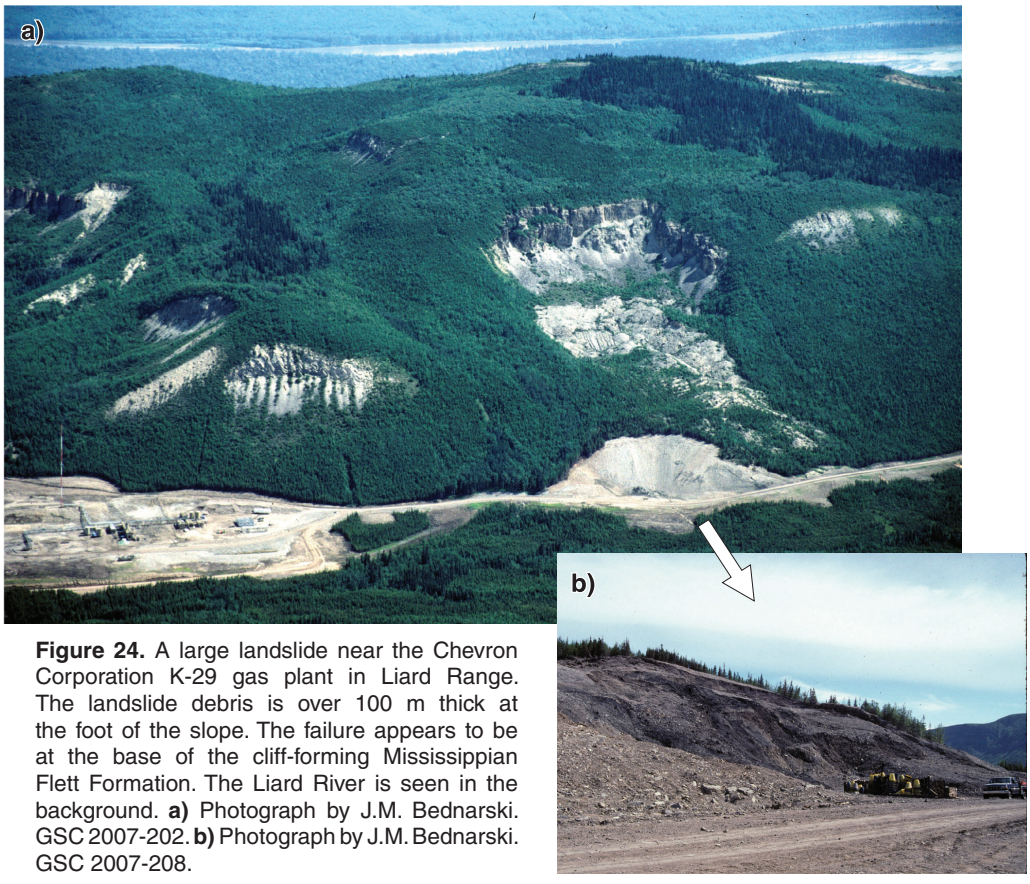

Figure 24. A large landslide near the Chevron Corporation K-29 gas plant in Liard Range. The landslide debris is over 100 m thick at the foot of the slope. The failure appears to be at the base of the cliff-forming Mississippian Flett Formation. The Liard River is seen in the background. **a)** Photograph by J.M. Bednarski. GSC 2007-202. **b)** Photograph by J.M. Bednarski. GSC 2007-208.

study area (Huscroft et al., 2004). At least 58 major recent landslides and numerous inactive landslides were mapped in Liard Range (Fig. 25). The vegetative cover on inactive landslides varies significantly, suggesting a wide range of ages. In general, the presence of steep slopes is conducive to landslides, but when comparing the location of current landslides with airphotos taken 40 years earlier, their location does not seem to be systematic. For example, sometime before August 1991 (based on Landsat imagery), an active landslide and/or debris flow occurred 5 km northeast of Fisherman Lake on a west-facing mountain flank. The initial failure occurred near the ridge crest and extended down a steep-sided gully, until it was about 3.5 km long and less than 200 m wide. It is not known how long the slide was active, but, by 2002, it was recolonized by shrubs (Fig. 25a). In about 1995, a similar failure, in the form of a debris flow, occurred 5 km north of the previous slide, on the same ridge so that in 2002 it extended over 3 km downvalley (Fig. 25b). Although the conditions for landslides to occur in this area are favourable, locating the next failure would require more detailed study beyond the present mapping effort.

Most of the colluvium outside the mountains is in the form of slumps and earth flows, particularly along active river cutbanks. The largest failures occur where rivers undercut exposures of Cretaceous bedrock, although Quaternary sediments play a larger role in the failures than in the mountains.

Landslides are common along Kotaneelee River where Cretaceous shale is exposed along steep banks. In places, extensive slumping of the shale has produced a step-like topography. At one site the slump blocks are over 1600 m long with a total relief of over 180 m (BJB010050; Fig. 12). A wood fragment extracted from a slump scarp about 80 m above the river ^{14}C dated 1120 ± 50 BP (GSC-6762; Fig. 12). The wood, giving a maximum age of one of the slumps, was charred. Consequently, slumping may be related to the destabilizing effects of a forest fire, as well as aggradation on Liard River, as noted earlier.

Eolian deposits and landforms

A thin cover of wind-blown silt is common throughout the area. It is usually confined to the top few centimetres of the soil horizon and was not mapped as a unit. Sand ridges (map unit Er on the GSC Open File maps), which are thought to be relic dunes, occur in a few isolated areas and cover less than 1 km^2 of the entire map area. Overall, eolian deposits cover less than 1 km^2 of the map area. A few active sand dunes occur on sandy banks in isolated places along Liard River.

Organic deposits and landforms

Organic deposits are most common in flat-lying, poorly drained areas such as valley floors and depressions in alpine areas, and broad flat areas on the plains. Organic deposits are most extensive east of Liard River because the area is underlain by flat-lying shale, clayey tills, and extensive areas of fine-grained glaciolacustrine sediments. Large areas of hummocky muskeg around Celibeta Lake are likely underlain by ground ice. Two main organic units were mapped: bogs (GSC Open File map unit O^{1}h), which are composed of *Sphagnum* or forest peat formed in an ombrotrophic environment, and fens (GSC Open File map unit O^2), which are composed of peat derived mainly from sedges and partially decayed shrubs under eutrophic conditions. Fens form relatively open peatlands with a mineral-rich water table that persists seasonally near the surface and are often covered with low shrubs and sometimes a sparse layer of trees, usually black spruce. Bogs may be treed or treeless with a cover of ericaceous shrubs, but tend to be more hummocky (GSC Open File map unit O^{1}h) due to thick accumulation of peat and the growth of ground ice. As noted earlier, this area is within the zone of discontinuous permafrost and the growth of ground ice is enhanced by the insulative properties of an organic mat. Consequently, there is a positive feedback between the accumulation of organic matter and the growth of ground ice, particularly where the groundwater table has recently dropped. Peat plateaus and palsas grow until there is a disturbance to the insulative cover allowing the ground ice to melt out.

Significant organic deposits may also exist in lake-bottom sediments. For example, Fisherman Lake has numerous methane gas seeps produced by the anaerobic decomposition of sedimentary organic matter; however, it is not known whether the source of the decomposing organic matter is underlying organic-rich shale or more recent organic sedimentation (Smith et al., 2005).

PATTERNS OF GLACIAL FLOW AND ICE RETREAT NEAR FORT LIARD

The previous sections described numerous glaciogenic features related to the last glacial cycle. These are used to reconstruct the pattern of deglaciation from the last glacial maximum in the Fort Liard map area. Although the western parts of the area may have been overridden by Cordilleran glaciers, any evidence of these advances was obscured by the subsequent advance and retreat of the Laurentide Ice Sheet. Consequently, the reconstructions described here are confined to the Laurentide Ice Sheet. Laurentide deposits are readily identified by their content of Canadian Shield erratics.

Landforms formed by actively flowing ice are widespread in the area and, in most places, provide unequivocal information about the direction of former ice flow. Nonetheless, these features are often found in discrete swarms with significant gaps in between. In order to facilitate the reconstructions several assumptions were made in interpreting the data succinctly described by Mathews (1980). Concerning ice-flow features, most apparent is that the ice-flow patterns

are usually not synchronous between areas. Ice-flow patterns in any given area reflect only the last time that the ice was active there, and this may be unrelated to adjacent areas. Consequently, it is unlikely that a regional assemblage of flow patterns reflects the flow at one instance of time, such as the last glacial maximum. In general, ice-flow features near the ice limits, or at higher elevations are likely older that those in valley bottoms, or nearer the ice sources. Topography has strong influence on ice flow, but again, larger topographic features need thicker ice to be affected, and thickest ice is most likely to have occurred during the last glacial maximum. The diachronous nature of ice-flow patterns is clear where sharp discordances occur between adjacent patterns, or where the patterns crosscut.

Ice-sheet reconstruction also requires a few assumptions about the surface profile of the ice sheet and its constituent lobes. In general, ice sheets are expected to slope down from the ice divide to the margin. In the eastern parts of the study area, which are underlain by deformable Cretaceous shale, the surface gradient of the Laurentide Ice Sheet was probably only 2–5 m/km (Mathews, 1974; Fisher et al., 1985). Two adjacent ice lobes within the ice sheet would meet along a

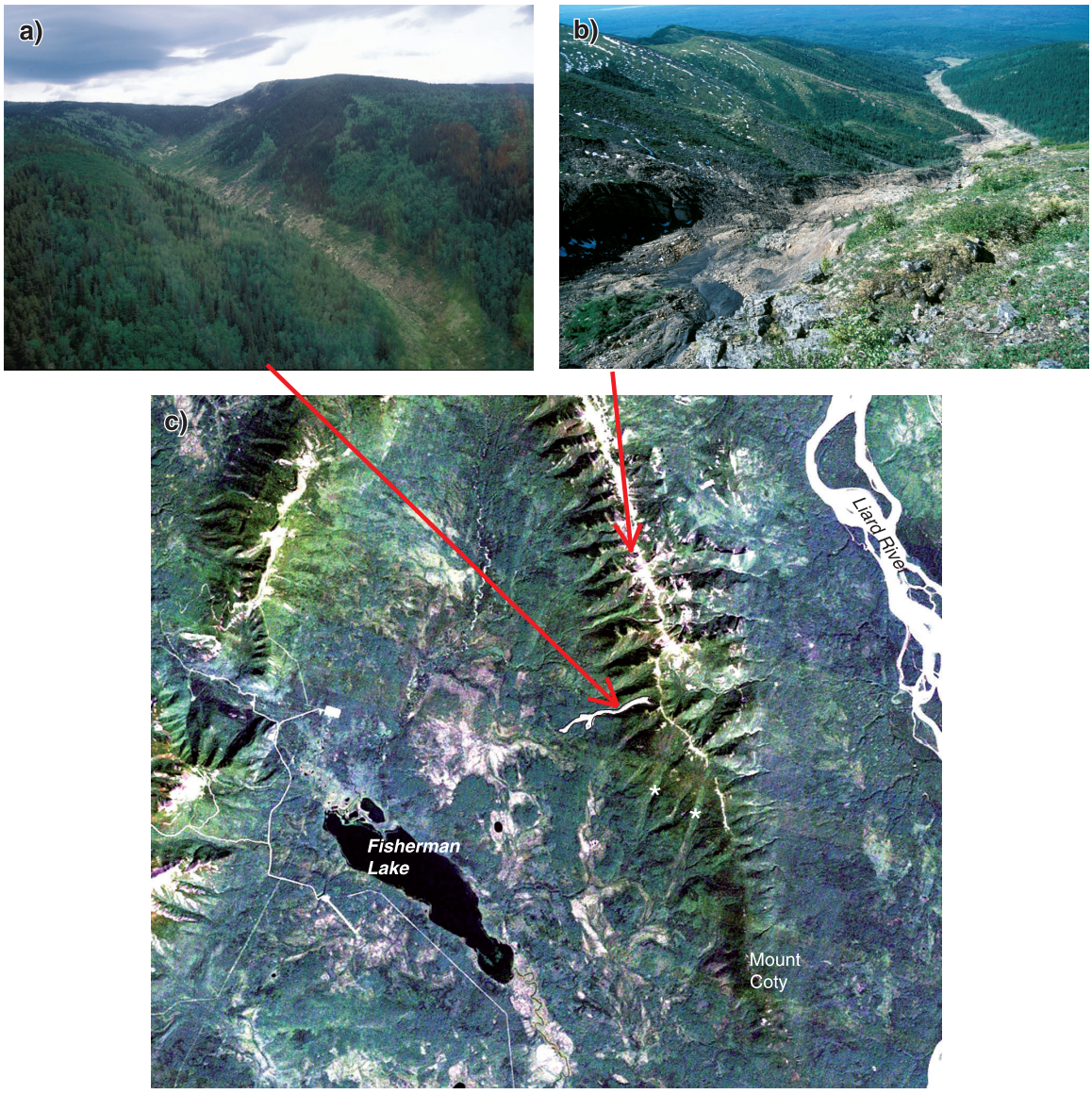

Figure 25. Examples of mass movement in the Fort Liard map area. **a)** Landslide and debris flow in Liard Range, which in 2002 had been active for about five years. Prominent levees occur along the lateral margins of the runoff area. Photograph by J.M. Bednarski. GSC 2007-206. **b)** Inactive landslide and debris flow 5 km south of Figure 25a. Photograph by J.M. Bednarski. GSC 2007-209. **c)** Landsat imagery shows this feature to be active in 1991 (outlined). Asterisks show old, vegetated debris-flow paths.

medial trough, which would slope toward the terminus, and the flow along the interlobate margin would become parallel. These medial margins could become the locus of meltwater channelling and glaciofluvial deposition during deglaciation. When separate lobes of glacial ice are confined within valleys it is assumed that the lobe is approximately symmetrical across the valley, which means that lateral moraines, meltwater channels, or glaciofluvial deposits are correlated on either side of valleys based on their relative position (cf. Dyke, 1990).

During deglaciation it is obvious that the Laurentide ice margin migrated across the study area, but this is not usually marked by large end moraines and the configuration of the margin must be deduced by other means. On flat ground it is assumed that the ice margin would be at right angles to the direction of local flow. This is partly confirmed by the numerous small moraines and crevasse fills described in previous sections, although, as was discussed, some of these small ridges may have formed some distance behind the ice margin; however, marginal and submarginal meltwater channels along valley sides show that the ice margin can be almost parallel to the ice flow. This, of course, depends on the relative thickness of the ice relative to the topographic relief. In places, meltwater channels can be correlated by extrapolating the gradients from one channel to the next, but given the transient nature of the ice front, this has limited utility in areas of low relief.

The configuration of large meltwater channels also provides information on the position of the ice front, especially where the regional drainage was blocked during ice retreat. The locus of meltwater emanating from the ice front could be a channel draining to the local base level, which was some stage of a glacial lake in this area. Consequently, the abrupt start of a channel could be an indication of the ice front;

Figure 25. d) Large rock fall along an upper tributary to Flett Creek. Individual blocks are several metres in diameter. Photograph by J.M. Bednarski. GSC 2007-211. **e)** Rockfall-slump of sandstone blocks along the Petitot River canyon. Photograph by J.M. Bednarski. GSC 2007-201. **f)** Recent landslide along a pipeline infill just north of Mount Coty. Photograph by J.M. Bednarski. GSC 2007-217. **g)** Older, tree-covered landslide on an outlying ridge of Liard Range (*see* cover photo). Photograph by J.M. Bednarski. GSC 2007-218.

however, these channels must be distinguished from channels that were glacial lake spillways distal to the ice front, or channels that were subglacial tunnel valleys, formed behind the ice front.

Proglacial lakes also provide constraints on the location of the ice margin because for a given lake elevation it can be determined which possible outlets would have to have been ice dammed at the time. Every lake would have decanted into another by a series of spillways and channels on its way to the sea. The spatial extent of these glacial lakes can provide a means of correlation, but distinct shorelines are rare in the study area. Lastly, as the Laurentide ice margin retreated, major disruptions of subaerial drainage, hence stream diversion, can also give indication of former ice positions.

When using the current topography to reconstruct the former extents of glacial lakes, the effects of glacioisostatic tilting must be considered (cf. Lemmen et al., 1994). This is especially important for large glacial lakes that extended well away from the ice front. Nevertheless, this factor is thought to be negligible in the Fort Liard area because the glacial lakes in the area were of short duration, and extended along the ice front rather than away from it. Also, crustal loading by the Cordilleran Ice Sheet in the west was roughly balanced by Laurentide Ice Sheet loading in the east (cf. Dyke, 1996).

The chronological control shown in this reconstruction is determined by correlations with other areas because of the paucity of deglacial radiocarbon dates in the immediate study area. The reader is directed to radiocarbon data provided by Lemmen et al. (1994), Dyke et al. (2003), and Dyke (2004) for further details.

Last glacial maximum (ca. 18 ka BP)

As previously noted, the presence of Canadian Shield erratics west of the Fort Liard area shows that continental ice definitely penetrated beyond the study area into the Yukon. West of Liard Range, granite erratics were found on Kotaneelee Range up to 1450 m a.s.l. and the highest granite erratic on La Biche Range, even farther west, was found at 1620 m a.s.l. (Smith, 2003a, b, c). In Liard Range quartzite and granite boulders were found up to 1400 m a.s.l. and Hage (1945) reported quartzite boulders to nearly 1370 m a.s.l. on Nahanni Butte, just north of the study area. Similarly, Ford (1976) reported on Laurentide till up to 1400 m a.s.l. on Nahanni Plateau and 1500 m a.s.l. on Ram Plateau (Fig. 1). Some of these granite erratics are thought to originate from the Great Bear Batholith, which outcrops in a narrow band between Great Bear and Great Slave lakes (Hoffman and McGlynn, 1977), a glacial transport distance of about 500 km. Well preserved glacial striae at an elevation of 1200 m a.s.l., north of Fisherman Lake, suggests that most of these erratics in the mountains were deposited during the last glaciation because they show substantial thickness of continental ice flowing northwestward into Kotaneelee River valley. This advance may also have produced the east-northeast-trending striae on the crest of Liard Range at 1120 m a.s.l., northeast of Fisherman Lake; however, the possibility remains that these striae could have been produced by an earlier advance by Cordilleran ice from the west. The ice flow over the southern Liard Range complements the curving flowlines on the plains, which are thought to date from the last glaciation. In addition, the most extensive continental glaciation in the Mackenzie Mountains to the north occurred during the last glaciation (Duk-Rodkin et al., 1996), which further supports the hypothesis that the eastern erratics in Liard Range were deposited during the last glaciation. The sandstone erratic from the crest of Kotaneelee Range (1820 m a.s.l.) was dated at 25.6 ± 3.2 ka BP (calibrated years) (Smith, 2004a, b), which confirms extensive glaciation during the Late Wisconsinan. If western in origin, the erratic also confirms that the Cordilleran and Laurentide ice sheets coalesced during the Late Wisconsinan.

Hage (1945) found that the tills on the plains contained dark cordierite-biotite schist erratics that originated from the Yellowknife area to the northeast. These erratics were absent in the mountains, leading him to suggest that the mountain erratics where deposited by ice from a different source area, probably from the "west or northwest" (Hage, 1945). Nevertheless, many of the erratics in the mountains originate from the Great Bear Batholith, which is also in the same direction as the schist, except farther from it (Fig. 26). Consequently, the observed distribution of erratics could be related to the transport distance and transport height within the same ice sheet. In reconstructing the paleogeography of the Laurentide Ice Sheet at 18 ka BP, Dyke and Prest (1987) drew a regional ice divide extending westward from an ice dome (Keewatin Sector) situated west of Great Slave Lake to Trout Lake (Fig. 26). This "Plains Ice Divide" separated ice flowing northwest to Beaufort Sea from ice flowing southwest, which would have affected the study area. This configuration, however, is not compatible with transporting erratics from the Great Bear Batholith to the study area and farther south. For this to have occurred the divide must have been farther north at some point in time. In any event, the southwestward progression to the Laurentide Ice Sheet from its Keewatin source was halted when the continental ice impinged on the Cordilleran Ice Sheet and caused a mutual northward deflection. A general southwest flow of the Laurentide Ice Sheet prior to the mutual deflection can only be inferred from the provenance of the shield erratics.

During the last glacial maximum, meltwater drainage to the east was blocked along the entire mountain front with most of the drainage diverted to the northwest into the Yukon and the Yukon River drainage (Lemmen et al., 1994; Duk-Rodkin and Hughes, 1995). A complex system of meltwater channels cutting across interfluves and exploiting pre-existing valleys can be traced from South Nahanni River to Bonnet Plume Basin (Duk-Rodkin and Hughes, 1991, 1995). During this time glacial Lake Nahanni was thought to occupy much of the South Nahanni and Flat

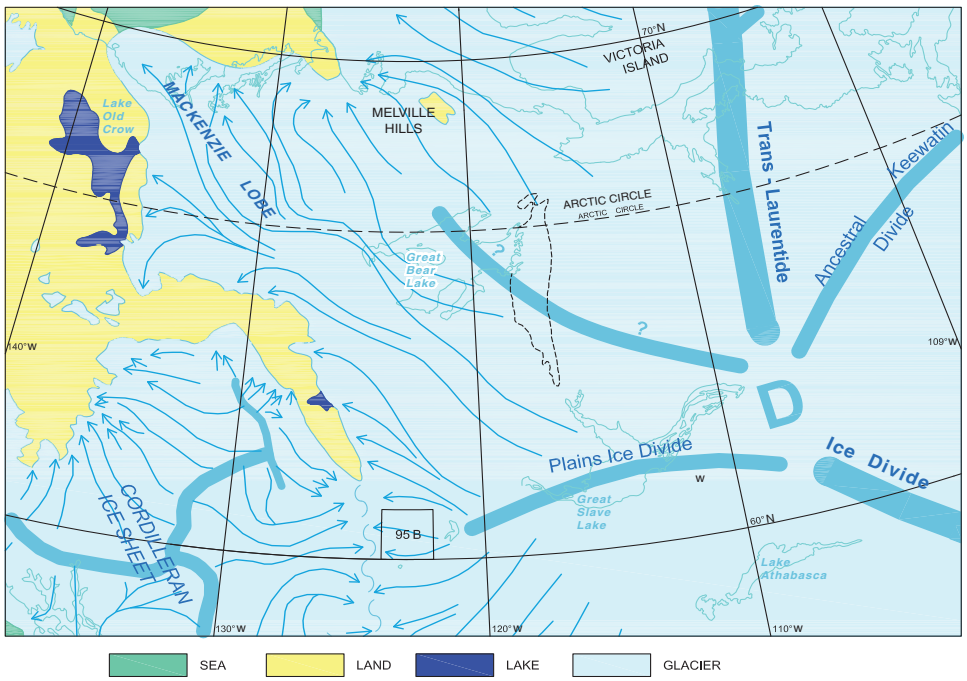

Figure 26. Paleogeography of the Laurentide Ice Sheet at about 18 ka BP, showing the confluence of the Laurentide and Cordilleran ice sheets. Arrows indicate major flow lines emanating from ice divides (thick lines). A large ice-dispersal centre formed a dome east of Great Slave Lake (Keewatin Ice Divide, D). This figure is derived from the paleogeography proposed by Dyke and Prest (1987), with ice and lake margins proposed by Dyke et al. (2003). The ice-free area in the Fort Liard map area (NTS 95 B) shown by Dyke et al. (2003) was removed. Also note that the glacial flow lines indicated in NTS map area 95 B are not entirely compatible with the surface features mapped in Figure 16, nor with the presence of erratics originating from the Great Bear Batholith (fine dashed line).

river valleys beyond the ice limit, reaching at least 650 m a.s.l. (Ford, 1976). In the interpretation presented here (Fig. 27), Ford's (1976) glacial Lake Nahanni is thought to date from the last glaciation and not the penultimate one. In the Fort Liard area, where the Cordilleran and Laurentide ice sheets were in contact, northward-flowing meltwater was probably concentrated along the suture zone. As discussed earlier, the maximum extent of the Laurentide Ice Sheet in the northernmost part of this region is thought have occurred ca. 30 ka BP (Duk-Rodkin and Hughes, 1995), which is considerably earlier than for the rest of the Laurentide Ice Sheet (e.g. Dyke et al., 2003). According to this model, proglacial drainage did not enter the Beaufort Sea until the Laurentide Ice Sheet retreated and then readvanced ca. 21 ka BP. South of the Mackenzie Mountains the maximum extent of the Laurentide Ice Sheet occurred after ca. 24.4 ka BP (Levson et al., 2004) and before ca. 14 ka cal BP (Bednarski, 2001). Consequently, the glacial maximum is near the approximate time of the globally recognized last glacial maximum at 18 ka BP (21.4 ka BP (calendar years), Mix et al. (2001)), when global sea levels were at their lowest.

In summary, during the last glacial maximum the entire Liard Range was probably totally ice covered, given the high-elevation erratics east of the map area (Smith, 2003a, b, c, 2004a, b). If the Nahanni region was ice-free as proposed by Ford (1976), meltwater would have been channelled northward along the mountain flanks, forming an integrated drainage network into glacial Lake Nahanni. Meltwater drainage would be most pronounced along the contact zone between the Laurentide and Cordilleran ice masses, especially when the Laurentide ice margin separated from Cordilleran ice, with a drainage area extending well into northern British Columbia. Figure 27a shows the paleogeography of the region soon after the last glacial maximum. When the Cordilleran and Laurentide ice sheets were in contact, the general southwest flow of Laurentide ice was diverted northward over the Fisherman Lake area and along the western flank of Liard Range. The deflection is well documented by the curving flutings on the plains, east of Liard Range. Ice flow on the plains was mainly toward the southwest, but in Liard River valley, north of Muskeg River, a southward ice flow prevailed below about 350 m a.s.l. (Fig. 16, 27a). North of Muskeg River there is a narrow zone where the two flows overlapped, but the relative age of these two ice flows is not clear. Three possibilities exist.

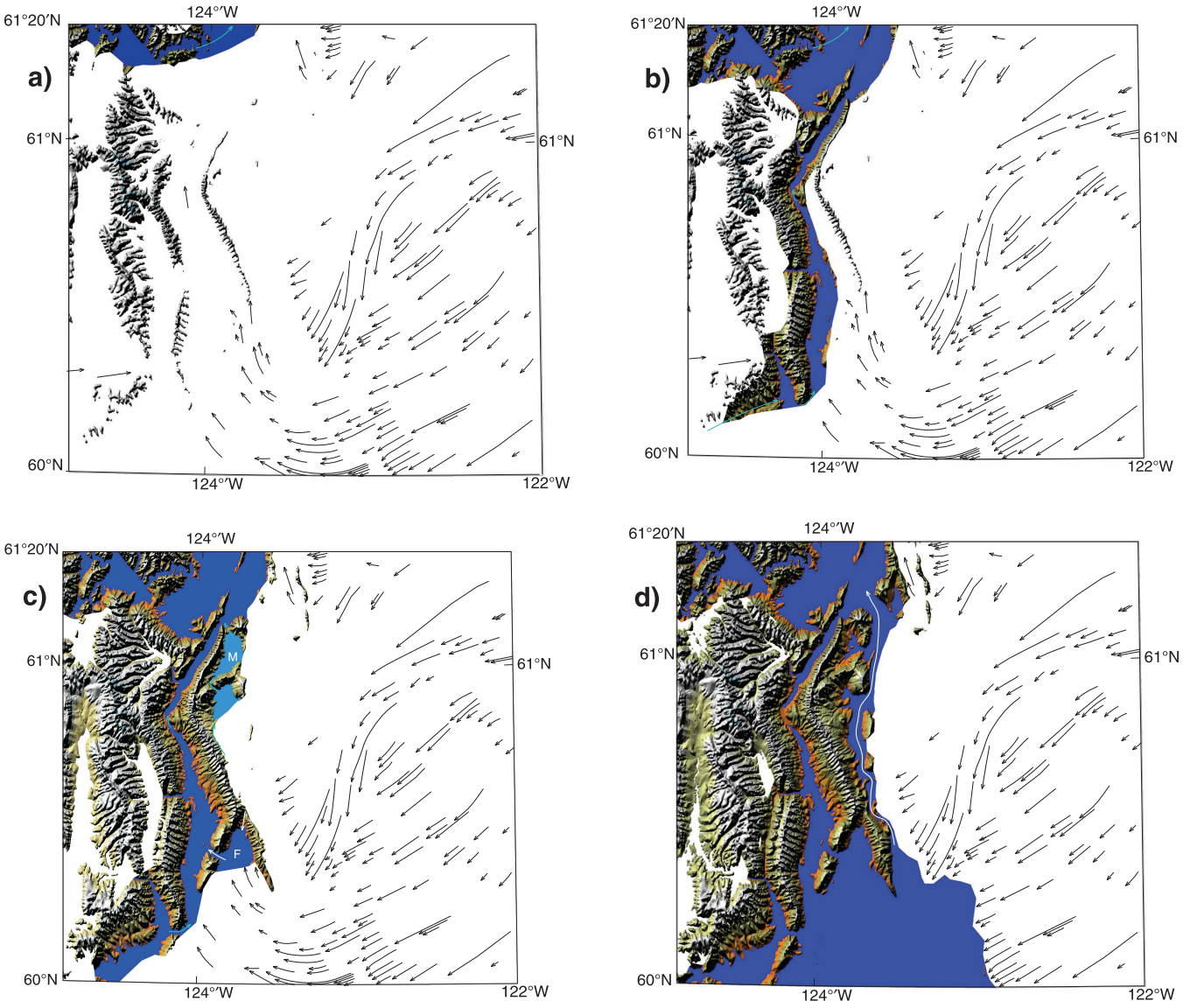

Figure 27. a) Paleogeography after the last glacial maximum when the Laurentide Ice Sheet thinned to about 1300 m a.s.l. over the Franklin Mountains. The entire Fort Liard map area is still engulfed in ice. Some of the ice flow lines (black arrows) shown in Figure 27 are not necessarily contemporaneous (*see* text). The existence of glacial Lake Nahanni at 650 m a.s.l. and its northward drainage (cyan arrow) is based on Ford (1976). **b)** Paleogeography ca. 16–13 ka BP. The Laurentide Ice Sheet retreated west of Liard Range. Glacial lakes formed in the La Biche and Kotaneelee river valleys. A lake level more than 600 m a.s.l. would have spilled into Lake Nahanni in the north via Chinkeh Creek and lower Jackfish River. Cyan arrows mark meltwater routes. **c)** Paleogeography ca. 13–12 ka BP. The Laurentide Ice Sheet retreated to the east side of Liard Range and proglacial lakes formed along the mountain flanks at high elevations. An outlet at about 790 m a.s.l. spilled meltwater into Mattson Creek basin (M) in the northern part of the study area. More retreat on the southern part of the study area allowed a lake to form within Fisherman Lake basin (F), which spilled into Kotaneelee River valley, where the divide into Chinkeh Creek maintained the lake level at 600 m a.s.l. These lakes joined the lake in the lower Beaver River, and eventually merged with a proglacial lake occupying the lower Toad and Liard rivers farther south (Mathews, 1980). **d)** Paleogeography ca. 12 ka BP. Glacial Lake Liard expanded south of Liard Range as the ice front rapidly retreated eastward. Drainage of glacial Lake Liard through Kotaneelee River valley at about 600 m a.s.l. was abandoned when the eastern system of proglacial lakes and channels connected to the lower South Nahanni River (cyan arrow). The new divide was at about 576 m a.s.l., but rapidly dropped as the Laurentide ice margin retreated from the flanks of the Liard Range.

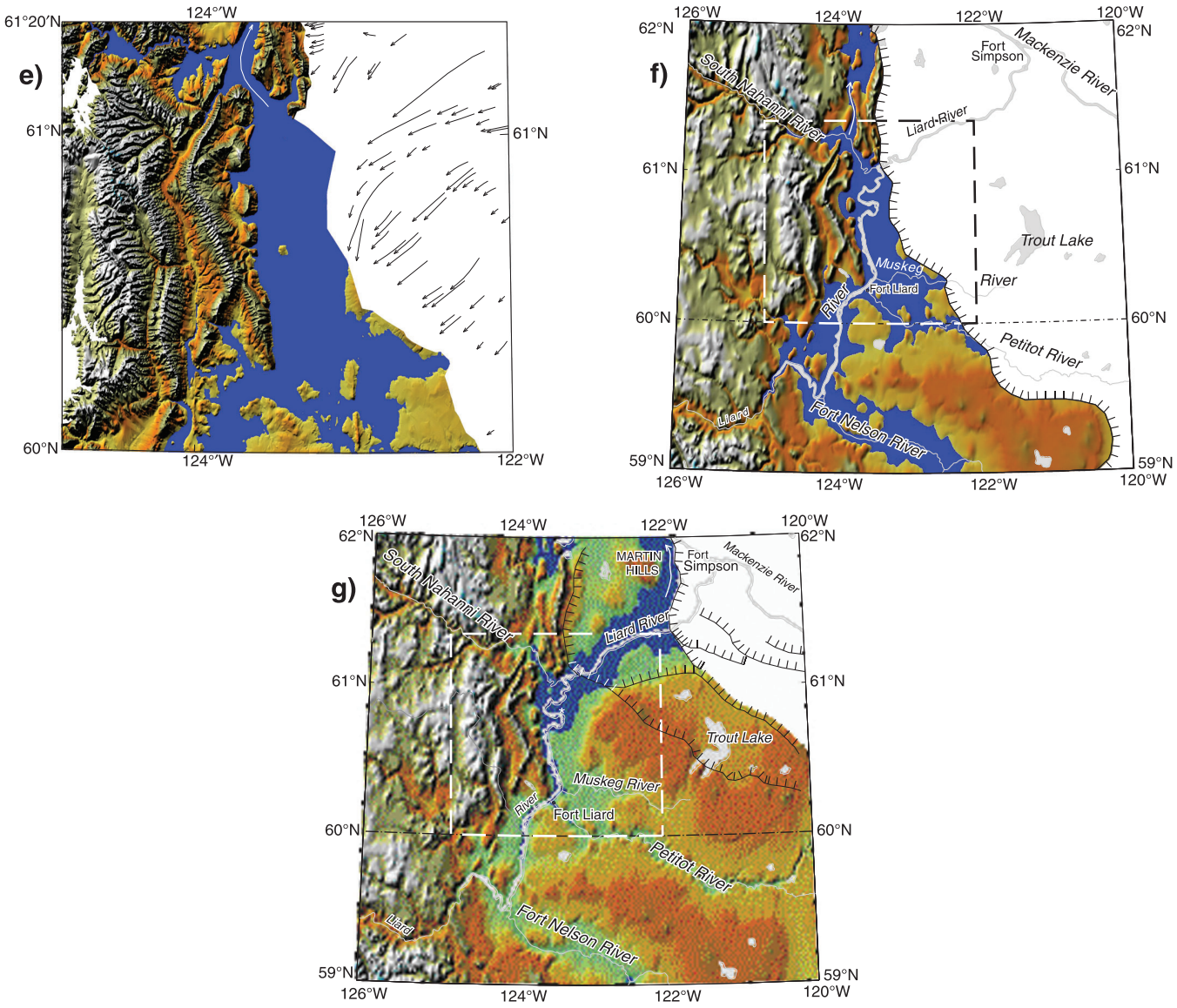

Figure 27. e) Paleogeography ca. 11.5 ka BP. The Laurentide Ice Sheet is no longer in contact with Liard Range, but still against the eastern flanks of Nahanni Range farther north. The level of glacial Lake Liard is maintained at about 400 m a.s.l. by drainage up the mouth of South Nahanni River. In the south, the lower Muskeg and Petitot rivers are inundated as the ice front receded. **f)** Regional paleogeography of the Laurentide Ice Sheet, ca. 11.5 ka BP, showing the southern extension of glacial Lake Liard up Fort Nelson River, given a lake level of 400 m a.s.l. This is probably the greatest areal expansion of the lake. The Cordilleran ice is not depicted. Dashed line shows the extent of Figures 27a to 27e. **g)** Regional paleogeography of the Laurentide Ice Sheet, ca. 11 ka BP, showing glacial Lake Liard at a level of 254 m a.s.l., when a prominent delta formed near Fort Liard. The outlet is east of Martin Hills. Hachured lines depict various ice-front positions defined by moraines and meltwater channels. Asterisk shows the location of deltaic sediments that were deposited when the lake dropped to about 220 m a.s.l. The Cordilleran ice is not depicted. Dashed line shows the extent of Figures 27a to 27e.

If the two flows were contemporaneous, the southward flow up Liard River valley would have to make a very abrupt turn northward as it met the main flow south of Mount Coty. Alternatively, an independent lobe of the Laurentide Ice Sheet may have flowed up Liard River valley from Mackenzie River valley prior to the main advance of the ice front. In this way the lobe would have been subsequently overridden by the main advance preserving the original bed forms at the lower elevations (*see* 'Glacial readvances'). The last possibility is that a lobe of the Laurentide Ice Sheet advanced up Liard River valley after the area was first deglaciated by the main ice front. While an attractive alternative, there are no moraines delineating such a lobate advance. Moraines and meltwater channels across the entire area show a coherent pattern of a common ice margin retreating northeastward.

Liard Range early phase (ca. 16–13 ka BP)

Rising global sea level shows that deglaciation of the continent was underway shortly after ca. 18 ka BP (Dyke, 2004). In the northwest sector of the Laurentide Ice Sheet, the Mackenzie lobe began retreating from Herschel Island ca. 16.2 ka BP (Dyke, 2004). The initial response in the Fort Liard area was likely thinning of the ice sheet and the formation of nunataks around the peaks of Liard Range. Eventually the Laurentide Ice Sheet retreated from the west side of Liard Range and glacial lakes formed in the exposed Kotaneelee, Chinkeh, and Jackfish river valleys (Fig. 27b). Stratigraphic sections along the lower Kotaneelee River have glaciolacustrine deposits to at least about 500 m a.s.l. If the lake level was more than 600 m a.s.l., water would have spilled into Chinkeh Creek, then to Jackfish River, and glacial Lake Nahanni. During this phase of deglaciation, the western margin of the Laurentide Ice Sheet abutted the eastern flanks of Liard Range. Meltwater was channelled westward through low spots along the mountains, especially north and west of Fisherman Lake, and through Kotaneelee River valley, south of Pointed Mountain.

During this phase of deglaciation, large volumes of meltwater would have been channelled along the Laurentide ice margin from the south. In British Columbia, Mathews (1980) described glaciolacustrine clay up to 820 m a.s.l. west of Fort Nelson, which he suggested was deposited in an early proglacial lake that extended along the lower valleys of the Dunedin, Toad, Liard, and Beaver rivers. He also identified a possible spillway on the east side of La Biche Range at 755 m a.s.l. (the possible site of Etanda Lakes) that would have drained northward along the western foot of Liard Range. The Etanda Lakes area has a large ice-contact delta on the southern end of the pass and signs of very large drainage events, but none of the thick glaciofluvial deposits was found to contain shield erratics, suggesting a Cordilleran ice source for the meltwater (Smith, 2003c). Mathews (1980) thought that a proglacial lake persisted in the lower Toad and Liard rivers, which drained from Beaver River valley at 520 m a.s.l., and then into La Biche and finally Kotaneelee river valleys, at about 440 m a.s.l., but, as noted earlier, the water level in the Kotaneelee River valley would have been impounded to more than 600 m a.s.l., which is the divide for northward drainage into Chinkeh Creek and glacial Lake Nahanni. Consequently, it is likely that the lower outlets described by Mathews (1980) could not have been used until the Laurentide Ice Sheet retreated east of Liard Range and exposed lower outlets into South Nahanni River drainage.

When the ice front retreated away from the crests of Liard Range, meltwater from the Laurentide Ice Sheet was diverted to the eastern flanks of the mountains and small proglacial lakes would have formed at the mouths of any ice-free valleys or indentations (Fig. 27c). At some point when the ice front retreated in the northwest part of the map area, meltwater spilled into Mattson Creek through several cols at about 790 m a.s.l. Farther south, near Fisherman Lake, glaciolacustrine sediments indicate a glacial lake formed in the basin at least 500 m a.s.l. Nevertheless, at a lake level of about 520 m a.s.l., this lake would have extended through the gap west of Fisherman Lake and joined the glacial lake in Kotaneelee River valley. Consequently, as noted above, it is likely that the lake level was about 600 m a.s.l., given the divide in Kotaneelee River valley. As the Laurentide margin retreated from Pointed Mountain, the lakes in the Fisherman Lake basin and Kotaneelee River valley would have become contiguous with the proglacial lake occupying the lower La Biche, Beaver, Toad, and Liard rivers (Mathews, 1980), thus forming the precursor to glacial Lake Liard.

Regionally, by 13 ka BP there was an overall thinning of Laurentide ice over the uplands that led to definition of individual lobes over the plains and a proto–Mackenzie delta was established in the north (Dyke et al., 2003). In the south, early phases of glacial Lake Peace drained into the Missouri River system, whereas, most proglacial drainage north of Lake Peace flowed to Beaufort Sea (Mathews, 1980). During the interval 13 ka BP to 11.5 ka BP the drainage of the eastern and western parts of the Mackenzie lobe merged into a single channel along the route of the postglacial Mackenzie River (Duk-Rodkin and Hughes, 1995). Further retreat of the Mackenzie lobe led to the formation of glacial Lake Mackenzie within Mackenzie River valley about 12 ka BP (Smith, 1992).

Liard Range late phase: early glacial Lake Liard (ca. 12 ka BP)

The retreat pattern of moraines suggests that deglaciation progressed at a greater rate in the southern part of the map area than in the north. In the south, the plains east of Lake Bovie were deglaciated while the ice margin remained against the mountain flanks in the north (Fig. 16, 27d). The faster retreat in the south may have been enhanced by calving into an expanding glacial Lake Liard, which maintained a level of about 600 m a.s.l., because the northern outlets east of Liard Range remained closed. In the north, as long as the Laurentide margin pressed against the eastern flanks of

Liard Range, meltwater continued to be channelled between the Liard and Kotaneelee ranges to the west. Nevertheless, on the eastern side of Liard Range, small, isolated proglacial lakes expanded within the mouths of recently exposed valleys. These lakes would have merged when north-trending mountain valleys were deglaciated. The result would have been an interconnected drainage system routing meltwater northward into proglacial lakes west of Mount Flett and Sawmill Mountain. The main spillway would have been into Mattson Creek at about 790 m a.s.l. until the Laurentide ice margin evacuated the mouth of South Nahanni River and a connection with glacial Lake Nahanni was made, making water levels drop below 600 m a.s.l. Early glacial Lake Liard did not drain through the eastern system until the Laurentide margin retreated from the easternmost ridges of the Liard Range at about 60°31.5'N, exposing a drainage divide at 576 m a.s.l. and finally abandoning the outlet west of Liard Range (Fig. 27d). Subsequent lake drainage progressed northward in steps as the receding ice margin exposed lower divides breaching into the north-trending valleys. Once the Laurentide ice margin left the easternmost flank of Liard Range, in the north part of the map area, glacial Lake Liard would have dropped to less than 400 m a.s.l. and joined with the glacial lake occupying the lower South Nahanni River valley (glacial Lake Tetcela; Ford (1976)).

Glacial Lake Liard (ca. 11.5 ka BP)

The most extensive phase of glacial Lake Liard formed when the Laurentide ice margin pulled away from the mountain front and glacial Lake Liard merged with the Tetcela phase of Lake Nahanni, forming a lake at about 400 m a.s.l. (Fig. 27e). During this period the patterns of moraines and meltwater channels indicate that the Laurentide ice margin retreated uniformly to the northeast across the map area so that the northeast corner of the map area was the last to be deglaciated. In the southern part of the map area glacial Lake Liard would have inundated broad lowlands along the lower Muskeg and Petitot rivers. Farther south in British Columbia, glacial Lake Liard may have extended more than 200 km up the Liard and Fort Nelson rivers to the Fort Nelson area, given the present-day topography (Fig. 27f). The southernmost extent of the lake would have been controlled by a bedrock canyon on Fort Nelson River, about 30 km upstream from the juncture with Liard River (Rampton, 1987).

The level of glacial Lake Liard fell quickly as the Laurentide ice margin receded from Liard Range and exposed lower outlets. Farther north, the Laurentide margin was still in contact with Nahanni Range and northward drainage continued to be directed through the lower South Nahanni and Tetcela river valleys. A lake level of about 362 m would be maintained as water flowed over the divide into Tetcela River, lower Nahanni River, and finally, Mackenzie River valley. Once the front of the Laurentide Ice Sheet receded from Nahanni Range, drainage of Lake Liard would have shifted to the east side of Nahanni Range, with a further drop in lake level to about 345 m a.s.l., as drainage was directed northward through the Sibbeston Lake area.

Regionally, by ca. 11.5 ka BP the northwestern Laurentide ice margin was marked by a series of meltwater channels along the Mackenzie Mountains front, which is traceable for over 600 km from South Nahanni River to Mountain River (Duk-Rodkin and Hughes, 1995), and glacial Lake Mackenzie occupied the lower Mackenzie River valley (Smith, 1992). In the south, the retreating Fort Nelson and Peace River lobes resulted in the formation of glacial Lake Hay and expansion of glacial Lake Peace (Mathews, 1980). Glacial Lake Hay drained northwest into glacial Lake Liard via Fort Nelson River and eventually into glacial Lake Mackenzie and the Beaufort Sea. Later, during this interval, a new spillway opened between glacial lakes Hay and Peace. The capture of Lake Peace increased the meltwater flow into glacial Lake Liard and along the Mackenzie Mountains front (Lemmen et al., 1994).

Glacial Lake Liard: late phase (ca. 11 ka BP)

The final stages of glacial Lake Liard were controlled by the Mackenzie lobe as it retreated toward Great Slave Lake. In the Fort Liard area during this phase the ice front formed a sublobe extending from the Mackenzie lobe. Varied ice flows just north of confluence of the South Nahanni and Liard rivers show the actions of the subsidiary lobe flowing up the lower Liard River valley. Consequently, fluctuations along the front of this lobe directly impacted the level of Lake Liard. On the plains to the southeast, the Laurentide ice margin stood at the moraines adjacent Trout and Tetcho lakes, east of the study area (Craig, 1965; Rutter et al., 1993) and a small proglacial lake was impounded in Trout Lake basin, which drained through successive spillways into Lake Liard via Muskeg River (Fig. 27g). Later stillstands are defined by meltwater channels and northwest-trending moraines northwest of Trout Lake, which show the ice margin receding toward Mackenzie River valley (Rutter et al., 1993). One of the final stages of glacial Lake Liard is defined by the prominent delta at Fort Liard at 254 m a.s.l., at the confluence of the Liard and Petitot rivers (Fig. 19). The lake dropped to this level when the Laurentide ice margin stood between the confluence of the Liard and Mackenzie rivers and Martin Hills (Fig. 27g). At this level, Lake Liard was restricted to the lower Liard and lower South Nahanni rivers. The next major lake level is indicated by the extensive deltaic sand at 220 m a.s.l., when glacial Lake Liard was confined the broad valley at the confluence of the South Nahanni and Liard rivers, narrowing northeastward within Liard River valley toward Mackenzie River. Finally, glacial Lake Liard drained into glacial Lake Mackenzie once the ice margin retreated east of the confluence of the Liard and Mackenzie rivers and a large delta was constructed at the mouth of Liard River (Smith, 1992, 1994).

Regionally, when the Mackenzie and Hay River ice lobes pulled back from Cameron Hills sometime after ca. 11 ka BP, glacial Lake Hay suddenly drained into the upper Mackenzie basin (Lemmen et al., 1994). Westward drainage was circumvented and the Liard and Fort Nelson rivers were no longer major conduits for Laurentide meltwater. The Mackenzie lobe retreated rapidly and by ca. 10.5 ka BP, it stood along the south shore of Great Slave Lake, marked by the Snake River moraine (Lemmen et al., 1994). In Great Bear Lake basin, major shifts in ice-flow direction took place due to calving into an expanding glacial Lake McConnell between 11 ka BP and 10.5 ka BP. In Great Slave Lake basin, once the ice front retreated from the Snake River moraine, glacial Lake Mackenzie was subsumed under glacial Lake McConnell after ca. 10.5 ka BP.

Glacial readvances

The history of deglaciation presented here shows the margin of the Laurentide Ice Sheet retreating progressively across the map area from about 13 ka BP to 10.5 ka BP (Fig. 27). In reality, however, overall ice retreat was probably punctuated by stillstands and readvances. Stillstands are marked by the larger moraine segments and meltwater channels in the study area, but moraine systems showing distinct glacial readvances are absent, although some readvances are recognized in the stratigraphic sections (e.g. Fig. 13). Nevertheless, there are features that appear to be overridden end moraines in several places. Generally, these are broad ridges of till, trending across the direction of former ice flow that have been fluted by the ice sheet (*see* 'Till and till landforms'; Fig. 16). If these features are end moraines, they suggest that significant readvances of the ice margin occurred. Less probably, these features could be subglacial bedforms from shearing and stacking of till, or even end moraines dating from the advance phase of glaciation. Further work would be necessary to determine their true nature.

The overridden ridges are concentrated in two main parts of the map area (Fig. 16). The first area is north of Muskeg River, mainly in Liard River valley where a series of subparallel ridges trend north to northwest, with a spacing of about 1 km. The second area is a broad ridge extending southeastward from Nahanni Range to Trout Lake, and beyond (*see* 'Till and till landforms'; Fig. 4). This ridge connects to similar ridges that follow the same trend as unaltered marine systems between Trout Lake and Trainor Lake with at least three other moraine complexes toward Mackenzie River valley. In detail, the broad ridge lies along the northeastern edge of an upland and is composed of a series of smaller ridges that were streamlined, with numerous intervening kettles. In both areas where the probable overridden moraines occur, the extent of the overriding advance is undetermined, because either the end moraines are masked within subsequent ice-retreat margins, or end-moraine building may have been hindered because the ice advanced into glacial Lake Liard. Surges under low basal shear stresses, such as would have occurred into a lake are suggested by the patterns of crevasse fillings in the map.

Dating these moraines based on their geographic position is also a problem because the ice front would have occupied the same location at least twice during deglaciation. The magnitude of the dating error would depend on the relative extent of the ice-marginal fluctuation, but if the readvances were limited, the general chronology presented earlier should provide a reasonable estimate. Consequently, the Laurentide ice margin stood at the western set of overridden moraines during the glacial Lake Liard phase at about 11.5 ka BP, during which time the lake outlet was west of Nahanni Range. The Laurentide ice margin stood at the easternmost moraines during the late phase of glacial Lake Liard between 11 ka BP and 10.5 ka BP, shortly before the final drainage of the lake into Mackenzie River basin.

Both changing glacier dynamics and climatic deterioration can cause a glacial readvance. The likelihood of the latter is greater if readvances took place across large areas of the Laurentide Ice Sheet. Dyke (2004) noted several intervals on a continental scale, when the Laurentide Ice Sheet paused or readvanced during overall retreat. An early readvance occurred from 14.5 ka BP to 14 ka BP, when ice readvanced on Kodiak Island, Alaska and the Hudson Strait ice stream re-expanded, which seemed to coincide with a sharp temperature decline at about 14.2 ka BP in the Summit ice core, Greenland. Nevertheless, when this readvance occurred the present study area was probably little affected because the Laurentide ice margin would have been west of the map area at the time. Following this, the Mackenzie lobe readvanced to the Tutsieta Lake and then the Kelly Lake moraines (Hughes, 1987) that Dyke (2004) placed at 12.5 ka and 12 ka BP, respectively. In the study area, these readvances would have occurred when the Laurentide ice was just retreating from the southern end of Liard Range, consequently the westernmost area of overridden moraines near the confluence of the Liard and Muskeg rivers may date from these readvances.

Correlations of major moraine systems have shown that perhaps the most widespread readvances of the Laurentide Ice Sheet took place during the Younger Dryas cold interval (11–10 ka BP) (Dyke and Saville, 2000; Dyke et al., 2003; Dyke, 2004). During this period, the Laurentide Ice Sheet retreated from the northeast part of the study map to just east of Slave River, Alberta (Bednarski, 1999). Consequently, the moraines in the northeastern part of the study area could have been overridden by a readvance related to the onset of the Younger Dryas interval.

ECONOMIC AND ENGINEERING GEOLOGY

This report describes the main physical properties and distribution of surficial materials in the Fort Liard area. Some aspects of surficial geology relevant to land-use concerns are outlined in this section.

Sand and gravel

Sand and gravel deposits in the form of glaciofluvial and alluvial terraces are found throughout most of the mountain valleys in the western part of the study area, providing a source for building aggregate. On the eastern plains, however, large boggy areas are devoid of aggregate on the surface, with most deposits being restricted to terraces along contemporary river valleys and some former meltwater channels. Although eskers are generally a good source of sand and gravel and a few small eskers were mapped in the eastern part of the study area, they do not appear to be well enough developed to be significant sources of aggregate. Nevertheless, small occurrences of gravel may be found by carefully tracing meltwater channels and end moraines. Other restricted deposits may be found along crevasse-fill ridges, but the gravel may be buried under a thin cover of till. The shotpoint data (Appendix B) suggest that substantial thicknesses of gravel lie below clay and till in some areas.

Peatlands and permafrost

The Fort Liard area lies within the southern fringe of discontinuous permafrost (Brown, 1967). Sporadic frozen ground can be found in peatlands and lacustrine sediments, but is absent in glaciofluvial materials and till, unless in the high alpine. In the eastern part, frozen ground is most likely in organic terrain dominated by peat plateaus and palsas, but even here large unfrozen areas occur (Zoltai and Tornacai, 1975) and collapse scars attest to the sensitivity of the substrate to disturbance. Organic terrain is detrimental to construction because peat has poor tractive strength when unfrozen. Moreover, in permafrost areas, any disturbance to the insulative cover is likely to cause surface instability by melting of any ground ice and liquefaction of soils. In the eastern part of the study area, fens, bog pools, and collapse scars are common along old cutlines where the vegetative cover has been disturbed. There is also a limited amount of data to suggest that permafrost is degrading in response to recent climatic warming (e.g. Nixon, 2000). Areas with high amounts of ground ice will be particularly vulnerable to further warming.

Landslides

The mountainous western part of the map area is subject to mass movement on steep mountain slopes, particularly as catastrophic landslides and debris flows, which is a major hazard for roads, pipelines, and buildings (e.g. Fig. 24). In Liard Range some large landslides occur along strike in cliffs of the Flett Formation, but, it is impossible to predict where and when the next one will occur. Consequently, it is recommended that a warning system be established by close monitoring of similar slopes. Another aspect concerning mountain slopes is that removal of the forest cover can cause substrate instability, especially along pipelines routed directly downslope (e.g. Fig. 25). As noted previously, outside of the mountains most landslides occurred along incised river valleys. These areas must be considered when planning river crossings for pipelines.

FUTURE RESEARCH

This study of the Quaternary geology of the Fort Liard area identifies a number of topics for future research under several broad categories:

- Geochronology: there is a need to address the lack of absolute chronological control for the deglacial sequence presented here. Deglacial dates may be obtained from bog coring, but the few basal dates from bogs in the surrounding region are usually younger than deglaciation (based on similar ages farther east; cf. Dyke et al. (2003)). In the mountains, cosmogenic exposure dating of large erratics or glacially polished mountain surfaces may prove useful in dating initial ice retreat and the establishment of the ice-free corridor between the Laurentide and Cordilleran ice sheets. This is important because all northward meltwater drainage between the two ice sheets was controlled by deglaciation of the corridor. Consequently, the existence and configuration of large ice-dammed lakes that extended far south would ultimately have been controlled by divides along the ice-free corridor. Some dating control may also be found in the subsurface. For example, some of the shotpoint logs (Appendix B) allude to woody material within the auger holes. In some places this organic material appears to be overlain by till, which may elucidate the timing of the glacial advance to the last glacial maximum or the readvances noted earlier.
- Cosmogenic exposure dating: striated bedrock on the crest of Liard Range indicates ice flow toward the east-northeast, which is opposite to the main Laurentide ice flow on the plains. This flow may be related to the main northward deflection of the Laurentide Ice Sheet or to an earlier Cordilleran advance from the west. Cosmogenic exposure dating of the striated surfaces may resolve this ambiguity.

- Mapping: the surficial geology mapping should be extended southward into British Columbia to further resolve the interaction of the Cordilleran and Laurentide ice sheets along Liard River and how meltwater was routed northward.
- Glacial processes: the rich assemblage of glacial bedforms found in the study area warrants further study. Morphostratigraphic relationships, structure, and sedimentology of the various ridges would establish their genesis; however, the few number of exposures available for study limits opportunities, and various means of imaging the subsurface would be necessary.
- Holocene fluvial geomorphology: numerous terrace exposures along Liard River could provide a wealth of information that could be used to reconstruct the recent fluvial history.
- Landslides: the Liard Range, an area of active economic development, has several large active and inactive landslides that should be monitored.
- Wetland and permafrost stability: a chronology of the major wetlands and their responses to past and future climate change should be established.

ACKNOWLEDGMENTS

The author wishes to acknowledge the help from many of the participants in the Geological Survey of Canada's Central Foreland NATMAP Project, and is grateful to A.S. Dyke and I.R. Smith for their thorough review of the manuscript.

REFERENCES

Bednarski, J.M., 1996. Preliminary report on mapping surficial geology of Trutch map area, northeastern British Columbia; *in* Current Research, Part A; Geological Survey of Canada, Paper 1999-A, p. 35–43.

Bednarski, J.M., 1999. Quaternary geology of northeastern Alberta; Geological Survey of Canada, Bulletin 535, 29 p.

Bednarski, J.M., 2001. Drift composition and surficial geology of the Trutch map area (94G), northeastern British Columbia; Geological Survey of Canada, Open File D3815 (CD-ROM).

Bednarski, J.M., 2002. Surficial geology, Fisherman Lake, Northwest Territories–Yukon Territory–British Columbia; Geological Survey of Canada, Open File 4360, scale 1:50 000.

Bednarski, J.M., 2003a. Surficial geology, Arrowhead Lake, Northwest Territories; Geological Survey of Canada, Open File 1775, scale 1:50 000.

Bednarski, J.M., 2003b. Surficial geology, Arrowhead River, Northwest Territories; Geological Survey of Canada, Open File 4483, scale 1:50 000.

Bednarski, J.M., 2003c. Surficial geology, Betalamea Lake, Northwest Territories–Yukon Territory–British Columbia; Geological Survey of Canada, Open File 4502, scale 1:50 000.

Bednarski, J.M., 2003d. Surficial geology, Celibeta Lake, Northwest Territories–British Columbia; Geological Survey of Canada, Open File 1754, scale 1:50 000.

Bednarski, J.M., 2003e. Surficial geology, Denedothada Creek, Northwest
Territories; Geological Survey of Canada, Open File 4480, scale 1:50 000.

Bednarski, J.M., 2003f. Surficial geology, Emile Lake, Northwest Territories;
Geological Survey of Canada, Open File 4477, scale 1:50 000.

Bednarski, J.M., 2003g. Surficial geology, Fort Liard, Northwest Territories–British Columbia; Geological Survey of Canada, Open File 1760, scale 1:50 000.

Bednarski, J.M., 2003h. Surficial geology, Lake Bovie, Northwest Territories–British Columbia; Geological Survey of Canada, Open File 1761, scale 1:50 000.

Bednarski, J.M., 2003i. Surficial geology, Mount Flett, Northwest Territories; Geological Survey of Canada, Open File 4481, scale 1:50 000.

Bednarski, J.M., 2003j. Surficial geology, Muskeg River, Northwest Territories; Geological Survey of Canada, Open File 1753, scale 1:50 000.

Bednarski, J.M., 2003k. Surficial geology, Netla River, Northwest Territories; Geological Survey of Canada, Open File 4478, scale 1:50 000.

Bednarski, J.M., 2003l. Surficial geology, Pointe-de-flèche River, Northwest Territories; Geological Survey of Canada, Open File 1773, scale 1:50 000.

Bednarski, J.M., 2003m. Surficial geology, Rabbit Creek, Northwest Territories; Geological Survey of Canada, Open File 4486, scale 1:50 000.

Bednarski, J.M., 2003n. Surficial geology, Sawmill Mountain, Northwest Territories; Geological Survey of Canada, Open File 4476, scale 1:50 000.

Bednarski, J.M., 2003o. Surficial geology, Tourbière River, Northwest Territories; Geological Survey of Canada, Open File 4487, scale 1:50 000.

Bednarski, J.M. and Smith, I.R., 2007. Laurentide and Montane glaciation along the Rocky Mountain Foothills of northeastern British Columbia; Canadian Journal of Earth Sciences, v. 44, p. 445–457.

Bell, R., 1900. An exploration of Great Slave Lake, N.W.T.; Geological Survey of Canada, Summary Report 1899, p. 103–110.

Bostock, H.S., 1970. Physiographic regions of Canada; Geological Survey of Canada, Map 1254A, scale 1:5 000 000.

Brown, R.J.E., 1967. Permafrost map of Canada; Geological Survey of Canada; Map 1246A, scale 1: 7 603 200.

Cameron, A.E., 1922. Post-glacial lakes in the Mackenzie River basin, North West Territories, Canada; Journal of Geology, v. 30, p. 337–353.

Catto N., Liverman, D.G.E., Bobrowsky, P.T., and Rutter, N., 1996. Laurentide, Cordilleran, and Montane glaciation in the western Peace River–Grand Prairie region, Alberta and British Columbia, Canada; Quaternary International, v. 32, p. 21–32.

Craig, B.G., 1965. Glacial Lake McConnell, and the surficial geology of parts of Slave River and Redstone River map-areas, District of Mackenzie; Geological Survey of Canada, Bulletin 122, 33 p.

Day, J.H., 1966. Reconnaissance soil survey of the Liard River valley, Northwest Territories; Research Branch, Canada Department of Agriculture, Ottawa, Ontario, 71 p.

Douglas, R.J.W., 1959. Great Slave and Trout River map areas, Northwest Territories, 85 S1/2 and 95 A, H; Geological Survey of Canada, Paper 58-11, 23 p.

Douglas, R.J.W. and Norris, D.K., 1959. Fort Liard and La Biche map areas, Northwest Territories and Yukon, 095B and 095C; Geological Survey of Canada, Paper 59-06, 23 p.

Douglas, R.J.W. and Norris, D.K., 1976. Geology, Fort Liard, District of Mackenzie; Geological Survey of Canada, Map 1379A, scale 1: 250 000.

Duk-Rodkin, A. and Huges, O.L., 1991. Age relationships of Laurentide and Montane glaciations, Mackenzie Mountains, Northwest Territories; Géographie physique et Quaternaire, v. 45, p. 79–90.

Duk-Rodkin, A. and Huges, O.L., 1992. Pleistocene montane glaciations in the Mackenzie Mountains, Northwest Territories; Géographie physique et Quaternaire, v. 46, p. 69–83.

Duk-Rodkin, A. and Huges, O.L., 1995. Quaternary geology of the northeastern part of the central Mackenzie Valley corridor, District of Mackenzie, Northwest Territories; Geological Survey of Canada, Bulletin 458, 45 p.

Duk-Rodkin, A., Barendregt, R.W., Tarnocai, C., and Philips, F.M., 1996. Late Tertiary to late Quaternary record in the Mackenzie Mountains, Northwest Territories, Canada: stratigraphy, paleosols, paleomagnetism, and clorine-36; Canadian Journal of Earth Sciences, v. 33, p. 875–895.

Dyke, A.S., 1990. Quaternary geology of the Frances Lake map area Yukon and Northwest Territories; Geological Survey of Canada, Memoir 426, 39 p.

Dyke, A.S., 1996. Preliminary paleogeographic maps of glaciated North America; Geological Survey of Canada, Open File 3296, 6 p.

Dyke, A.S., 2004. An outline of North American deglaciation with emphasis on central and northern Canada; *in* Quaternary Glaciations - Extent and Chronology, Part II, North America; (ed.) J. Ehlers and P.L. Gibbard; Elsevier, Amsterdam, Developments in Quaternary Science, p. 373–424.

Dyke, A.S. and Prest, V.K., 1987. Paleogeography of northern North America, 18 000-5000 years age; Geological Survey of Canada, Map 1703A, scale 1:12 500 000.

Dyke, A.S. and Savelle, J.M., 2000. Major end moraines of Younger Dryas age on Wollaston Peninsula, Victoria Island, Canadian Arctic: implications for paleoclimate and for formation of hummocky moraine; Canadian Journal of Earth Sciences, v. 37, p. 601–619.

Dyke, A.S., Moore, A., and Robertson, L., 2003. Deglaciation of North America; Geological Survey of Canada; Open File 1574 (CD-ROM).

Evans, D.J.A., Lemmen, D.S., and Brice, R.R., 1999. Glacial landsystems of the southwest Laurentide Ice Sheet: modern Icelandic analogues; Journal of Quaternary Science, v. 14, p. 673–691.

Fallas, K.M. and Lane, L.S., 2001. Geology of the Mount Martin, Fisherman Lake, and Mount Flett map areas, Yukon Territory and Northwest Territories; Geological Survey of Canada, Current Research 2001-A5, 19 p.

Fisher, D.A., Reeh, N., and Langely, K., 1985. Objective reconstruction of the Late Wisconsin Laurentide Ice Sheet and the significance of deformable beds; Géographie physique et Quaternaire, v. 39, p. 229–238.

Ford, D.C., 1976. Evidences of multiple glaciations in South Nahanni National Park, Mackenzie Mountains, Northwest Territories; Canadian Journal of Earth Sciences, v. 13, p. 1433–1445.

Fulton, R.J., (comp.) 1995. Surficial materials of Canada; Geological Survey of Canada, Map 1880A, scale 1:5 000 000.

Gordey, S.P. and Makepeace, A.J., (comp.), 1999. Yukon bedrock geology; *in* Yukon Digital Geology, (comp.) S.P. Gordey and A.J. Makepeace; Geological Survey of Canada, Open File D3826 (*also* Exploration and Geological Services Division, Yukon, Indian and Northern Affairs Canada, Open File 1999-1(D)).

Gough, L.P., Severson, R.C., and Shacklette, H.T., 1988. Element concentrations in soils and other surficial materials in Alaska; United States Geological Survey, Professional Paper 1458, 53 p.

Govett, G.J.S., 1983. Rock geochemistry in mineral exploration; *in* Volume 3, Handbook of Exploration Geochemistry. (ed.) G.J.S. Govett; Elsevier, New York, New York, 461 p.

Hage, C.O., 1944. Geology adjacent to the Alaska highway between Fort St. John and Fort Nelson, British Columbia; Geological Survey of Canada, Paper 44-30, 22 p.

Hage, C.O., 1945. Geological reconnaissance along lower Liard River, British Columbia, Yukon, and Northwest Territories; Geological Survey of Canada, Paper 45-22, 33 p.

Harington, C.R., (ed.) 2003. Annotated bibliography of Quaternary vertebrates of northern North America - with radiocarbon dates; University of Toronto Press, Toronto, Ontario, 360 p.

Hoffman, P.F. and McGlynn, J.C., 1977. Great Bear Batholith: a volcano-plutonic depression; *in* Volcanic Regimes in Canada, (ed.) W.R.A Baragar, L.C. Coleman, and J.M. Hall; The Geological Association of Canada, Special Paper Number 16, p. 169–192.

Hughes, O.L., 1987. Late Wisconsinan Laurentide glacial limits of northwestern Canada: the Tutsieta Lake and Kelly Lake phases; Geological Survey of Canada, Paper 85-25, 19 p.

Huscroft, C.A., Lipovsky, P.S., and Bond, J.D., 2004. A regional characterization of landslides in the Alaska Highway corridor; Yukon Geological Survey, Open File 2004-18, 76 p.

Hynes, G.F., Dixon, J.M., and Lane, L.S., 2002. Structural geology of the northern Liard Range, Franklin Mountains, Northwest Territories; Geological Survey of Canada, Current Research 2002-A5, 9 p.

Jackson, L.E., Jr., Phillips, F.M., Shimamura, K., and Little, E.C., 1997. Cosmogenic ^{36}Cl dating of the Foothills Erratics Train, Alberta Canada; Geology, v. 25, p. 195–198.

Jackson, L.E., Jr., Ward, B., Duk-Rodkin, A., and Huges, O., 1991. The last Cordilleran Ice Sheet in southern Yukon Territory; Géographie physique et Quaternaire, v. 45, p. 341–354.

Kigoshi, K., Aizawa, H., and Suzuki, N., 1969. Gakushuin natural radiocarbon measurements VII; Radiocarbon, v. 11, no. 2, p. 311–312.

Klassen, R.W., 1987. The Tertiary-Pleistocene stratigraphy of the Liard Plain, southeastern Yukon; Geological Survey of Canada, Paper 86-17, 16 p.

Lane, L.S., 2001. Geology, Fisherman Lake, Northwest Territories; Geological Survey of Canada, Open File 4161, scale 1:50 000.

Lane, L.S., 2006. Geology, Mount Flett, District of Mackenzie, Northwest Territories; Geological Survey of Canada, Open File 5236, scale 1:50 000.

Lane, L.S. and Hynes, G.F., 2005. Geology, Sawmill Mountain (95 B/13), District of Mackenzie, Northwest Territories; Geological Survey of Canada, Open File 4940, scale 1:50 000.

Lane, L.S., Cecile, M.P., Currie, L.D., and Stockmal, G.S., 1999. Summary of 1998 fieldwork in Trutch and Toad River map areas, Central Forelands NATMAP Project, northeastern British Columbia; *in* Current Research 1999-E, Part E; Geological Survey of Canada, Paper 1999-E, p. 1–8.

Lemmen, D.S., Duk-Rodkin, A., and Bednarski, J.M., 1994. Late glacial drainage systems along the northwestern margin of the Laurentide Ice Sheet; Quaternary Science Reviews, v. 13, p. 805–828.

Levinson, A.A., 1974. An Introduction to Exploration Geochemistry; Applied Publishing Ltd., Wilmette, Illinois, 612 p.

Levinson, A.A., 1980. An Introduction to Exploration Geochemistry. The 1980 Supplement; Applied Publishing Ltd., Wilmette, Illinois, p. 615–924.

Levson, V., Ferbey, T., Kerr, B., Johnsen, T., Bednarski, J., Smith, R., Blackwell, J., and Jonnes, S., 2004. Quaternary geology and aggregate mapping in northeast British Columbia: applications for oil and gas exploration and development; *in* Regional Overview Papers, Overview 2003–2004; Oil and Gas Division, British Columbia Ministry of Energy, Mines and Petroleum Resources, 12 p.

Lowdon, J.A., Wilmeth, R., and Blake, W., Jr., 1970. Geological Survey of Canada Radiocarbon Dates X; Geological Survey of Canada, Paper 70-2, Part B (second report), p. 482–483.

Massey, N.W.D., MacIntyre, D.G., Okulitch, A.V., and Desjardins, P.J., 2003. Digital geology map of British Columbia: tile NO10 northeast B.C.; British Columbia Ministry of Energy and Mines, Geofile 2003-14, scale 1:250 000.

Mathews, W.H., 1963. Quaternary stratigraphy and geomorphology of the Fort St. John area, northeastern British Columbia; Department of Mines and Petroleum Resources, Victoria, British Columbia, 22 p.

Mathews, W.H., 1974. Surface profiles of the Laurentide Ice Sheet in its marginal areas; Journal of Glaciology, v. 13, p. 37–43.

Mathews, W.H., 1978. Quaternary stratigraphy and geomorphology of Charlie Lake (94A) map area, British Columbia; Geological Survey of Canada, Paper 76-20, 25 p.

Mathews, W.H., 1980. Retreat of the last ice sheets in northeastern British Columbia and adjacent Alberta; Geological Survey of Canada, Bulletin 331, 22 p.

Matthews, J.V., Jr., 1980. Paleoecology of John Klondike Bog, Fisherman Lake region, southwest District of Mackenzie; Geological Survey of Canada, Paper 80-22, 12 p.

McConnell, R.G., 1891. Report on an exploration in the Yukon and MacKenzie Basins, N.W.T.; Geological Survey of Canada, Annual Report IV, Part D.

McNeely, R., 1989. Geological Survey of Canada Radiocarbon Dates XXVIII; Geological Survey of Canada, Paper 88-7, p. 57.

McNeely, R. and McCuaig, S., 1991. Geological Survey of Canada Radiocarbon Dates XXIX; Geological Survey of Canada, Paper 89-7, 134 p.

Millar, J.F.V., 1968. Archeology of Fisherman Lake, western District of MacKenzie, N.W.T.; Ph.D. dissertation, University of Calgary, Calgary, Alberta, 496 p.

Mix, A.C., Dard, E., and Schneider, R., 2001. Environmental processes of the ice age: land ocean, glaciers (EPILOG); Quaternary Science Reviews, v. 20, p. 627–657.

Nixon, F.M., 2000. Thaw-depth monitoring; *in* The Physical Environment of the Mackenzie Valley, Northwest Territories: a Base Line for the Assessment of Environmental Change, (ed.) L.D. Dyke and G.R. Brooks; Geological Survey of Canada, Bulletin 547, p. 119–126.

Piët, L.J.M., 1992. Paleogeography and sedimentology of fluvial point bars, chute-fills and oxbow-fills in the lower Liard River, NWT; M.Sc. thesis, University of Calgary, Calgary, Alberta, 107 p.

Prest, V.K., 1983. Canada's heritage of glacial features; Geological Survey of Canada, Miscellaneous Report 28, 119 p.

Rampton, V.N., 1987. Late Wisconsin deglaciation and Holocene river evolution near Fort Nelson, northeastern British Columbia; Canadian Journal of Earth Sciences, v. 24, p. 188–191.

Rutter, N.W., 1974. Surficial geology and land classification, Mackenzie valley transportation corridor (85D, E, 95A, B, G, H, I, J, K, N, O); *in* Report of Activities, Part A; Geological Survey of Canada, Paper 74-1A, p. 285.

Rutter, N.W. and Boydell, A.N., 1973. Surficial geology and land classification, Mackenzie valley transportation corridor (85D, 95B (north half), 95 G, I, K (east half), N, O); *in* Report of Activities, Part A; Geological Survey of Canada, Paper 73-1A, p. 239–241.

Rutter, N.W. and Minning, G.V., 1972. Surficial geology and land classification, Mackenzie valley transportation corridor (85E, 95A, B (south half), H, J); *in* Report of Activities, Part A; Geological Survey of Canada, Paper 72-1A, p. 178.

Rutter, N.W., Hawes, R.J., and Catto, N.R., 1993. Surficial geology, southern Mackenzie River valley, District of Mackenzie, Northwest Territories; Geological Survey of Canada, Map 1693A, scale 1: 500 000.

Rutter, N.W., Minning, G.V., Netterville, J.A., and Boydell, A.N., 1980. Surficial geology and geomorphology, Fort Liard, District of Mackenzie, Northwest Territories; Geological Survey of Canada, Map 11-1979, scale 1: 125 000.

Sharp, M., 1984. Annual moraine ridges at Skálafellsjökull, south-east Iceland; Journal of Glaciology, v. 30, p. 82–93.

Smith, D.G., 1992. Glacial Lake Mackenzie, Mackenzie valley, Northwest Territories, Canada; Canadian Journal of Earth Sciences, v. 29, p. 1756–1766.

Smith, D.G., 1994. Glacial Lake McConnell: paleogeography, age, duration, and associated river deltas, Mackenzie River basin, western Canada; Quaternary Science Reviews, v. 13, p. 829–843.

Smith, I.R., 2000. Preliminary report on surficial geology investigations of La Biche River map area, southeast Yukon Territory; *in* Current Research 2000; Geological Survey of Canada, 9 p. (CD-ROM).

Smith, I.R., 2002a. Surficial geology, Mount Martin, Yukon Territory–Northwest Territories–British Columbia; Geological Survey of Canada, Open File 4260, scale 1:50 000.

Smith, I.R., 2002b. Surficial geology, Mount Merrill, Yukon Territory–British Columbia; Geological Survey of Canada, Open File 4324, scale 1:50 000.

Smith, I.R., 2003a. Surficial geology, Babiche Mountain, Yukon Territory–Northwest Territories; Geological Survey of Canada, Open File 1558, scale 1:50 000.

Smith, I.R., 2003b. Surficial geology, Chinkeh Creek, Northwest Territories–Yukon Territory; Geological Survey of Canada, Open File 1615, scale 1:50 000.

Smith, I.R., 2003c. Surficial geology, Etanda Lakes, Northwest Territories–Yukon Territory; Geological Survey of Canada, Open File 1671, scale 1:50 000.

Smith, I.R., 2003d. Surficial geology, Brown Lake, Yukon Territory; Geological Survey of Canada, Open File 1771, scale 1:50 000.

Smith, I.R., 2004a. Surficial geology, Tika Creek, Yukon Territory–British Columbia; Geological Survey of Canada, Open File 4702, scale 1:100 000.

Smith, I.R., 2004b. Surficial geology, La Biche River (southwest), Yukon Territory–British Columbia; Geological Survey of Canada, Open File 4680, scale 1:100 000.

Smith, I.R., Grasby, S.E., and Lane, L.S., 2005. An investigation of gas seeps and aquatic chemistry in Fisherman Lake, southwest Northwest Territories; Geological Survey of Canada, Current Research 2005-A3, 8 p.

Tarnocai, C., 1973. Soils of the Mackenzie River area; Environmental-Social Committee, Northern Pipelines, Report 73-26, 136 p.

Tempelman-Kluit, D., 1980. Evolution of physiography and drainage in southern Yukon; Canadian Journal of Earth Sciences, v. 17, p. 1189–1203.

Wheeler, J.O., Hoffman, P.F., Card, K.D., Davidson, A., Sanford, B.V., Okulitch, A.V., and Roest, W.R., (comp.), 1997. Geological Map of Canada; Geological Survey of Canada, Map D1860A, scale 1: 5 000 000.

Zoltai, S.C. and Tarnocai, C., 1975. Perennially frozen peatlands in the western Arctic and Subarctic of Canada; Canadian Journal of Earth Sciences, v. 12, p. 28–43.

Appendix A. Sample analyses. See also data on CD-ROM (not edited to GSC style)

Appendix A1. Analysis of samples from Fort Laird area.

SAMPLE		UTM LOCATION			MATERIAL	GRAIN SIZE (wt %)				ATTERBERG LIMITS			CARBON (%) by LECO			CHITTICK			
		UTM Zone 10; NAD 83				<2 mm fraction (% sand-silt-clay)											Total		
Sample no.	Easting	Northing	Latitude (N)	Longitude (W)		>2 mm (%)	2 mm–63 µm	63–2 µm	<2 µm	Liquid limit	Plastic limit	Plasticity index	Total C (%)	LOI	Inorganic	Organic	Calcite (%)	Dolomite (%)	Carbonate	C/D ratio
00BJB0002	491379	6663807	60.1112135	123.15508	Diamicton	21.87	29.51	61.32	9.16	30.83	17.02	13.81	1.5	4.1	0.9	0.6	—	—	—	—
00BJB0003	501330	6655303	60.0349433	122.97613	Diamicton	9.14	30.94	58.08	10.98	35.80	16.85	18.95	2.0	4.4	1.5	0.5	—	—	—	—
00BJB0007	501629	6653762	60.0211053	122.97078	Diamicton	5.01	16.02	81.22	2.76	25.03	18.51	6.52	2.1	2.2	1.7	0.4	—	—	—	—
00BJB0008	482985	6670961	60.1751858	123.30667	Diamicton	11.75	35.26	53.73	11.01	31.29	16.21	15.08	1.6	4.2	1.2	0.4	—	—	—	—
00BJB0009	483020	6685914	60.3094473	123.3073	Sand	0.05	95.22	4.47	0.30	Too sandy	—	—	4.3	4.0	3.4	0.9	—	—	—	—
00BJB0010	482334	6692904	60.3721788	123.32033	Diamicton	0.11	1.49	69.78	28.72	56.85	25.87	30.97	2.1	5.7	1.3	0.8	—	—	—	—
00BJB0011	481408	6696193	60.4016679	123.33742	Diamicton	17.50	38.20	52.86	8.94	28.89	14.92	13.97	1.9	3.6	1.4	0.5	—	—	—	—
00BJB0012	480488	6699834	60.4343154	123.35447	Diamicton	17.45	37.18	54.83	7.99	30.59	16.40	14.19	2.9	4.8	1.9	1.0	—	—	—	—
00BJB0013	474484	6710908	60.5334064	123.46497	Diamicton	29.80	47.44	47.38	5.18	Too sandy	—	—	2.2	3.0	1.7	0.5	—	—	—	—
00BJB0014	473735	6716316	60.5819123	123.47933	Diamicton	6.97	21.56	66.25	12.19	40.19	18.23	21.96	1.3	4.2	0.7	0.6	—	—	—	—
00BJB0015	472707	6723338	60.6448878	123.49907	Diamicton	5.65	32.64	57.94	9.42	32.96	17.47	15.48	1.9	4.8	1.1	0.8	—	—	—	—
00BJB0016	475502	6726312	60.4343154	123.35447	Sand	60.57	90.45	8.85	0.70	Too sandy	—	—	—	—	—	—	—	—	—	—
00BJB0017	480850	6731670	60.7201661	123.35098	Sand	0.06	2.32	92.92	4.76	26.24	20.44	5.79	4.3	1.8	4.0	0.3	—	—	—	—
00BJB0018	487064	6743891	60.8301376	123.23791	Clay	0.02	0.98	87.86	11.16	39.34	21.31	18.03	2.4	4.0	1.9	0.5	—	—	—	—
00BJB0019	494900	6756041	60.9393988	123.09412	Sand	0.03	6.67	91.03	2.30	28.76	24.54	4.22	2.5	2.0	2.1	0.4	—	—	—	—
00BJB0021	473243	6680600	60.2612085	123.48353	Diamicton	5.31	30.73	57.89	11.38	38.43	18.35	20.08	2.2	5.4	1.4	0.8	—	—	—	—
00BJB0022	471850	6686431	60.3134682	123.50951	Diamicton	20.20	36.84	51.86	11.30	33.75	15.27	18.49	2.0	4.4	1.2	0.8	—	—	—	—
00BJB0023	470702	6696805	60.4065287	123.53181	Diamicton	4.56	48.21	44.41	7.38	24.38	16.45	7.93	2.3	2.7	1.9	0.4	—	—	—	—
00BJB0024	469346	6702793	60.4601899	123.55734	Diamicton	24.32	32.26	54.98	12.76	34.68	15.32	19.35	3.0	4.4	2.3	0.7	—	—	—	—
00BJB0025	464945	6708660	60.5125057	123.63838	Diamicton	25.27	37.37	49.95	12.68	35.60	16.36	19.25	2.1	4.8	1.7	0.4	—	—	—	—
00BJB0026	469142	6721944	60.6321137	123.56403	Clay	0.82	5.14	80.78	14.08	42.11	20.84	21.27	2.1	4.5	1.6	0.5	—	—	—	—
00BJB0028	463099	6723719	60.6475382	123.67481	Silt	11.45	27.78	68.78	3.45	23.82	19.44	4.38	0.7	3.1	0.0	0.7	—	—	—	—
00BJB0029	468011	6704247	60.4731405	123.58184	Diamicton	25.00	24.85	67.19	7.96	32.04	17.30	14.74	2.9	3.4	2.5	0.4	—	—	—	—
00BJB0030	479869	6675355	60.2144969	123.36327	Diamicton	0.45	4.75	66.24	29.00	57.62	24.69	32.93	2.2	5.5	1.6	0.6	—	—	—	—
00BJB0031	482317	6671616	60.1810386	123.31877	Diamicton	14.73	42.78	48.36	8.87	25.99	14.44	11.55	1.5	4.1	1.0	0.5	—	—	—	—
01BJB0002	447151	6679768	60.2511855	123.95476	Diamicton	6.04	28.32	61.87	9.81	33.15	15.08	18.07	2.0	4.7	1.1	0.9	3.5	6.33	9.83	0.55
01BJB0003	449979	6700214	60.4351005	123.90877	Diamicton	36.84	32.75	60.63	6.62	24.55	15.66	8.88	1.4	3.9	0.8	0.6	1.69	4.51	6.2	0.37
01BJB0004	454953	6673411	60.1950507	123.81242	Diamicton	0.82	21.32	72.77	5.90	21.69	17.48	4.20	0.5	3.2	0.0	0.5	1.37	0.91	2.28	1.51
01BJB0006	538899	6682840	60.2803396	122.29664	Diamicton	0.00	4.17	80.47	15.36	35.25	19.50	15.74	2.5	5.2	1.4	1.1	2.63	4.52	7.15	0.58
01BJB0007	538899	6682840	60.2803396	122.29664	Diamicton	12.16	27.34	60.18	12.48	34.79	18.00	16.79	2.0	3.9	1.3	0.7	5.13	6.79	11.92	0.76
01BJB0008	489134	6666401	60.1344516	123.1956	Diamicton	16.16	56.34	40.31	3.35	21.07	16.00	5.07	2.4	5.2	1.6	0.8	5.65	5.43	11.08	1.04
01BJB0009	501164	6656217	60.0431508	122.9791	Diamicton	13.54	34.03	56.36	9.61	30.30	18.58	11.71	2.1	4.5	1.3	0.8	5.07	7.91	12.98	0.64
01BJB0010	498884	6692356	60.3676424	123.02023	Diamicton	14.68	38.29	53.50	8.20	28.04	16.74	11.30	2.4	4.0	1.2	1.2	3.95	6.79	10.74	0.58
01BJB0011	498978	6692401	60.3680467	123.01853	Diamicton	9.01	24.80	69.73	5.47	24.68	17.17	7.51	1.9	6.0	0.8	1.1	3.22	7.46	10.68	0.43

— no data

Appendix A1. (cont.)

SAMPLE		UTM LOCATION			MATERIAL	GRAIN SIZE (wt %)				ATTERBERG LIMITS			CARBON (%) by LECO			CHITTICK				
UTM Zone 10; NAD 83						<2 mm fraction (% sand-silt-clay)											Total			
Sample no.	Easting	Northing	Latitude (N)	Longitude (W)		>2 mm (%)	2 mm–63 µm	63–2 µm	<2 µm	Liquid limit	Plastic limit	Plasticity index	Total C (%)	LOI	Inorganic	Organic	Calcite (%)	Dolomite (%)	Carbonate	C/D ratio
01BJB0012	498978	6692401	60.3680467	123.01853	Sand	7.90	92.69	6.71	0.60	—	—	—	—	—	—	—	—	—	—	—
01BJB0013	502810	6649791	59.9854423	122.94964	Diamicton	6.34	42.71	48.96	8.33	32.66	19.66	13.00	1.1	2.9	0.6	0.5	2.45	3.17	5.62	0.77
01BJB0014	500662	6650511	59.9919164	122.98813	Sand	3.62	72.06	26.54	1.40	Too sandy	—	—	1.5	6.0	0.8	0.7	2.42	4.07	6.49	0.59
01BJB0015	494512	6658194	60.0608676	123.09857	Silt	14.67	61.50	36.79	1.72	28.60	20.98	7.62	2.8	3.7	1.7	1.1	3.85	9.04	12.89	0.43
01BJB0018	462782	6672299	60.1858565	123.67103	Diamicton	8.47	24.77	62.23	12.99	36.06	19.70	16.36	2.1	5.1	1.1	1.0	3.95	6.54	10.49	0.6
01BJB0021	456397	6660624	60.0804031	123.78364	Diamicton	6.10	20.63	67.21	12.16	32.03	18.79	13.24	1.9	4.1	1.0	0.9	2.13	5.19	7.32	0.41
01BJB0022	456397	6660624	60.0804031	123.78364	Diamicton	13.67	30.15	56.60	13.25	36.23	19.74	16.49	1.5	4.9	0.9	0.6	2.63	4.51	7.14	0.58
01BJB0023	460107	6668155	60.1483975	123.71844	Diamicton	0.66	29.93	60.27	9.80	28.94	18.72	10.21	1.5	6.0	0.0	1.5	0.7	0	0.7	
01BJB0024	480459	6688382	60.3314914	123.35388	Diamicton	23.42	74.72	24.29	0.99	Too sandy	—	—	1.7	3.0	1.4	0.3	2.72	7.88	10.6	0.35
01BJB0025	477799	6696736	60.4063612	123.40298	Diamicton	6.55	29.24	64.49	6.27	28.75	16.40	12.35	1.7	4.9	1.0	0.7	3.1	4.28	7.38	0.72
01BJB0027	521608	6681435	60.2690119	122.60943	Diamicton	25.59	42.56	50.25	7.19	26.10	14.30	11.80	2.4	4.6	1.4	1.0	2.2	9.02	11.22	0.24
01BJB0028	509733	6686582	60.3156836	122.82382	Diamicton	15.71	30.02	61.62	8.36	32.28	19.02	13.26	2.4	5.2	1.4	1.0	5.12	6.55	11.67	0.78
01BJB0030	482782	6736678	60.7652166	123.31602	Clay	0.00	0.45	88.11	11.44	35.20	20.81	14.39	3.1	4.4	1.9	1.2	5.19	11.1	16.29	0.47
02BJB0004	445894	6711609	60.5368699	123.98607	Diamicton	14.67	49.77	45.88	4.35	21.10	15.63	5.47	1.3	2.9	0.7	0.6	2.66	3.36	6.02	0.79
02BJB0005	453065	6738977	60.783463	123.86194	Diamicton	4.21	12.53	74.12	13.35	36.84	20.46	16.38	1.8	4.0	1.1	0.7	4.03	4.49	8.52	0.90
02BJB0008	460260	6738763	60.7823249	123.72978	Gravel	43.48	81.95	16.15	1.90	Too sandy	—	—	3.1	3.1	2.3	0.8	9.3	7.64	16.94	1.22
02BJB0009	454629	6750572	60.8877346	123.83594	Diamicton	9.39	22.92	65.70	11.39	37.68	17.83	19.86	1.7	4.4	0.9	0.8	3.82	4.04	7.86	0.95
02BJB0010	512449	6716667	60.5857299	122.77278	Diamicton	11.81	28.82	59.56	11.62	32.79	15.50	17.29	2.5	3.7	1.5	1.0	5.61	5.83	11.44	0.96
02BJB0011	536641	6748959	60.8741569	122.3252	Diamicton	3.91	30.50	61.76	7.74	36.42	22.10	14.33	0.6	4.8	0.0	0.6	0.7	0	0.7	
02BJB0012	502381	6739395	60.7899752	122.95627	Diamicton	24.64	54.01	42.39	3.60	33.03	22.47	10.56	0.6	3.4	0.0	0.6	1.15	0.23	1.38	5.00
02BJB0013	509771	6686378	60.313851	122.82314	Diamicton	5.56	27.23	59.43	13.34	39.31	19.26	20.04	2.8	4.8	1.5	1.3	2.69	8.32	11.01	0.32
02BJB0014	516430	6687002	60.3192388	122.70257	Diamicton	0.34	27.47	65.21	7.32	33.61	20.16	13.45	0.6	3.6	0.0	0.6	1.16	0.23	1.39	5.04
02BJB0015	529059	6691366	60.3577127	122.47332	Diamicton	4.53	26.21	61.23	12.56	38.00	18.23	19.77	2.4	4.6	1.0	1.4	3.23	6.28	9.51	0.51
02BJB0016	545774	6682380	60.2754935	122.17244	Diamicton	11.85	27.47	59.93	12.60	36.43	16.69	19.75	2.6	4.1	1.4	1.2	5.55	6.04	11.59	0.92
02BJB0017	487056	6743909	60.830299	123.23805	Clay	0.00	1.98	85.69	12.33	33.59	18.72	14.87	2.9	3.0	2.5	0.4	5.78	12.32	18.1	0.47
02BJB0018	494921	6756053	60.9395068	123.09373	Sand	0.00	37.00	60.89	2.11	Too sandy	—	—	3.1	1.5	2.9	0.2	4.91	16.86	21.77	0.29
02BJB0019	454313	6689420	60.3387078	123.82758	Clay	1.03	9.07	75.11	15.82	44.11	25.45	18.66	2.9	4.6	2.0	0.9	11.02	4.29	15.31	2.57
02BJB0020	456795	6658882	60.064805	123.77612	Clay	0.00	0.63	92.25	7.11	38.84	22.29	16.55	2.5	4.0	1.0	1.5	2.29	6.5	8.79	0.35
02BJB0021	467303	6671258	60.1768973	123.58936	Clay	0.09	2.06	78.63	19.31	47.87	25.83	22.04	1.9	3.4	1.4	0.5	4.91	5.63	10.54	0.87
02BJB0022	485274	6668090	60.1494963	123.26521	Diamicton	7.74	28.10	60.44	11.45	36.31	20.98	15.34	1.8	4.4	0.9	0.9	2.62	4.26	6.88	0.62
02BJB0023	459617	6719493	60.6092625	123.73761	Diamicton	21.68	48.13	43.60	8.26	31.71	19.33	12.37	1.1	5.5	0.0	1.1	1.15	0.23	1.38	5.00

— no data

Appendix A2. Instrumental neutron activation analysis data for all surficial material samples.

Sample ID	Au (ppb)	Ag (ppm)	As (ppm)	Ba (ppm)	Br (ppm)	Ca (%)	Cd (ppm)	Co (ppm)	Cr (ppm)	Cs (ppm)	Fe (%)	Hf (ppm)	Hg (ppm)	Ir (ppb)	Mo (ppm)	Na (%)	Ni (ppm)	Rb (ppm)	Sb (ppm)	Sc (ppm)
00BJB0002	-2	3	19	940	1.6	na	-5	16	71	5.7	4.1	9	na	-50	3	0.55	47	100	1.2	12
00BJB0003	-2	-2	17	860	2.1	na	-5	18	94	5.8	4.1	7	na	-50	4	0.57	29	93	1.1	13
00BJB0007	-2	-2	11	840	1.7	na	-5	10	49	2.8	2.4	9	na	-50	3	0.83	25	56	0.7	8.6
00BJB0008	-2	-2	19	980	2.4	na	-5	15	110	6	4.2	7	na	-50	4	0.55	57	100	1.3	13
00BJB0009	7	-2	36	1100	4.2	na	-5	42	56	2.8	5.7	11	na	-50	19	0.66	120	67	2.3	10
00BJB0010	-2	-2	13	880	3.5	na	-5	15	100	7.2	3.8	5	na	-50	2	0.41	35	110	1.3	15
00BJB0011	-2	-2	14	810	1.6	na	-5	14	95	4.8	3.8	7	na	-50	3	0.57	49	90	0.9	12
00BJB0012	-2	-2	14	710	3.9	na	-5	13	73	4.6	3.5	8	na	-50	2	0.62	39	69	1	10
00BJB0013	-2	-2	16	830	3.4	na	-5	12	53	3	3.2	13	na	-50	1	0.69	43	56	0.9	8.1
00BJB0014	5	-2	13	870	1.2	na	-5	19	90	6.3	3.5	7	na	-50	1	0.45	35	97	0.8	13
00BJB0015	4	-2	13	790	1.4	na	-5	14	82	6	3.8	8	na	-50	4	0.51	46	89	0.9	13
00BJB0017	4	-2	9.4	1100	1.4	na	-5	7	63	2.9	2.5	6	na	-50	1	0.57	34	66	1.1	8
00BJB0018	4	-2	13	910	1	na	-5	11	83	5.5	3.5	7	na	-50	3	0.53	50	97	1.1	11
00BJB0019	-2	-2	9.1	1000	1.9	na	-5	7	80	2.5	2.5	8	na	-50	1	0.88	29	55	1.1	8.2
00BJB0021	4	-2	13	830	5.4	na	-5	16	88	5.6	3.5	7	na	-50	3	0.56	48	81	1.1	12
00BJB0022	-2	-2	16	800	0.9	na	-5	15	100	5.8	4.1	8	na	-50	3	0.45	35	95	0.8	14
00BJB0023	-2	-2	10	390	1.5	na	-5	7	97	3.1	2.4	16	na	-50	2	0.3	31	55	0.6	8.2
00BJB0024	-2	-2	12	610	1.6	na	-5	14	92	5.3	3.6	6	na	-50	2	0.45	50	89	0.7	12
00BJB0025	-2	-2	14	460	1.8	na	-5	16	120	6.2	3.8	7	na	-50	2	0.3	44	97	0.7	12
00BJB0026	5	-2	15	970	1.5	na	-5	14	97	7.1	4	6	na	-50	3	0.46	66	98	1.4	12
00BJB0028	-2	2	13	390	0.9	na	-5	-5	110	1.7	1.6	22	na	-50	-1	0.12	-10	34	0.6	11
00BJB0029	-2	3	12	680	2.6	na	-5	10	93	4.6	3.1	8	na	-50	1	0.55	50	78	0.9	11
00BJB0030	4	2	14	680	1.9	na	-5	15	88	6.8	3.7	5	na	-50	4	0.41	47	110	1	14
00BJB0031	-2	-2	19	940	1.5	na	-5	14	100	5.8	3.6	8	na	-50	2	0.56	57	97	1.2	12
01BJB0002	-2	-2	12	690	0.8	na	-5	10	65	4.5	3	6	na	-50	2	0.47	23	78	0.8	9.3
01BJB0003	10	-2	13	360	1.1	na	-5	7	120	4.4	2.7	11	na	-50	2	0.3	38	73	0.6	9.1
01BJB0004	8	-2	21	830	1.4	na	-5	9	100	4.1	2.6	15	na	-50	1	0.1	27	61	1.1	10
01BJB0006	4	-2	13	680	1.1	na	-5	17	83	5.2	3.6	5	na	-50	4	0.49	43	84	1	12
01BJB0007	4	-2	12	650	1.3	na	-5	14	92	5	3.3	5	na	-50	5	0.52	47	88	0.9	12
01BJB0008	-2	-2	24	770	2.5	na	-5	11	68	3.1	3.4	10	na	-50	2	0.68	24	60	1	8.5
01BJB0009	-2	-2	15	590	2.6	na	-5	16	80	4.3	4.1	8	na	-50	4	0.47	47	63	0.9	11
01BJB0010	4	-2	13	630	0.9	na	-5	11	77	4.6	3.5	7	na	-50	3	0.56	26	79	0.7	11
01BJB0011	-2	-2	11	620	1	na	-5	12	72	3.7	2.9	8	na	-50	3	0.57	24	66	0.8	9.1
01BJB0013	5	-2	18	710	1.2	na	-5	19	70	4.5	3.9	7	na	-50	9	0.56	42	83	1.3	11
01BJB0014	4	-2	12	740	0.9	na	-5	10	66	2.4	2.5	12	na	-50	6	0.64	26	58	0.9	6.4
01BJB0015	-2	-2	14	600	1.1	na	-5	11	51	3.3	2.9	8	na	-50	4	0.55	25	60	0.8	7.7
01BJB0018	4	-2	12	650	1.7	na	-5	13	76	5.4	3.3	6	na	-50	2	0.52	46	86	0.8	11
01BJB0021	11	-2	11	710	0.7	na	-5	13	83	4.5	2.8	8	na	-50	2	0.56	29	77	0.8	10
01BJB0022	5	-2	14	780	1.5	na	-5	14	84	5.4	3.4	7	na	-50	2	0.53	31	87	1	11
01BJB0023	-2	-2	19	900	2	na	-5	17	100	6.5	2.4	9	na	-50	3	0.24	43	88	1.2	13
01BJB0024	3	-2	13	700	1.2	na	-5	13	71	1.9	2.9	13	na	-50	3	1	27	48	0.8	7.7
01BJB0025	-2	-2	12	580	0.6	na	-5	15	71	4.6	3.4	7	na	-50	1	0.57	37	79	0.6	12
01BJB0027	3	-2	11	680	1.4	na	-5	14	72	4.5	3.3	7	na	-50	3	0.58	34	78	0.8	10
01BJB0028	5	3	17	630	1.6	na	-5	17	78	4.1	3.8	7	na	-50	8	0.48	34	67	1.1	10
01BJB0030	6	-2	11	770	0.6	na	-5	10	78	4.6	3.3	5	na	-50	2	0.47	37	75	1	10
02BJB0004	5	-5	14.4	810	-0.5	3	na	11	84	5	3.06	11	-1	-5	-1	0.51	-32	77	0.7	9.5
02BJB0005	8	-5	15.3	910	-0.5	3	na	11	95	7	3.7	6	-1	-5	5	0.52	-36	98	1.1	12.2
02BJB0008	-2	-5	17.3	600	2	7	na	8	95	3	2.92	19	-1	-5	-1	0.4	-30	41	0.7	8.2
02BJB0009	9	10	14.8	810	1.3	3	na	12	88	7	3.92	7	-1	-5	-1	0.44	-35	118	0.8	12.5
02BJB0010	3	-5	13.5	960	2	5	na	14	93	7	3.65	7	-1	-5	5	0.59	-38	104	1	12.6
02BJB0011	7	-5	14.6	870	2.1	1	na	12	105	7	4.08	8	-1	-5	-1	0.65	-36	106	1.5	10.8
02BJB0012	-2	-5	8.4	650	-0.5	-1	na	6	116	5	2.42	19	-1	-5	-1	1.24	-42	89	0.4	11.5
02BJB0013	4	-5	23.7	870	2.5	4	na	13	85	6	4.05	6	-1	-5	7	0.47	-37	115	1.3	11.5
02BJB0014	-2	-5	16.8	690	1.1	-1	na	7	104	5	2.95	12	-1	-5	-1	0.85	-35	96	0.5	12.2
02BJB0015	-2	-5	20	980	2	4	na	22	95	8	3.89	6	-1	-5	8	0.51	-38	110	1.2	12.9
02BJB0016	-2	-5	15.4	740	2.1	5	na	14	80	7	3.63	6	-1	-5	6	0.52	159	94	1.1	11.8
02BJB0017	8	-5	13.5	1000	1.9	6	na	9	78	5	3.25	5	-1	-5	3	0.47	-32	93	1.3	10.7
02BJB0018	4	-5	11.6	1000	1.8	7	na	6	57	2	2.23	9	-1	-5	-1	0.56	-25	55	1	6.7
02BJB0019	-2	-5	13.9	840	3.7	7	na	13	85	7	3.36	5	-1	-5	4	0.47	-33	99	1	11.5
02BJB0020	-2	-5	16.8	770	2	4	na	13	77	5	3.46	5	-1	-5	5	0.53	-31	75	1	10.7
02BJB0021	5	-5	16	990	2.6	3	na	10	78	5	3.48	6	-1	-5	3	0.58	-32	93	1	10.6
02BJB0022	11	-5	18.7	1100	-0.5	4	na	14	103	8	4	7	-1	-5	5	0.55	-37	102	1.2	13.3
02BJB0023	-2	-5	15.3	420	2	-1	na	11	106	4	3.56	16	-1	-5	-1	0.33	-31	75	0.5	10.1

— no data
na = not available

ITS-Bondar Clegg				Activation laboratories		
Element	Units	Lower limit		Element	Units	Lower limit
Ag	ppm	2		Ag	ppm	5
As	ppm	0.5		As	ppm	2
Au	ppb	1		Au	ppb	2
Ba	ppm	50		Ba	ppm	100
Br	ppm	0.5		Br	ppm	0.05
—	—	—		Ca	%	1
Cd	ppm	5		—	—	—
Co	ppm	5		Co	ppm	1
Cr	ppm	20		Cr	ppm	2
Cs	ppm	0.5		Cs	ppm	1
Fe	%	0.2		Fe	%	0.01
Hf	ppm	1		Hf	ppm	0.5
—	—	—		Hg	ppm	1
Ir	ppm	50		Ir	ppb	5
Mo	ppm	1		Mo	ppm	1
Na	%	0.02		Na	%	0.01
Ni	ppm	10		Ni	ppm	100
Rb	ppm	5		Rb	ppm	20
Sb	ppm	0.1		Sb	ppm	0.2
Sc	ppm	0.2		Sc	ppm	0.1
Se	ppm	5		Se	ppm	3
Sn	ppm	100		Sn	%	0.01
—	—	—		Sr	%	0.05
Ta	ppm	0.5		Ta	ppm	0.5
Te	ppm	10		—	—	—
Th	ppm	0.2		Th	ppm	0.5
U	ppm	0.2		U	ppm	0.5
W	ppm	1		W	ppm	1
Zn	ppm	100		Zn	ppm	50
Zr	ppm	200		—	—	—
La	ppm	2		La	ppm	0.2
Ce	ppm	5		Ce	ppm	3
—	—	—		Nd	ppm	5
Sm	ppm	0.1		Sm	ppm	0.1
Eu	ppm	1		Eu	ppm	0.1
Tb	ppm	0.5		Tb	ppm	0.5
Yb	ppm	2		Yb	ppm	0.1
Lu	ppm	0.2		Lu	ppm	0.05
Mass	g	0.01		Mass	g	0.01

Appendix A2. (cont.)

Sample ID	Se (ppm)	Sn (ppm,%)	Sr (%)	Ta (ppm)	Te (ppm)	Th (ppm)	U (ppm)	W (ppm)	Zn (ppm)	Zr (ppm)	La (ppm)	Ce (ppm)	Nd (ppm)	Sm (ppm)	Eu (ppm)	Tb (ppm)	Yb (ppm)	Lu (ppm)	Weight (g)
00BJB0002	-5	-100	na	1.2	-10	13	4.9	2	140	510	37	75	na	6.9	2	1.3	2	0.7	32
00BJB0003	-5	-100	na	1.1	-10	13	4.7	1	130	-200	39	79	na	6.6	3	0.9	3	0.7	29.8
00BJB0007	-5	-100	na	1	-10	10	4.4	1	-100	560	30	64	na	5.6	4	0.9	-2	0.7	30.7
00BJB0008	-5	-100	na	1.1	-10	13	4.7	1	120	340	38	80	na	6.5	3	1.1	2	0.7	33
00BJB0009	-5	-100	na	-0.5	-10	14	8.8	-1	430	-200	37	98	na	7.8	-1	1	3	0.7	6.99
00BJB0010	-5	-100	na	1.1	-10	12	4.2	1	100	420	40	83	na	6.2	2	0.8	-2	0.5	31.8
00BJB0011	-5	-100	na	1	-10	12	4.3	-1	-100	320	36	71	na	6	3	0.9	3	0.6	31.7
00BJB0012	-5	-100	na	0.9	-10	11	3.9	-1	-100	670	32	65	na	5.7	3	0.9	2	0.6	31.4
00BJB0013	-5	-100	na	1	-10	11	4.1	1	-100	460	32	58	na	6.5	2	1.1	3	0.7	30.9
00BJB0014	-5	-100	na	1	-10	12	4.3	-1	140	280	39	74	na	6.6	3	0.9	3	0.7	30
00BJB0015	-5	-100	na	1.1	-10	12	4.2	1	140	300	37	76	na	6.4	3	1	2	0.8	31
00BJB0017	-5	-100	na	0.6	-10	8.9	3.9	1	110	-200	28	54	na	4.7	1	-0.5	-2	0.5	32.7
00BJB0018	-5	-100	na	1	-10	11	4.2	1	120	-200	37	76	na	6	2	0.9	2	0.7	32.8
00BJB0019	-5	-100	na	0.8	-10	10	3.7	2	-100	290	35	70	na	5.7	1	1.1	-2	0.6	32.1
00BJB0021	-5	-100	na	1.2	-10	11	3.7	2	-100	270	36	67	na	5.9	-1	0.7	2	0.7	29.4
00BJB0022	-5	-100	na	0.9	-10	12	5.1	-1	120	-200	40	81	na	6.6	2	0.9	2	0.6	29.5
00BJB0023	-5	-100	na	0.8	-10	8.8	3.8	-1	-100	740	28	49	na	4.9	1	0.7	3	0.8	30.1
00BJB0024	-5	-100	na	0.8	-10	11	4.2	1	-100	350	35	70	na	5.6	2	0.8	-2	0.7	30.7
00BJB0025	-5	-100	na	0.8	-10	11	3.6	-1	-100	-200	35	69	na	5.4	1	0.7	-2	0.5	30.5
00BJB0026	-5	-100	na	1.1	-10	13	4.6	2	110	470	36	66	na	6.4	-1	0.6	2	0.7	31.5
00BJB0028	-5	-100	na	1.4	-10	16	5.4	2	-100	790	49	110	na	9.2	2	1.8	4	1.3	33.3
00BJB0029	-5	-100	na	0.9	-10	10	3.6	1	110	270	34	70	na	5.6	2	0.9	2	0.7	31.3
00BJB0030	-5	-100	na	0.9	13	12	4.3	-1	110	-200	39	76	na	6	2	1.1	2	0.6	30.3
00BJB0031	-5	-100	na	1	-10	12	4.5	-1	-100	-200	38	77	na	6.3	2	0.9	3	0.6	30.5
01BJB0002	-5	-100	na	0.9	-10	10	4.9	-1	100	-200	30	62	na	5.4	2	0.9	2	0.4	32.7
01BJB0003	-5	-100	na	0.8	-10	9.4	4.9	2	-100	430	30	56	na	5.2	1	0.9	3	0.7	31.9
01BJB0004	-5	-100	na	0.9	-10	9.3	4.5	-1	120	440	30	60	na	5.2	1	0.9	3	0.7	34.2
01BJB0006	-5	-100	na	0.8	-10	10	5	2	120	-200	34	69	na	5.3	1	0.9	2	0.5	33.9
01BJB0007	-5	-100	na	0.8	-10	11	5.3	3	-100	-200	33	70	na	5.1	1	0.7	-2	0.4	31.3
01BJB0008	-5	-100	na	0.7	-10	9.2	4	-1	-100	290	28	64	na	5.4	2	1.1	2	0.7	36
01BJB0009	-5	-100	na	0.9	-10	10	4.3	-1	510	320	34	74	na	5.6	1	0.8	3	0.5	30.8
01BJB0010	-5	-100	na	0.8	-10	10	4.8	-1	110	260	32	70	na	5.3	2	0.9	3	0.6	32.1
01BJB0011	-5	-100	na	0.9	-10	9.1	4.4	-1	120	220	29	54	na	4.9	2	1	2	0.5	30.6
01BJB0013	-5	-100	na	0.9	-10	10	7.3	2	180	340	32	73	na	5.6	1	0.8	-2	0.4	31.5
01BJB0014	-5	-100	na	0.8	-10	10	5.6	-1	110	420	25	56	na	5.4	2	1	-2	0.5	32.7
01BJB0015	-5	-100	na	0.7	-10	8.8	5.3	-1	-100	310	26	52	na	4.7	-1	0.8	2	0.5	32.1
01BJB0018	-5	-100	na	0.8	-10	11	4.4	-1	-100	250	31	64	na	5.4	2	0.8	-2	0.5	31.7
01BJB0021	-5	-100	na	1	-10	10	4.8	-1	110	280	31	61	na	5.1	1	0.8	3	0.6	31
01BJB0022	-5	-100	na	1.1	-10	11	4.8	-1	110	340	33	74	na	5.5	1	0.9	3	0.7	33
01BJB0023	-5	-100	na	1	-10	10	4.6	2	110	350	35	72	na	5.3	2	0.8	3	0.6	32.2
01BJB0024	-5	-100	na	0.8	-10	10	4.3	-1	-100	360	30	68	na	5.3	1	1.1	2	0.6	31.1
01BJB0025	-5	-100	na	0.8	-10	11	4	-1	110	270	33	70	na	5.6	2	1	3	0.7	31.3
01BJB0027	-5	-100	na	0.8	-10	10	4.6	-1	100	350	32	72	na	5.1	-1	0.7	2	0.6	35.3
01BJB0028	7	-100	na	0.6	-10	9.5	6.9	2	160	220	30	65	na	4.9	2	0.8	-2	0.4	31
01BJB0030	-5	-100	na	0.9	-10	8.5	4.3	-1	110	380	29	61	na	4.6	-1	0.7	-2	0.4	35
02BJB0004	-3	-0.01	-0.05	-0.5	na	10.3	3.8	-1	122	na	35.3	70	20	5.9	1.4	-0.5	3.7	0.55	22.52
02BJB0005	-3	-0.01	-0.05	-0.5	na	11.6	4	-1	145	na	40.1	76	22	6.5	1.4	-0.5	3.2	0.5	19.92
02BJB0008	-3	-0.01	-0.05	0.7	na	10.6	4.2	-1	103	na	34.2	70	21	5.7	1.4	0.8	3.8	0.58	23.2
02BJB0009	-3	-0.01	-0.05	0.9	na	11	4.3	-1	118	na	40	76	22	6.5	1.4	1	3.4	0.51	21.06
02BJB0010	-3	-0.01	-0.05	1.1	na	11.9	5	-1	103	na	40.2	78	21	6.3	1.4	1	3	0.46	18.85
02BJB0011	-3	-0.01	-0.05	1.8	na	9.8	3.9	-1	115	na	36.3	62	17	4.2	1.1	-0.5	2.8	0.42	20.06
02BJB0012	-3	-0.01	-0.05	1.1	na	11.6	4	-1	-50	na	52.7	102	28	7.3	1.6	-0.5	4.6	0.7	19.21
02BJB0013	8	-0.01	-0.05	1.1	na	11.5	6.1	-1	118	na	39.6	81	20	6.2	1.5	-0.5	3	0.45	19.19
02BJB0014	-3	-0.01	-0.05	1.6	na	9.9	3.9	-1	70	na	43.9	83	23	6.7	1.5	1.1	3.9	0.59	23.68
02BJB0015	-3	-0.01	-0.05	1.4	na	12	6.1	-1	147	na	42.4	83	22	6.6	1.5	1.3	3.3	0.51	19.56
02BJB0016	-3	-0.01	-0.05	1	na	11.4	4.8	-1	170	na	39.3	75	26	6	1.4	1	2.8	0.42	21.08
02BJB0017	-3	-0.01	-0.05	1	na	10.2	3.8	-1	132	na	36.6	68	18	5.7	1.2	-0.5	2.8	0.43	22.55
02BJB0018	-3	-0.01	-0.05	0.8	na	7.8	3.2	-1	107	na	29.3	55	12	4.8	1.2	-0.5	2.6	0.4	29.38
02BJB0019	-3	-0.01	-0.05	0.9	na	11	3	-1	119	na	38.5	75	15	6	1.5	0.9	2.7	0.42	20.99
02BJB0020	-3	-0.01	-0.05	0.9	na	11.1	5	-1	134	na	35.8	73	14	5.8	1.6	1	2.9	0.41	22.97
02BJB0021	-3	-0.01	-0.05	1.1	na	11.3	4.5	-1	131	na	40.2	77	13	6.3	1.4	1.1	3	0.47	23.68
02BJB0022	-3	-0.01	-0.05	1.3	na	11.9	5.4	-1	164	na	42.6	86	19	6.8	1.7	1.3	5.4	0.52	19.24
02BJB0023	-3	-0.01	-0.05	1.2	na	12.3	4.7	-1	116	na	38.9	78	15	5.2	1.1	0.8	3.6	0.58	22.27

— no data
na = not available

Appendix A3. Descriptive statistics and outliers for all sample types.

	Au (ppb)	Ag (ppm)	As (ppm)	Ba (ppm)	Br (ppm)	Ca (%)	Cd (ppm)	Co (ppm)	Cr (ppm)	Cs (ppm)	Fe (%)	Hf (ppm)	Hg (ppm)	Ir (ppb)	Mo (ppm)	Na (%)	Ni (ppm)	Rb (ppm)	Sb (ppm)
Cases	63	63	63	63	63	18	45	63	63	63	63	63	18	63	63	63	63	63	63
Mean	2.80952	0.36507	14.8016	772.222	1.70159	3.66667	0	12.9048	85.1587	4.94444	3.37476	8.50794	0	0	2.95238	0.53333	30.7143	81.8571	0.96666
Standard error	0.40658	0.18003	0.5325	21.9603	0.12666	0.54831	0	0.66424	2.07331	0.19456	8.10E-02	0.46477	0	0	0.38827	2.21E-02	3.52936	2.38658	3.68E-02
Variance	10.4147	2.04199	17.864	30382.1	1.0108	5.41176	0	27.7972	270.813	2.38477	0.41384	13.6088	0	0	9.4977	3.07E-02	784.754	358.834	8.52E-02
Standard deviation	3.22719	1.42898	4.22659	174.305	1.00539	2.32632	0	5.27231	16.4564	1.54427	0.6433	3.68901	0	0	3.08183	0.17523	28.0135	18.9429	0.29182
Variation coefficient	1.14866	3.91417	0.28555	0.22571	0.59085	0.63445	—	0.40855	0.19324	0.31232	0.19062	0.43359	—	—	1.04385	0.32856	0.91206	0.23141	0.30188
Relative variation coefficient	14.4718	49.3138	3.59759	2.84378	7.44404	14.9542	—	5.14731	2.43464	3.93491	2.40162	5.4628	—	—	13.1512	4.13948	11.4909	2.91555	3.80342
Skewness	0.82884	5.32269	2.28033	-0.29798	1.1362	-0.18911	0	2.44956	-7.68E-02	-0.14163	0.15141	1.82591	0	0	2.31469	1.00526	1.81071	-0.33987	1.39304
Kurtosis	-0.25653	31.5008	8.55977	-0.187	2.26725	-0.87334	0	13.2928	-0.33483	-0.60361	1.77333	3.05079	0	0	10.0455	4.2025	6.42255	-0.51724	5.28116
Minimum	0	0	8.4	360	0	0	0	0	49	1.7	1.6	5	0	0	-1	0.1	1.00E-04	34	0.4
Maximum	11	10	36	1100	5.4	7	0	42	120	8	5.7	22	0	0	19	1.24	159	118	2.3
Range	11	10	27.6	740	5.4	7	0	42	71	6.3	4.1	17	0	0	20	1.14	159	84	1.9
Sum	177	23	932.5	48650	107.2	66	0	813	5365	311.5	212.61	536	0	0	186	33.6	1935	5157	60.9
1st percentile	—	—	—	—	—	—	—	—	—	—	—	—	—	—	—	—	—	—	—
5th percentile	0	0	9.52	396	0	—	0	6.2	53.6	2.08	2.4	5	—	0	-1	0.252	1.00E-04	49.4	0.52
10th percentile	0	0	11	584	0.64	0	0	7	63.8	2.8	2.452	5	0	0	-1	0.312	1.00E-04	55.4	0.6
25th percentile	0	0	12	650	1.1	2.5	0	10	73	4.1	2.92	6	0	0	1	0.47	1.00E-04	67	0.8
Median	3	0	14	780	1.6	4	0	13	84	5	3.48	7	0	0	3	0.53	31	84	1
75th percentile	5	0	16.8	900	2	5.25	0	15	97	6	3.8	9	0	0	4	0.57	46	97	1.1
90th percentile	8	1.2	19	996	3.08	7	0	17	105.6	7	4.092	14.2	0	0	6	0.686	50	105.2	1.3
95th percentile	9.8	3	23.16	1080	3.86	—	0	19	114.8	7.18	4.1	18.4	—	0	8	0.874	64.2	110	1.38
99th percentile	—	—	—	—	—	—	—	—	—	—	—	—	—	—	—	—	—	—	—
10% trimmed mean	2.33333	0	14.3036	779.286	1.60536	3.70833	0	12.6151	85.377	4.97936	3.3906	7.80952	0	0	2.64881	0.52474	27.9961	82.381	0.95297
10% winsorized mean	2.53968	0	13.9667	756.349	1.5619	3.27778	0	12.1111	82.6032	4.80794	3.26603	7.7619	0	0	2.53968	0.50476	26.6032	79.3651	0.92222
Geometric mean	2.47E-02	2.69E-04	14.3295	750.475	0.87831	0.68374	0	10.286	83.5082	4.67065	3.31111	7.92602	—	—	0.67744	0.50161	0.99183	79.4304	0.92665
Geometric standard deviation	238.278	21.6373	1.28032	1.28509	11.3179	59.6444	0	4.54332	1.22564	1.43181	1.22336	1.43092	—	—	39.4826	1.47124	356.263	1.29348	1.3426

Descriptive statistics for each element measured by INAA. Values below detection levels were assigned zero values in order to facilitate computation. The background levels of various elements in the surficial materials must be established so that threshold values between background and possible anomalies can be identified. The problem is that a single value usually cannot represent the elemental composition of an entire area. Govett (1983) argued that the geometric mean (antilog of the arithmetic mean of the log10 of the values) provides a useful indicator of background values for geochemical data. Because the geometric mean can not be calculated for data sets that contain zeros, an arbitrary small value of 0.0001 replaced zero for these calculations.
— no data

Sample no.	Element	Value	n(σ)	p	Soil mean[1]	Range	Alaska surficial materials[2]
02BJB0009	Ag (ppm)	10	6.74251	4.90E-10	0.1	—	—
00BJB0009	As (ppm)	36	5.01549	1.67E-05	5	1–50	—
	U (ppm)	8.8	4.48132	2.34E-04	1	—	<0.22–45
	Co (ppm)	42	5.5185	1.08E-06	10	1–40	<2–55
	Fe (%)	5.7	3.61452	0.00943	—	—	0.55–10%
	Mo (ppm)	19	5.46344	1.47E-06	2	1–5	<2–15
	Ni (ppm)	120	3.23798	0.03722	30	5–500	<3–320
	Sb (ppm)	2.3	4.56896	1.54E-04	10	1–40	<2–55
	Zn (ppm)	430	3.71464	0.00638	50	10–300	<20–2700
00BJB0021	Br (ppm)	5.4	3.67859	0.00736	—	—	—
00BJB0028	Ce (ppm)	110	3.47976	0.01568	~5	—	<5–180
	Hf (ppm)	22	3.65737	0.00799	—	—	—
	Lu (ppm)	1.3	4.90039	3.01E-05	—	—	—
	Sm (ppm)	9.2	4.09729	0.00131	—	—	—
	Th (ppm)	16	3.63579	0.00869	13	—	<1.6–76
00BJB0030	Te (ppm)	13	6.55913	1.70E-09	—	—	—
01BJB0009	Zn (ppm)	510	4.60974	1.27E-04	50	10–300	<20–2700
01BJB0028	Se (ppm)	7	5.08979	1.13E-05	0.2	—	—
02BJB0012	La (ppm)	52.7	3.35006	0.02513	—	—	<2–120
	Na (%)	1.24	4.03274	0.00173	—	—	<0.07–3.6%
02BJB0013	Se (ppm)	8	5.8425	1.62E-07	0.2	—	—
02BJB0016	Ni (ppm)	159	4.878	3.38E-05	30	5–500	<3–320

Sample no.	Element	Value	n(σ)	p	Soil mean[1]	Range	Alaska surficial materials[2]
00BJB0030	Te (ppm)	13	6.55913	1.70E-09	—	—	—
01BJB0009	Zn (ppm)	510	4.60974	1.27E-04	50	10–300	<20–2700
01BJB0028	Se (ppm)	7	5.08979	1.13E-05	0.2	—	—
02BJB0012	La (ppm)	52.7	3.35006	0.02513	—	—	<2–120
	Na (%)	1.24	4.03274	0.00173	—	—	<0.07–3.6%
02BJB0013	Se (ppm)	8	5.8425	1.62E-07	0.2	—	—
02BJB0016	Ni (ppm)	159	4.878	3.38E-05	30	5–500	<3–320
None	Au (ppb)						
None	Ba (ppm)						
None	Ca (%)						
None	Cr (ppm)						
None	Cs (ppm)						
None	Eu (ppm)						
None	Nd (ppm)						
None	Rb (ppm)						
None	Sc (ppm)						
None	Ta (ppm)						
None	Tb (ppm)						
None	W (ppm)						
None	Yb (ppm)						

Notes:
Outliers: Anomalies were identified as outliers which lie so far from the mean that they may not be representative of the normal background fluctuation of the element. The outliers table lists all cases of suspected anomalous values based on the distance from the mean. The distance from the mean is defined by multiples (n) of σ (the standard deviation). For a given (n), the probability of such an occurrence increases with sample size. The outliers table lists the cases where (n) σ is greater than 4, which means all cases where the probability of finding at least one value at this distance from the mean in a normally distributed sample is less than 0.05 (95th percentile). The average abundance and range of values in soils and surficial materials reported elsewhere is also provided in the table for comparison.

[1] Levinson (1974, 1980)
[2] Gough et al. (1988)
— no data

Appendix A3. (cont.)

	Sc (ppm)	Se (ppm)	Sn (ppm,%)	Sr (%)	Ta (ppm)	Te (ppm)	Th (ppm)	U (ppm)	W (ppm)	Zn (ppm)	Zr (ppm)	La (ppm)	Ce (ppm)	Nd (ppm)	Sm (ppm)	Eu (ppm)	Tb (ppm)	Yb (ppm)	Lu (ppm)
Cases	63	63	63	18	63	45	63	63	63	63	45	63	63	18	63	63	63	63	63
Mean	10.8603	-0.57142	0	0	0.92539	0.28888	10.8683	4.6	0.52381	98	286	35.2365	71.3175	19.3333	5.83333	1.56032	0.81746	2.27778	0.58444
Standard error	0.23497	0.25066	0	0	3.77E-02	0.28888	0.17782	0.11807	0.10334	11.2603	30.3771	0.65676	1.40054	1.03532	0.10352	0.10326	4.58E-02	0.16351	1.84E-02
Variance	3.47856	3.95853	0	0	8.97E-02	3.75556	1.9922	0.87838	0.67281	7988.06	41524.5	27.1743	123.575	19.2941	0.67516	0.67178	0.13211	1.68434	2.13E-02
Standard deviation	1.86509	1.9896	0	0	0.29944	1.93793	1.41145	0.93722	0.82025	89.376	203.776	5.2129	11.1164	4.39251	0.82168	0.81962	0.36346	1.29782	0.14602
Variation coefficient	0.17173	—	—	—	0.32358	6.7082	0.12986	0.20374	1.56593	0.912	0.7125	0.14794	0.15587	0.22719	0.14086	0.52529	0.44463	0.56977	0.24984
Relative variation coefficient	2.16365	—	—	—	4.07679	100	1.6362	2.56694	19.7289	11.4901	10.6214	1.86387	1.96381	5.35512	1.77467	6.61809	5.60183	7.17849	3.14774
Skewness	-0.34052	1.71029	0	0	-0.69429	6.48249	0.71849	1.99666	1.24897	2.08938	0.21075	0.64069	0.80996	6.09E-02	1.16345	0.25528	-0.96851	-0.52288	1.78195
Kurtosis	-0.36354	6.7061	0	0	3.46936	40.0227	1.56739	5.95456	0.2135	7.98199	-0.10944	1.03161	1.9557	-0.65541	3.16164	0.59112	1.44366	-0.20289	7.15358
Minimum	6.4	-3	0	0	0	0	7.8	3	0	0	0	25	49	12	4.2	0	0	0	0.4
Maximum	15	8	0	0	1.8	13	16	8.8	3	510	790	52.7	110	28	9.2	4	1.8	5.4	1.3
Range	8.6	11	0	0	1.8	13	8.2	5.8	3	510	790	27.7	61	16	5	4	1.8	5.4	0.9
Sum	684.2	-36	0	0	58.3	13	684.7	289.8	33	6174	12870	2219.9	4493	348	367.5	98.3	51.5	143.5	36.82
1st percentile	—	—	—	—	—	—	—	—	—	—	—	—	—	—	—	—	—	—	—
5th percentile	7.7	-3	0	0	0.12	0	8.8	3.6	0	0	0	28	54	—	4.7	0	0	0	0.4
10th percentile	8.14	-3	0	0	0.7	0	9.14	3.74	0	0	0	29	56	12.9	4.9	0.4	0	0	0.404
25th percentile	10	-3	0	0	0.8	0	10	4	0	0	110	31	64	15	5.3	1	0.8	2	0.5
Median	11	0	0	0	0.9	0	11	4.4	0	110	300	35	70	20	5.7	1.5	0.9	2.8	0.6
75th percentile	12	0	0	0	1.1	0	11.9	4.9	1	122	400	39	76	22	6.4	2	1	3	0.7
90th percentile	13	0	0	0	1.2	0	12.72	5.52	2	154.8	530	40.2	83	26.2	6.66	3	1.1	3.66	0.7
95th percentile	13.86	0	0	0	1.4	0	13	6.74	2	178	719	43.64	95.6	—	7.22	3	1.3	3.98	0.78
99th percentile	—	—	—	—	—	—	—	—	—	—	—	—	—	—	—	—	—	—	—
10% trimmed mean	10.9313	-0.6369	0	0	0.93511	0	10.8006	4.47302	0.38492	89.6012	273.75	35.0067	70.8194	19.2222	5.78274	1.5496	0.85853	2.32183	0.57712
10% winsorized mean	10.5286	-0.7619	0	0	0.90793	0	10.4492	4.35238	0.47619	84.0476	258.667	33.827	68.3492	17.1111	5.59365	1.57619	0.77936	2.16032	0.55507
Geometric mean	10.6908	1.43E-04	—	—	0.61405	1.30E-04	10.7811	4.52102	2.45E-03	2.29699	8.96256	34.8689	70.4991	18.845	5.78019	0.58187	0.28839	0.38952	0.56889
Geometric standard deviation	1.20076	7.26811	—	—	7.22036	5.78551	1.13579	1.19895	95.9259	606.719	710.065	1.15659	1.16474	1.26656	1.14421	17.5437	21.5004	57.337	1.25796

Descriptive statistics for each element measured by INAA. Values below detection levels were assigned zero values in order to facilitate computation. The background levels of various elements in the surficial materials must be established so that threshold values between background and possible anomalies can be identified. The problem is that a single value usually cannot represent the elemental composition of an entire area. Govett (1983) argued that the geometric mean (antilog of the arithmetic mean of the log10 of the values) provides a useful indicator of background values for geochemical data. Because the geometric mean can not be calculated for data sets that contain zeros, an arbitrary small value of 0.0001 replaced zero for these calculations.
— no data

Appendix A4. Descriptive statistics and outliers for till samples.

	Au (ppb)	Ag (ppm)	As (ppm)	Ba (ppm)	Br (ppm)	Ca (%)	Cd (ppm)	Co (ppm)	Cr (ppm)	Cs (ppm)	Fe (%)	Hf (ppm)	Hg (ppm)	Ir (ppb)	Mo (ppm)	Na (%)	Ni (ppm)	Rb (ppm)	Sb (ppm)
Cases	49	49	49	49	49	12	37	49	49	49	49	49	12	49	49	49	49	49	49
Mean	2.65306	0.46938	14.7735	740	1.6449	2.66692	0	13.102	88.1837	5.17143	3.40837	8.65306	0	0	2.87755	0.52714	31.5919	84.1837	0.92244
Standard error	0.47697	0.2298	0.48173	23.4358	0.14339	0.55494	0	0.53946	2.27615	0.20582	8.17E-02	0.5229	0	0	0.31084	2.70E-02	3.76046	2.62651	3.54E-02
Variance	11.148	2.58758	11.3712	26912.5	1.00753	3.69552	0	14.2602	253.861	2.07583	0.32732	13.398	0	0	4.73469	3.57E-02	692.912	338.028	6.14E-02
Standard deviation	3.33886	1.6086	3.37211	164.05	1.00376	1.92237	0	3.77627	15.933	1.44078	0.57212	3.66032	0	0	2.17594	0.189	26.3232	18.3855	0.24771
Variation coefficient	1.25849	3.42701	0.22825	0.22169	0.61022	0.72082	—	0.28822	0.18068	0.2786	0.16785	0.423	—	—	0.75617	0.35853	0.83322	0.21839	0.26853
Relative variation coefficient	17.9785	48.9573	3.26078	3.16699	8.71748	20.8083	—	4.11743	2.58114	3.98004	2.39797	6.04298	—	—	10.8025	5.12194	11.9033	3.11997	3.83623
Skewness	1.01905	4.63745	0.84891	-0.41561	1.19329	-0.38567	0	-0.76245	-0.15048	-0.2289	-0.92336	1.875	0	0	0.89402	1.00702	2.0446	-0.44897	7.21E-02
Kurtosis	2.94E-02	23.6387	0.4487	-4.52E-03	2.92036	-1.34413	0	1.93072	-0.20415	-0.14931	0.55803	3.24639	0	0	0.61063	3.77935	9.27447	-0.11919	-0.60443
Minimum	0	0	8.4	360	0	1.00E-03	0	0	49	1.7	1.6	5	0	0	0	0.1	1.00E-04	34	0.4
Maximum	11	10	24	1100	5.4	5	0	22	120	8	4.2	22	0	0	9	1.24	159	118	1.5
Range	11	10	15.6	740	5.4	4.999	0	22	71	6.3	2.6	17	0	0	9	1.14	159	84	1.1
Sum	130	23	723.9	36260	80.6	32.003	0	642	4321	253.4	167.01	424	0	0	141	25.83	1548	4125	45.2
1st percentile	—	—	—	—	—	—	—	—	—	—	—	—	—	—	—	—	—	—	—
5th percentile	0	0	10.5	390	0	—	0	6.5	59	2.35	2.4	5	—	0	0	0.18	1.00E-04	51.5	0.5
10th percentile	0	0	11	460	0.6	1.00E-03	0	7	70	3.1	2.42	6	0	0	0	0.3	1.00E-04	56	0.6
25th percentile	0	0	12.5	650	1.1	0.25075	0	11	76.5	4.45	3.03	7	0	0	1.5	0.45	11.5	74	0.75
Median	0	0	14	740	1.5	3	0	14	88	5	3.5	7	0	0	3	0.52	34	87	0.9
75th percentile	4.5	0	16.9	865	2.05	4	0	15	100	6.1	3.8	9	0	0	4	0.57	46	97	1.1
90th percentile	8	2	19	940	2.6	5	0	17	110	7	4.1	15	0	0	6	0.69	50	110	1.3
95th percentile	10.5	3	22.35	980	3.7	—	0	19	118	7.6	4.1	17.5	—	0	8	0.925	57	112.5	1.3
99th percentile	—	—	—	—	—	—	—	—	—	—	—	—	—	—	—	—	—	—	—
10% trimmed mean	2.08673	5.61E-02	14.4847	750.51	1.56939	2.70852	0	13.3265	88.2143	5.22219	3.46536	7.96173	0	0	2.64286	0.51681	30.1021	84.9388	0.92066
10% winsorized mean	2.30612	0.20408	13.9755	711.837	1.5102	2.25017	0	12.5714	84.898	4.98163	3.29122	8.04082	0	0	2.59184	0.49224	28.0612	81.1633	0.88775
Geometric mean	1.63E-02	3.56E-04	14.4219	719.657	0.73102	0.4328	—	10.1734	86.6862	4.93939	3.35344	8.09602	—	—	0.66055	0.4899	1.66139	81.9263	0.8878
Geometric standard deviation	240.035	31.2287	1.24563	1.283	15.1089	39.8109	—	5.48948	1.21059	1.38517	1.21017	1.41488	—	—	39.1494	1.52806	270.428	1.27981	1.3328

Descriptive statistics for each element measured by INAA. Values below detection levels were assigned zero values in order to facilitate computation. The background levels of various elements in the surficial materials must be established so that threshold values between background and possible anomalies can be identified. The problem is that a single value usually cannot represent the elemental composition of an entire area. Govett (1983) argued that the geometric mean (antilog of the arithmetic mean of the log10 of the values) provides a useful indicator of background values for geochemical data. Because the geometric mean can not be calculated for data sets that contain zeros, an arbitrary small value of 0.0001 replaced zero for these calculations.
— no data

Sample no.	Element	Value	n(σ)	p	Soil mean[1]	Range	Alaska surficial materials[2]
02BJB0009	Ag (ppm)	10	5.9248	9.85E-08	0.1	—	—
00BJB0021	Br (ppm)	5.4	3.74105	0.00575	—	—	—
00BJB0028	Co (ppm)	0	3.46957	0.01628	10	1–40	<2–55
	Fe (%)	1.6	3.16081	0.04836	—	—	0.55–10%
	Hf (ppm)	22	3.64638	0.00834	—	—	—
	Th (ppm)	16	3.81091	0.00435	13	—	<1.6–76
	Ce (ppm)	110	3.52007	0.01349	~5	—	<5–180
	Sm (ppm)	9.2	4.07735	0.00143	—	—	—
	Lu (ppm)	1.3	4.64686	1.06E-04	—	—	—
00BJB0030	Te (ppm)	13	5.91836	1.02E-07	—	—	—
01BJB0009	Zn (ppm)	510	4.85013	3.89E-05	50	10–300	<20–2700
01BJB0013	U (ppm)	7.3	3.5091	0.01406	1	—	<0.22–45
01BJB0028	Se (ppm)	7	4.45418	2.65E-04	0.2	—	—
02BJB0011	Ta (ppm)	1.8	3.50238	0.01442	—	—	—
02BJB0012	Na (%)	1.24	3.77174	0.00509	—	—	<0.07–3.6%
	La (ppm)	52.7	3.24325	0.03655	—	—	<2–120
02BJB0013	Se (ppm)	8	5.11959	9.65E-06	0.2	—	—
02BJB0016	Ni (ppm)	159	5.32937	3.10E-06	30	5–500	<3–320

Sample no.	Element	Value	n(σ)	p	Soil mean[1]	Range	Alaska surficial materials[2]
None	Au (ppb)						
None	Ca (%)						
None	Cr (ppm)						
None	Cs (ppm)						
None	Eu (ppm)						
None	Nd (ppm)						
None	Rb (ppm)						
None	Sc (ppm)						
None	Ta (ppm)						
None	Tb (ppm)						
None	W (ppm)						
None	Yb (ppm)						
None	Au (ppb)						
None	Ca (%)						

Notes:
Outliers: Anomalies were identified as outliers which lie so far from the mean that they may not be representative of the normal background fluctuation of the element. The outliers table lists all cases of suspected anomalous values based on the distance from the mean. The distance from the mean is defined by multiples (n) of σ (the standard deviation). For a given (n), the probability of such an occurrence increases with sample size. The outliers table lists the cases where (n) σ is greater than 4, which means all cases where the probability of finding at least one value at this distance from the mean in a normally distributed sample is less than 0.05 (95th percentile). The average abundance and range of values in soils and surficial materials reported elsewhere is also provided in the table for comparison.

[1] Levinson (1974, 1980)
[2] Gough et al. (1988)
— no data

Appendix A4. (cont.)

	Sc (ppm)	Se (ppm)	Sn (ppm,%)	Sr (%)	Ta (ppm)	Te (ppm)	Th (ppm)	U (ppm)	W (ppm)	Zn (ppm)	Zr (ppm)	La (ppm)	Ce (ppm)	Nd (ppm)	Sm (ppm)	Eu (ppm)	Tb (ppm)	Yb (ppm)	Lu (ppm)
Cases	49	49	49	12	49	37	49	49	49	49	37	49	49	12	49	49	49	49	49
Mean	11.2755	0.30612	0	0	0.95918	0.35135	10.9898	4.60612	0.55102	90.9796	297.297	35.7612	72.2857	21.25	5.87551	1.71429	0.84898	2.38163	0.60224
Standard error	0.23902	0.21469	0	0	4.28E-02	0.35135	0.18781	0.10966	0.12044	12.3419	33.7333	0.74611	1.53058	1.0234	0.11647	0.11184	4.97E-02	0.18282	2.15E-02
Variance	2.79939	2.2585	0	0	9.00E-02	4.56757	1.72844	0.58933	0.71088	7463.85	42103.6	27.2774	114.792	12.5682	0.6648	0.61291	0.12088	1.63778	2.25E-02
Standard deviation	1.67314	1.50283	0	0	0.29994	2.13719	1.3147	0.76768	0.84314	86.3936	205.192	5.22278	10.7141	3.54516	0.81535	0.78289	0.34768	1.27976	0.15015
Variation coefficient	0.14838	4.90925	—	—	0.3127	6.08276	0.11962	0.16666	1.53014	0.94959	0.69019	0.14604	0.14821	0.16683	0.13877	0.45668	0.40953	0.53734	0.24932
Relative variation coefficient	2.11981	70.1321	—	—	4.46724	100	1.70899	2.38094	21.8592	13.5656	11.3467	2.08637	2.11741	4.816	1.98245	6.52408	5.85046	7.67635	3.56183
Skewness	-0.24196	4.67624	0	0	-0.5787	5.83333	1.05313	1.5663	1.20793	2.10381	0.28315	0.89173	0.9358	0.1814	1.3101	0.45428	-0.91367	-0.5251	1.91385
Kurtosis	-0.4752	19.9829	0	0	3.54787	32.0278	2.49434	2.91104	0.13565	9.26289	2.33E-02	1.06782	2.64682	-0.18852	3.90252	0.63906	2.19454	6.79E-02	7.55375
Minimum	7.7	0	0	0	0	0	8.8	3.6	0	0	0	28	49	15	4.2	0	0	0	0.4
Maximum	15	8	0	0	1.8	13	16	7.3	3	510	790	52.7	110	28	9.2	4	1.8	5.4	1.3
Range	7.3	8	0	0	1.8	13	7.2	3.7	3	510	790	24.7	61	13	5	4	1.8	5.4	0.9
Sum	552.5	15	0	0	47	13	538.5	225.7	27	4458	11000	1752.3	3542	255	287.9	84	41.6	116.7	29.51
1st percentile	—	—	—	—	—	—	—	—	—	—	—	—	—	—	—	—	—	—	—
5th percentile	8.15	0	0	—	0.3	0	9.15	3.65	0	0	0	28.5	55	—	4.9	0.5	0	0	0.4
10th percentile	8.6	0	0	0	0.8	0	9.4	3.8	0	0	0	30	60	15.6	5.1	1	0	0	0.42
25th percentile	10	0	0	0	0.8	0	10	4.05	0	0	220	32	65	19.25	5.3	1	0.8	2	0.5
Median	11.5	0	0	0	0.9	0	11	4.4	0	110	300	35	72	21.5	5.6	1.7	0.9	3	0.6
75th percentile	12.35	0	0	0	1.1	0	12	4.9	1	121	390	39.15	77.5	22.75	6.5	2	1	3	0.7
90th percentile	13	0	0	0	1.3	0	12.3	5.4	2	160	582	42.4	83	27.4	6.7	3	1.1	3.7	0.7
95th percentile	14	3.5	0	—	1.5	1.3	13	6.5	2	175	745	46.45	94	—	7.1	3	1.3	4.3	0.8
99th percentile	—	—	—	—	—	—	—	—	—	—	—	—	—	—	—	—	—	—	—
10% trimmed mean	11.3332	0	0	0	0.95943	0	10.9074	4.49796	0.41326	83.9286	284.054	35.3046	71.8189	21.1875	5.82092	1.66837	0.89056	2.43546	0.59443
10% winsorized mean	10.7857	0	0	0	0.93469	0	10.4531	4.33061	0.48979	79.8775	268.108	34.0061	68.8367	17.6667	5.59592	1.65306	0.8	2.24286	0.56469
Geometric mean	11.1481	1.58E-04	—	—	0.67177	1.37E-04	10.9171	4.55089	2.80E-03	1.28838	13.6761	35.4087	71.5441	20.9761	5.82425	1.11721	0.3651	0.5182	0.58656
Geometric standard deviation	1.16716	9.42806	—	—	6.34931	6.9299	1.12203	1.16509	101.799	782.747	546.792	1.15104	1.15521	1.18463	1.14094	7.23477	16.4405	45.8241	1.25492

Descriptive statistics for each element measured by INAA. Values below detection levels were assigned zero values in order to facilitate computation. The background levels of various elements in the surficial materials must be established so that threshold values between background and possible anomalies can be identified. The problem is that a single value usually cannot represent the elemental composition of an entire area. Govett (1983) argued that the geometric mean (antilog of the arithmetic mean of the log10 of the values) provides a useful indicator of background values for geochemical data. Because the geometric mean can not be calculated for data sets that contain zeros, an arbitrary small value of 0.0001 replaced zero for these calculations.
— no data

Appendix A5. Heavy-mineral separations.

	Minerals (%)			
Sample no.	Light	Heavy	Magnetics	Method loss
00BJB0002	99.375	0.548	0.101	-0.023
00BJB0003	99.500	0.466	0.093	-0.060
00BJB0004	99.892	0.216	0.017	-0.125
00BJB0005	100.047	0.205	0.006	-0.257
00BJB0007	99.521	0.354	0.057	0.067
00BJB0008	99.403	0.408	0.072	0.117
00BJB0009	99.654	0.302	0.053	-0.010
00BJB0010	99.025	0.322	0.087	0.566
00BJB0011	98.913	0.516	0.136	0.435
00BJB0012	99.229	0.569	0.055	0.147
00BJB0013	99.241	0.534	0.087	0.138
00BJB0014	99.609	0.321	0.072	-0.002
00BJB0015	99.453	0.448	0.087	0.013
00BJB0016	98.721	0.969	0.273	0.038
00BJB0017	99.919	0.015	0.002	0.064
00BJB0018	99.806	0.083	0.018	0.092
00BJB0019	99.867	0.037	0.003	0.093
00BJB0021	99.533	0.391	0.063	0.012
00BJB0022	99.541	0.322	0.051	0.087
00BJB0023	99.782	0.104	0.009	0.104
00BJB0024	99.466	0.520	0.064	-0.050
00BJB0025	99.735	0.115	0.031	0.119
00BJB0029	99.571	0.270	0.050	0.109
00BJB0030	99.436	0.461	0.109	-0.006
00BJB0031	99.428	0.389	0.073	0.111
01BJB0002	99.566	0.365	0.058	0.011
01BJB0003	99.863	0.074	0.009	0.054
01BJB0004	99.828	0.009	0.000	0.163
01BJB0006	98.651	0.419	0.086	0.844
01BJB0007	99.474	0.721	0.100	-0.295
01BJB0008	99.242	0.629	0.085	0.044
01BJB0009	99.471	0.412	0.078	0.038
01BJB0010	99.225	0.582	0.089	0.103
01BJB0011	98.874	0.923	0.083	0.120
01BJB0012	99.265	0.158	0.070	0.507
01BJB0013	99.333	0.543	0.059	0.065
01BJB0014	99.336	0.519	0.070	0.076
01BJB0015	99.393	0.202	0.011	0.394
01BJB0018	99.287	0.548	0.083	0.083
01BJB0021	99.550	0.397	0.060	-0.008
01BJB0022	99.532	0.333	0.066	0.068
01BJB0023	100.125	0.017	0.000	-0.142
01BJB0024	98.039	1.405	0.544	0.012
01BJB0025	99.409	0.514	0.086	-0.010
01BJB0027	98.777	1.033	0.104	0.086
01BJB0028	99.485	0.277	0.052	0.187
01BJB0030*	—	—	—	—
02BJB0004	99.392	0.518	0.071	0.019
02BJB0005	99.082	0.326	0.085	0.507
02BJB0008	99.492	0.349	0.103	0.056
02BJB0009	99.569	0.198	0.039	0.194
02BJB0010	98.968	0.854	0.106	0.073
02BJB0011	99.267	0.543	0.150	0.039
02BJB0012*	99.794	0.018	0.000	0.188
02BJB0013	98.951	0.640	0.091	0.319
02BJB0014	99.760	0.017	0.000	0.223
02BJB0015	98.210	1.411	0.119	0.260
02BJB0016	98.894	0.890	0.102	0.114
02BJB0017	99.381	0.145	0.000	0.474
02BJB0018	99.625	0.173	0.011	0.192
02BJB0019	99.102	0.357	0.081	0.460
02BJB0020*	96.832	0.081	0.000	3.087
02BJB0021	99.274	0.436	0.112	0.179
02BJB0022	99.439	0.419	0.066	0.075
02BJB0023	99.674	0.262	0.033	0.031

*too sandy
— no data

Appendix A6. Heavy-mineral counts.

Sample	PY	Pg	HM	Hr	IL	Ib	CM	RU	Ro	AT	LX	BA	Bc	Bs	KY	GO	Gp	SD	HB	CP	OP	EP	GA	ST	SP	MZ	ZR	Za	Al	X1	UK
00BJB0002	0.3	1.0	8.3	1.0	5.0	4.3	0.0	0.7	0.3	0.0	4.3	7.7	1.0	0.0	0.0	27.0	0.0	0.0	3.0	0.0	11.0	6.3	15.3	0.0	0.0	0.0	0.7	0.0	0.0	0.0	2.7
00BJB0003	0.0	1.0	6.0	0.0	4.7	4.3	0.0	0.7	0.0	0.3	5.7	2.0	0.0	0.0	0.0	24.0	0.0	0.0	4.0	0.7	7.3	5.7	31.3	0.0	0.3	0.0	1.0	0.0	0.0	0.0	1.0
00BJB0004	0.7	0.7	1.0	0.3	0.0	0.0	0.0	0.0	0.0	0.0	1.7	8.0	18.7	0.0	0.0	64.3	1.3	0.0	0.0	0.0	0.0	0.3	1.7	0.0	0.0	0.0	0.7	0.0	0.0	0.0	0.7
00BJB0006	0.0	3.3	2.3	5.3	0.3	0.0	0.0	0.0	0.0	0.0	0.7	2.3	14.7	0.0	0.0	61.7	5.7	0.0	0.0	0.0	0.0	0.3	0.7	0.0	0.0	0.0	0.0	0.7	0.7	0.0	1.3
00BJB0007	0.0	0.3	5.0	0.7	7.0	8.3	0.0	0.0	0.7	0.0	1.7	0.3	4.0	0.0	0.0	7.0	0.0	0.0	2.7	0.0	2.7	10.0	47.0	0.0	0.0	0.3	1.0	0.3	0.3	0.0	0.7
00BJB0008	0.3	0.3	9.3	0.0	3.0	10.7	0.0	0.7	0.3	0.0	3.7	1.3	3.0	0.0	0.0	19.3	0.0	0.0	2.7	0.0	10.3	4.7	25.7	0.0	0.0	0.7	1.3	0.3	0.0	0.3	2.0
00BJB0009	0.0	0.3	4.7	0.7	6.0	6.7	0.0	0.0	0.0	0.0	0.7	0.7	1.3	0.0	0.0	21.0	0.0	0.0	6.7	0.0	21.0	6.0	22.3	0.0	0.0	0.0	0.3	0.0	0.0	0.0	1.7
00BJB0010	0.0	0.7	7.7	5.3	3.3	7.3	0.0	0.3	0.0	0.0	3.7	1.0	1.7	0.0	0.0	23.7	0.0	0.0	2.3	0.0	13.7	4.0	24.3	0.0	0.0	0.0	0.3	0.0	0.0	0.0	0.7
00BJB0011	0.0	0.7	3.0	1.0	5.0	10.7	0.0	0.0	0.0	0.0	0.7	0.7	1.7	0.0	0.0	23.0	0.0	0.0	6.3	0.0	11.3	5.3	27.7	0.0	0.0	0.0	0.7	0.3	0.0	0.0	2.0
00BJB0012	0.0	2.0	5.0	4.0	2.0	8.3	0.0	0.0	0.0	0.3	4.0	0.0	0.3	0.0	0.0	32.3	0.3	0.0	6.7	0.0	4.3	2.3	26.0	0.0	0.0	0.0	0.0	0.0	0.0	0.0	2.3
00BJB0013	0.0	0.0	6.0	4.0	7.0	6.0	0.0	1.7	1.7	3.0	4.0	0.0	2.0	0.0	0.0	17.3	0.3	0.0	3.0	0.0	3.7	1.7	36.3	0.0	0.0	0.0	0.0	1.3	0.0	0.0	1.3
00BJB0014	0.0	2.3	6.3	0.0	5.3	10.3	0.0	0.7	0.3	0.0	2.7	2.7	0.0	0.0	0.0	13.0	2.7	0.0	2.0	0.0	6.0	10.0	29.7	0.0	0.0	0.0	0.7	1.3	0.3	0.0	3.7
00BJB0015	1.0	6.3	5.0	0.3	2.3	12.7	0.0	0.0	1.0	0.0	3.3	0.7	0.3	0.3	0.0	16.0	2.7	0.0	4.7	0.0	4.7	7.7	28.7	0.0	0.0	0.0	1.0	1.0	0.0	0.0	0.3
00BJB0016	0.0	0.0	3.7	1.0	8.7	3.7	0.0	0.0	0.0	0.0	1.0	1.7	0.0	1.0	0.0	40.0	0.0	4.0	4.3	0.0	8.7	9.0	10.3	0.0	0.0	0.0	1.3	0.0	0.0	0.0	1.7
00BJB0017	0.0	0.0	3.3	2.0	2.3	5.0	0.0	0.3	1.3	0.0	6.7	13.0	0.7	1.0	0.0	39.0	0.0	2.3	1.3	0.0	3.3	7.3	7.7	0.0	0.0	0.0	0.3	0.3	0.0	0.7	2.0
00BJB0018	0.0	0.0	3.0	2.3	2.3	3.0	0.0	0.7	0.7	0.0	3.0	1.7	0.7	0.3	0.0	34.0	1.3	0.0	2.7	1.0	8.3	12.3	14.3	0.0	0.0	0.3	0.7	0.3	0.3	3.7	3.0
00BJB0019	0.0	0.3	3.7	2.0	7.0	3.3	0.0	0.0	0.7	0.0	4.0	7.3	1.0	0.3	0.0	30.0	0.0	0.0	2.7	0.0	6.3	5.7	13.3	0.0	0.0	0.0	2.7	1.7	0.3	2.7	5.0
00BJB0021	0.0	0.0	2.3	1.3	6.3	10.7	0.0	0.7	1.3	0.7	7.3	2.0	0.3	0.0	0.0	7.0	0.3	0.0	4.3	0.7	8.7	9.3	32.3	0.0	0.0	0.0	2.0	0.3	0.0	0.0	2.0
00BJB0022	0.3	19.7	2.0	1.0	4.0	3.0	0.0	0.0	0.3	0.0	5.0	1.7	0.3	0.0	0.0	29.3	5.3	0.0	1.7	0.0	1.3	6.3	13.7	0.0	0.0	0.3	1.0	1.7	0.3	0.0	1.7
00BJB0023	0.0	0.0	1.0	1.0	7.3	3.0	0.0	3.7	3.0	0.0	13.7	0.0	0.0	0.0	0.0	17.3	0.7	0.0	2.7	0.0	2.7	3.0	19.3	0.0	0.0	1.3	0.7	16.0	0.0	0.0	3.7
00BJB0024	4.0	35.0	3.7	2.0	5.3	1.3	0.0	0.0	0.0	0.0	2.0	0.7	0.0	0.3	0.0	16.0	0.7	0.0	1.7	0.0	3.7	3.7	16.7	0.3	0.0	0.0	0.7	1.0	0.0	0.7	0.7
00BJB0025	0.0	3.0	4.0	1.3	3.7	0.7	0.0	0.7	2.3	0.0	6.7	0.3	0.0	0.0	0.0	21.0	0.7	0.0	3.0	0.0	1.3	5.0	16.0	0.0	0.0	1.3	0.0	26.7	0.3	0.0	2.0
00BJB0029	0.3	4.3	3.0	6.7	5.7	3.0	0.0	0.0	0.3	0.0	2.3	0.0	0.0	0.0	0.0	39.7	3.0	0.0	2.7	0.0	3.7	9.0	15.0	0.3	0.0	0.0	0.3	0.3	0.3	0.0	0.0
00BJB0030	0.0	0.0	5.7	3.3	7.3	7.3	0.0	0.7	0.0	0.0	2.0	0.0	0.0	0.0	0.0	9.7	0.0	0.0	4.0	0.0	12.0	7.0	37.7	0.0	0.0	0.0	1.0	0.0	0.3	0.0	2.0
00BJB0031	0.0	1.0	4.0	0.3	13.3	2.3	0.0	0.0	1.0	0.3	2.7	2.7	0.7	0.3	0.0	17.7	0.3	0.0	1.0	0.0	2.3	8.0	38.0	0.0	0.0	0.0	0.3	0.0	0.0	0.0	3.7

Notes:
PY = pyrite; Pg = pyrite, goethite covered; HM = hematite, grey; Hr = hematite, red; IL = ilmenite, grey; Ib = ilmenite, black; CM = chromite; RU = rutile, red; Ro = rutile, orange;
AT = anatase; LX = leucoxene; BA = barite, colourless; Bc = barite, milky; Bs = barite, stained; KY = kyanite; GO = yellow to brown; Gp = goethite after euhedral pyrite;
SD = siderite; HB = hornblende; CP = clinopyroxene; OP = orthopyroxene; EP = epidote; GA = garnet, pink; ST = staurolite; SP = titanite; MZ = monazite;
ZR = zircon, euhedral and irregular; Za = zircon, rounded; Al = aluminum shaving; X1 = unknown silver, maleable grain; UK = unknown and unidentifiables

00BJB0006	The Al shavings are almost certainly contamination (clean cut shavings).
00BJB0012	Three high lustre, black, submetallic grains placed in 5 mL vial. Also, nice blue anatase circled in ink (*see* figures below).
00BJB0015	Several varieties of black, high-lustre grains, may not all be ilmenite. This is true for several of the samples containing grains counted as black ilmenite.
00BJB0016	Some of the siderite grains may be goethite.
00BJB0019*	Five silver, maleable grains placed in 5 mL vial. These may be molybdenite grains. Unlikely graphite unless the till is extremely rich in this mineral. (*Contaminated by solder, *see* figures below)
00BJB0022	Many euhedral (octahedra and pyritohedra) pyrite grains covered with a very thin veneer of red goethite.

Appendix A6. (cont.)

Sample	PY	Pg	HM	Hr	IL	Ib	Io	CM	RU	Ro	AT	LX	BA	Bc	KY	GO	Gp	Gb	SD	HB	Ho	CP	OP	EP	GA	Gj	ST	SP	CH	MZ	ZR	Za	Al	UK
01BJB0002	0.0	1.0	3.0	0.3	6.3	8.0	0.0	0.7	0.7	0.3	0.0	7.3	1.7	0.3	0.0	14.7	0.7	0.3	0.3	2.7	0.0	0.3	3.7	12.0	30.3	1.3	0.0	0.3	0.0	0.0	0.3	0.0	0.0	3.3
01BJB0003	0.0	0.0	2.3	0.7	0.7	6.0	0.0	0.0	0.7	1.3	0.7	7.7	0.0	0.0	0.0	19.0	1.7	0.0	0.0	0.0	0.0	0.0	0.7	1.3	3.0	0.0	0.0	0.0	0.0	0.3	10.0	42.3	0.0	1.7
01BJB0004	0.0	0.3	4.3	1.0	0.3	1.7	0.0	0.0	0.7	0.0	0.0	5.3	4.7	11.0	0.0	54.7	3.7	4.0	0.0	0.0	0.0	0.0	0.0	2.0	1.7	0.7	0.0	0.0	0.7	0.0	0.3	0.3	0.0	2.7
01BJB0006	0.0	1.0	4.0	0.0	7.0	16.7	0.0	0.0	1.7	0.3	0.0	3.7	0.3	0.7	0.0	16.0	1.0	0.0	0.0	2.0	0.0	0.0	1.3	4.0	34.0	0.0	0.3	0.0	0.0	0.0	0.3	2.3	0.0	3.3
01BJB0007	1.3	12.4	5.3	0.7	1.7	6.0	1.0	0.0	0.0	0.0	0.0	0.3	0.0	0.0	0.0	36.0	1.7	0.7	2.7	2.0	0.0	0.0	2.3	3.7	16.7	0.3	0.0	0.0	0.3	0.0	0.3	0.0	0.0	4.7
01BJB0009	0.0	0.0	2.7	1.3	2.7	3.3	0.0	0.0	0.0	0.0	0.0	3.7	0.3	0.0	0.0	27.7	0.3	0.0	0.3	5.0	0.0	0.0	4.3	21.7	23.7	1.0	0.0	0.0	0.0	0.0	0.0	0.7	0.0	1.3
01BJB0008	0.0	0.3	5.3	5.7	4.0	5.0	0.0	0.0	0.3	0.3	0.0	2.3	0.3	0.0	0.0	39.0	0.3	0.3	0.0	2.3	0.0	1.7	4.3	7.6	17.0	2.0	0.0	0.0	0.0	0.0	0.0	0.3	0.0	1.7
01BJB0010	0.3	2.7	5.0	0.7	7.3	9.7	0.0	0.0	0.0	0.3	0.0	2.3	0.0	0.0	0.0	15.3	1.0	0.0	0.0	3.7	0.0	0.3	3.3	6.0	38.0	1.0	0.3	0.0	0.0	0.0	0.3	0.3	0.3	1.7
01BJB0011	34.0	0.3	2.0	1.3	5.0	2.3	0.0	0.0	0.7	0.0	0.0	1.3	0.0	0.0	0.0	7.3	0.0	0.0	24.3	0.7	0.0	0.0	1.7	3.0	14.3	0.0	0.0	0.0	0.0	0.0	0.0	0.0	0.0	1.7
01BJB0012	0.0	0.7	3.4	2.7	7.3	0.8	0.0	0.0	0.0	0.0	0.0	0.4	0.0	0.0	0.0	32.8	0.4	0.0	1.1	2.7	0.4	0.0	22.5	7.6	14.9	0.8	0.0	0.0	0.0	0.0	0.4	0.4	0.0	0.8
01BJB0013	0.3	36.3	10.0	0.7	4.0	1.3	0.0	0.0	0.3	0.0	0.3	1.7	0.3	0.0	0.0	9.0	0.0	0.7	0.0	3.0	0.7	0.0	2.7	5.7	19.0	2.3	0.0	0.0	0.0	0.0	0.0	0.3	0.0	1.3
01BJB0014	0.0	9.0	5.3	0.0	7.7	3.7	0.0	0.0	0.0	0.7	0.7	3.3	0.0	0.0	0.3	25.7	0.0	0.7	0.0	4.0	0.0	0.3	6.3	5.3	22.0	2.3	0.0	0.0	0.0	0.0	0.0	1.7	0.0	1.0
01BJB0015	3.0	13.3	2.0	1.3	1.3	0.3	0.0	0.0	0.0	0.0	0.0	0.3	0.0	0.0	0.0	12.0	0.0	0.3	56.3	1.0	0.0	0.0	0.3	2.3	3.3	0.0	0.0	0.3	0.0	0.0	0.0	0.0	0.0	2.7
01BJB0018	0.7	21.0	7.7	1.0	5.3	4.7	0.0	0.0	0.0	0.3	0.0	1.3	0.0	0.0	0.0	14.0	0.0	0.0	0.7	2.3	0.0	0.0	3.3	7.7	24.3	0.7	0.0	0.0	0.0	0.3	1.3	0.0	0.0	3.3
01BJB0021	9.3	16.0	5.3	0.3	4.3	4.0	0.0	0.0	0.0	0.0	0.0	1.0	0.0	0.0	0.0	13.0	0.3	0.7	13.7	1.0	0.0	0.0	1.7	4.0	19.3	0.0	0.0	0.0	0.0	0.0	1.3	3.0	0.0	1.7
01BJB0022	0.3	2.0	2.7	1.0	8.0	12.3	0.0	0.0	0.3	1.0	0.7	3.3	0.0	0.0	0.0	11.0	0.0	0.3	3.0	4.7	0.0	0.7	4.7	5.0	30.7	2.3	0.0	0.0	0.0	0.0	1.0	3.0	0.0	2.0
01BJB0023	0.0	2.0	0.3	0.0	0.0	2.3	0.0	0.0	0.7	3.7	0.0	19.3	0.0	0.0	0.0	1.0	0.0	0.0	2.7	0.3	0.0	0.0	1.3	0.0	1.0	0.3	0.0	0.0	0.0	0.3	7.0	56.0	0.0	1.7
01BJB0024	0.0	0.3	3.7	1.3	1.0	6.7	0.0	0.0	0.0	0.0	0.0	0.3	0.0	2.0	0.0	8.0	0.0	0.0	0.0	8.3	0.0	0.0	51.0	1.7	13.0	0.3	0.0	0.0	0.0	0.0	0.3	0.3	0.0	1.7
01BJB0025	1.7	40.7	4.7	1.0	2.0	3.0	0.0	0.0	0.0	0.0	0.0	2.0	0.0	0.7	0.0	10.7	0.0	0.3	0.7	3.3	0.0	0.0	5.3	6.3	14.7	0.7	0.0	0.0	0.0	0.0	0.3	1.3	0.0	0.7
01BJB0027	9.0	23.7	3.3	0.3	2.7	1.0	0.0	0.0	0.0	0.0	0.0	1.0	0.0	0.0	0.3	14.7	0.0	1.0	22.7	1.3	0.0	0.0	3.3	1.3	13.7	0.3	0.0	0.0	0.0	0.0	0.0	0.0	0.0	0.3
01BJB0028	0.3	1.0	8.0	0.3	4.3	6.3	0.0	0.0	0.0	0.0	0.7	1.3	0.0	0.0	0.0	11.0	0.0	0.0	0.3	1.3	0.3	0.0	5.7	4.3	51.7	1.3	0.0	0.0	0.0	0.0	0.7	0.0	0.0	1.0
02BJB0004	0.0	3.0	3.3	4.3	0.7	4.0	0.3	0.3	0.0	0.3	0.0	3.7	0.3	0.3	0.3	55.0	0.0	0.0	0.0	1.0	0.0	0.0	1.7	4.7	12.7	0.0	0.0	0.0	0.0	0.0	1.0	2.0	0.0	1.0
02BJB0005	0.3	2.7	3.7	1.7	8.0	4.0	0.3	0.0	0.0	0.3	0.3	2.3	0.0	0.3	0.0	9.7	0.3	0.0	0.0	4.3	0.0	0.7	9.3	10.3	39.3	0.0	0.0	0.0	0.0	0.0	0.7	0.7	0.0	0.7
02BJB0008	0.0	0.0	4.3	2.0	4.3	3.7	0.0	0.0	0.7	1.0	0.0	9.7	0.7	0.0	0.3	26.3	0.0	0.0	0.0	5.0	0.0	0.7	4.7	6.3	20.0	0.3	0.0	0.0	0.0	0.0	1.3	7.3	0.0	1.3
02BJB0009	0.0	4.0	3.0	3.0	3.0	2.7	0.0	0.0	0.0	1.3	0.0	5.3	0.0	1.3	0.0	29.3	1.3	0.0	0.0	3.7	0.0	0.7	5.0	10.0	18.0	0.0	0.0	0.0	0.0	0.3	0.3	6.0	0.0	1.7
02BJB0010	28.3	1.3	0.7	0.7	4.7	2.3	0.7	0.0	0.0	0.0	0.0	2.0	0.0	1.0	0.0	5.3	0.0	0.0	27.0	1.0	0.0	2.0	4.0	6.7	11.3	0.3	0.0	0.0	0.0	0.0	0.3	0.0	0.0	0.3
02BJB0011	0.0	0.3	2.0	10.7	1.7	4.7	0.0	0.0	0.0	0.0	0.0	1.0	0.0	0.0	0.0	28.7	0.0	0.0	0.0	4.7	0.0	0.3	22.7	4.3	16.3	0.7	0.0	0.0	0.0	0.3	0.3	0.0	0.0	1.3
02BJB0013	7.3	7.7	3.7	0.0	3.7	2.3	0.0	0.0	0.3	0.0	0.0	0.3	0.0	0.0	0.0	21.3	0.3	2.0	1.0	5.7	0.0	0.3	0.7	9.0	33.0	0.0	0.0	0.0	0.0	0.0	0.0	0.3	0.0	1.0
02BJB0014	0.0	0.0	11.3	0.0	0.0	1.3	0.0	0.0	0.3	0.3	0.0	72.7	0.0	0.0	0.0	4.0	0.0	0.0	1.3	0.3	0.0	0.0	0.3	0.3	5.0	0.0	0.0	0.0	2.0	0.0	0.0	0.0	0.0	0.7
02BJB0015	24.7	0.7	1.7	0.0	1.3	0.3	0.0	0.0	0.0	0.0	0.0	1.0	0.0	0.0	0.0	5.7	0.0	0.0	53.0	1.3	0.0	0.3	2.0	1.7	5.7	0.0	0.0	0.3	0.0	0.0	0.0	0.0	0.0	0.3
02BJB0016	23.7	3.0	3.7	1.3	2.7	1.3	0.0	0.0	0.0	0.0	0.0	3.3	0.0	0.0	0.3	14.3	0.0	0.0	19.7	1.0	0.0	0.3	4.7	4.3	14.0	0.0	0.0	0.0	0.0	0.3	0.3	0.7	0.0	1.0
02BJB0017	0.0	0.0	4.7	9.7	5.3	1.3	0.0	0.0	0.0	0.7	0.0	3.7	0.0	0.0	0.0	40.7	0.0	0.0	0.0	5.3	0.0	0.0	2.7	13.7	9.0	0.0	0.0	0.0	0.0	0.0	0.0	0.3	0.0	3.0
02BJB0018	0.0	0.0	1.3	7.7	0.0	2.3	0.0	0.0	0.0	0.0	0.3	5.3	0.0	0.0	0.0	41.7	0.0	0.0	0.3	1.3	0.0	0.0	3.0	17.3	18.0	0.3	0.0	0.0	0.0	0.0	0.0	0.0	0.0	1.0
02BJB0019	0.0	0.0	4.7	9.7	8.0	2.0	0.0	0.0	0.0	0.0	0.0	3.7	0.0	0.0	0.3	13.7	0.0	0.0	0.0	6.0	0.0	2.0	5.7	10.3	28.3	3.0	0.3	0.0	0.0	0.0	0.0	0.7	0.0	1.7
02BJB0021	0.0	1.7	2.7	2.0	6.0	5.0	0.3	0.0	0.0	0.3	0.0	4.0	0.0	0.0	0.0	12.7	0.0	0.0	0.0	8.0	0.0	3.3	2.0	16.0	32.7	0.7	0.0	0.0	0.3	0.0	1.7	0.0	0.0	0.7
02BJB0022	0.0	3.3	1.7	3.7	5.3	4.7	0.0	0.0	0.0	0.0	0.0	5.0	0.3	2.0	0.0	28.7	0.0	0.0	0.0	5.3	0.0	1.0	3.3	9.0	21.0	0.0	0.0	0.0	1.3	0.0	1.7	0.7	0.0	2.0
02BJB0023	0.0	0.0	1.0	0.3	3.0	3.7	0.0	0.0	1.3	1.3	0.7	21.0	0.0	0.0	0.0	16.3	0.0	0.0	0.0	3.7	0.0	0.3	1.7	2.3	14.7	0.0	0.0	0.0	0.3	1.7	5.3	18.0	0.0	3.3

Notes:
PY = pyrite; Pg = pyrite, goethite covered; HM = hematite, grey; Hr = hematite, red; IL = ilmenite, grey; Ib = ilmenite, black; CM = chromite; RU = rutile, red; Ro = rutile, orange;
AT = anatase; LX = leucoxene; BA = barite, colourless; Bc = barite, milky; Bs = barite, stained; KY = kyanite; GO = yellow to brown; Gp = goethite after euhedral pyrite;
SD = siderite; HB = hornblende; CP = clinopyroxene; OP = orthopyroxene; EP = epidote; GA = garnet, pink; ST = staurolite; SP = titanite; MZ = monazite;
ZR = zircon, euhedral and irregular; Za = zircon, rounded; Al = aluminum shaving; X1 = unknown silver, maleable grain; UK = unknown and unidentifiables

01BJB0003	Ten of the zircon grains counted were broken, irregular grains.
01BJB0005	Rutile with elbow twin at 001 005 on slide.
01BJB0011	Ilmenite and leucoxene with similar morphology.
01BJB0021	Some of the grey hematite grains are particularly silvery and may be interesting to verify using the SEM or microprobe.
01BJB0023	One nice, euhedral, possibly brookite grain classed as anatase (also TiO_2) at 002 004 on slide.

Appendix A6. (cont.)

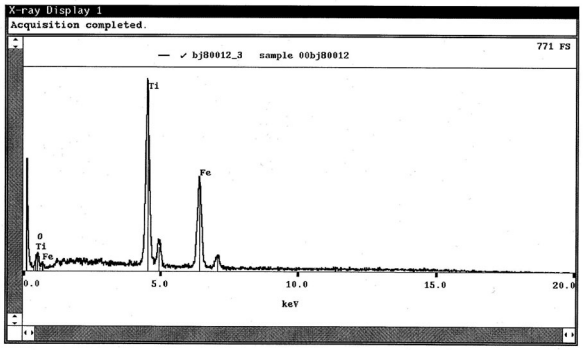

Figure A6-1

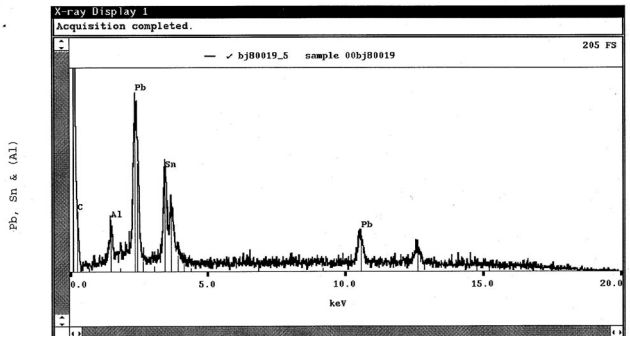

Figure A6-2

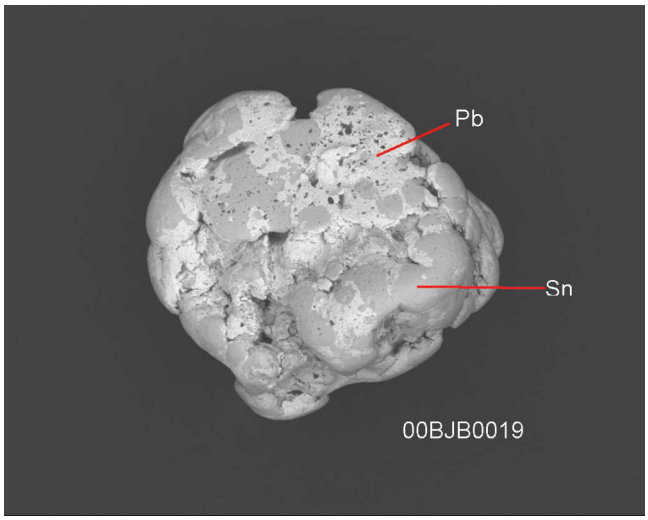

Figure A6-3

Contents
This CD-ROM contains the full contents of Bulletin 596 in .pdf, .shp, and .mdb formats, including any maps or oversized figures.

System requirements
PC with 486 or greater processor, or Mac® with OS® X v. 10.2.2 or later; Adobe® Reader® v. 6.0 (included for both PC and Mac) or later; ESRI® ArcExplorer™ v. 2.0 (included for PC) or any software capable of importing or translating shape files; Microsoft® Access® 2003 or later; video resolution of 1280 x 1024.

Quick start
This is a Windows®-based autoplay disk. Should the autoplay fail, navigate to the root of your CD-ROM drive and double-click on the autoplay.exe file. Mac® users must use this method to begin.

****

Contenu
Ce CD-ROM renferme le contenu intégral du Bulletin 596 en formats .pdf, .shp et .mdb y compris les figures surdimensionnées ou les cartes, s'il y a lieu.

Configuration requise
PC avec processeur 486 ou plus rapide, ou Mac® avec OS® X v. 10.2.2 ou ultérieure; Reader® v. 6.0 d'Adobe® (fourni pour PC et Mac) ou version ultérieure; ArcExplorer™ v. 2.0 d'ESRI® (fourni pour pc) ou tout logiciel capable d'importer ou de traduire les fichiers shape file; Access® 2003 de Microsoft® ou version ultérieure; résolution vidéo de 1280 x 1024.

Démarrage rapide
Ceci est un disque à lancement automatique pour les systèmes d'exploitation Windows®. Si le lancement automatique ne fonctionne pas, allez au répertoire principal du CD-ROM et faites un double clic sur le fichier autoplay.exe. Les utilisateurs de systèmes Mac® doivent procéder de cette façon pour débuter la consultation.